Results from the *Planck* satellite and their scientific implications

Carlo Burigana @ INAF/IASF Bologna

On behalf of the *Planck* Collaboration

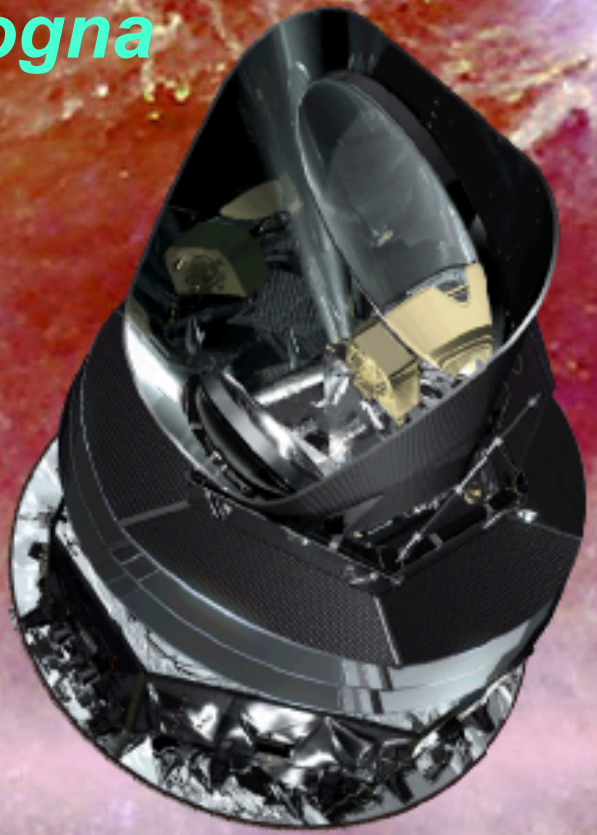

The 16th Paris Cosmology Colloquium 2012
"Lambda Warm Dark Matter:
the new Standard Model of the Universe.
Theory and Observations",
The International School Daniel Chalonge
The 16th Paris Cosmology Colloqium
Observatoire de Paris, Paris campus, 25-27 July 2012

Planck is a project of the European Space Agency - ESA - with instruments provided by two scientific Consortia funded by ESA member states (in particular the lead countries: France and Italy) with contributions from NASA (USA), and telescope reflectors provided in a collaboration between ESA and a scientific Consortium led and funded by Denmark.

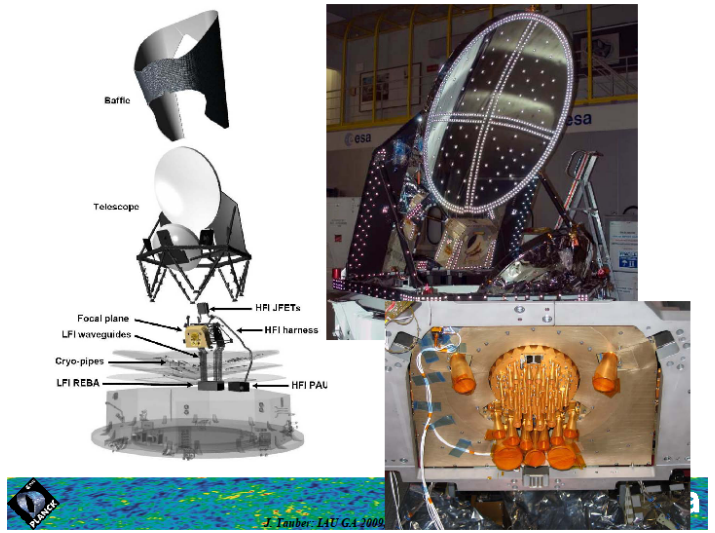

Principal Investigators
HFI: J.L. Puget,
LFI: R. Mandolesi,
Tel: H.U. Nørgaard-Nielsen

The European mission to map the Cosmic Microwave Background

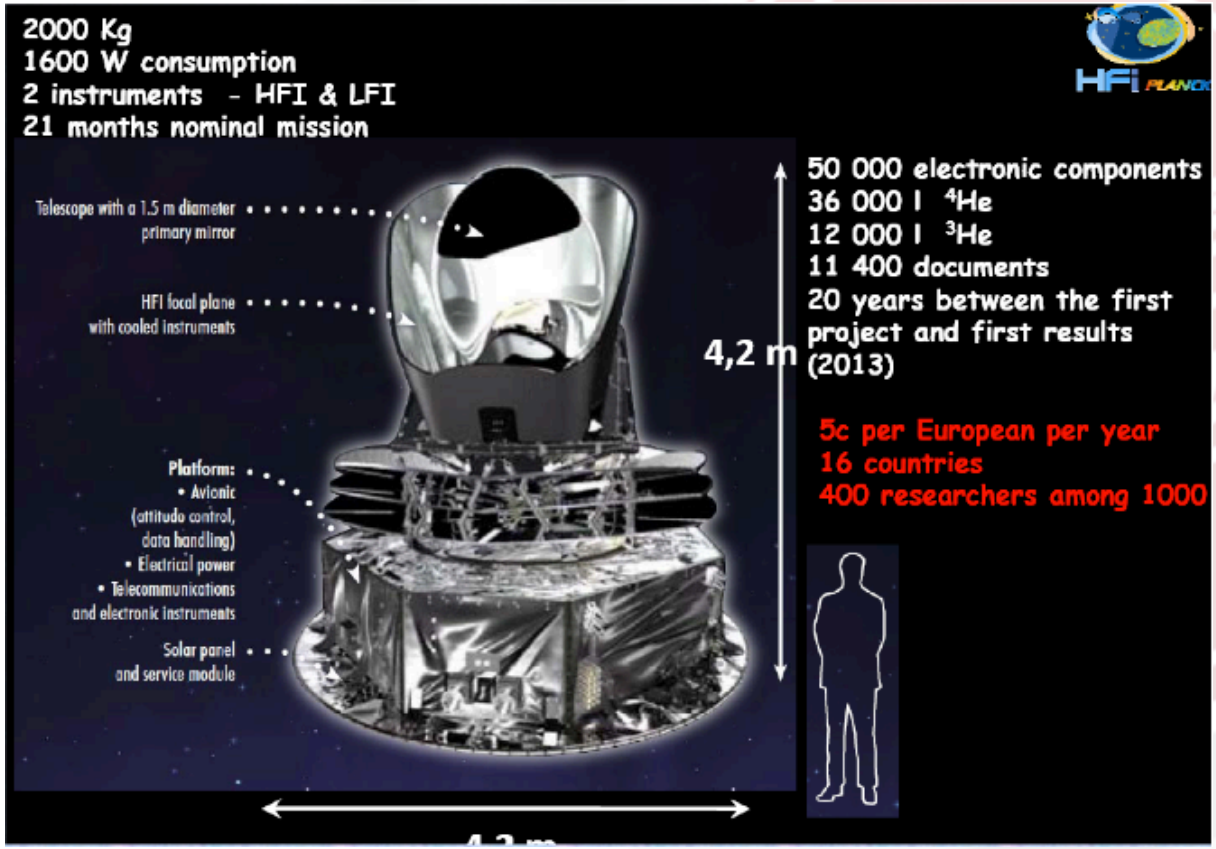

To image the temperature and polarisation anisotropies of the Cosmic Microwave Background (CMB), over the whole sky, with an uncertainty on the temperature limited by "natural causes" (foreground fluctuations, cosmic variance) rather than intrinsic or systematic detector noises, and an angular resolution ~5 arcminutes.

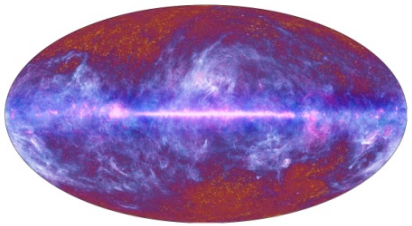

CMB space mission experiments overview – Planck: 3rd Generation

The oldest light or the first light of the Universe

1965 — Penzias and Wilson

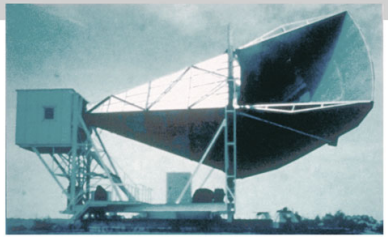

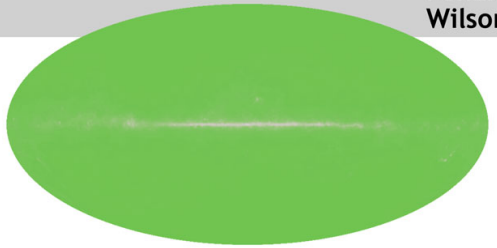

Discovered the remnant afterglow from the **Big Bang**.
→ **2.7 K**

1992 — COBE

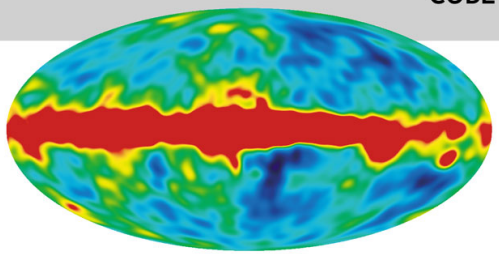

Blackbody radiation, Discovered the patterns (**anisotropy**) in the afterglow.
→ **angular scale ~ 7°** at a level ΔT/T of 10^{-5}

2003 — WMAP

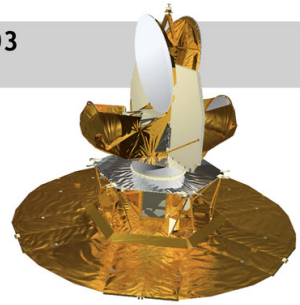

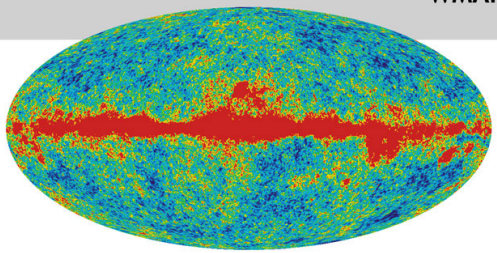

(Wilkinson Microwave Anisotropy Probe):
→ **angular scale ~ 15'**

2009 — *Planck*

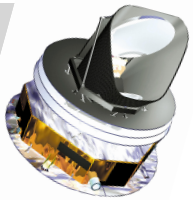

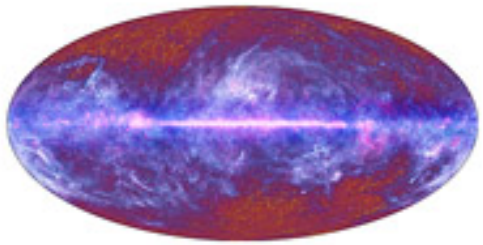

→ **angular scale ~ 5',**
ΔT/T ~ 2×10^{-6}, 30~867 Hz

Planck Scientific Objectives

The unrivalled accuracy of *Planck* on the whole sky will allow us to:

- **Pin down the basic characteristics of the Universe: age, contents, dynamics, geometry, …**
- **Examine the origins of the Universe and test inflation**
- **Probe physics at extremely high energies, e.g. superstrings, neutrinos**
- **Probe the birth of the first stars and galaxies**

But also

- **Understand the evolution of structures, galaxies and clusters of galaxies; Observe our own Galaxy as never seen before …**

→ **Key non-CMB science with *Planck* includes:**

- ❖ **The Cosmic Infrared Background**
- ❖ **Sunyaev-Zeldovich selected sources**
- ❖ **Extragalactic sources and backgrounds**
- ❖ **Maps of Milky Way at frequencies 30-1000 GHz**

… and all related science ☺

The Scientific Programme of Planck

This book describes the expected scientific output of the Planck mission, both cosmological and non-cosmological.

Title	Authors	Publication
The Scientific Programme of Planck (Bluebook)	Planck Collaboration	2005 ESA

Planck Pre-launch Papers

These papers contain detailed technical descriptions of the status of Planck immediately prior to launch, including the satellite, the optical system, its two scientific instruments, and the main results of its multiple ground characterization and calibration campaigns.

Title	Authors	Publication
Planck pre-launch status: High Frequency Instrument polarization calibration	Rosset et al.	2010 A&A 520, A13
Planck pre-launch status: HFI ground calibration	Pajot et al.	2010 A&A 520, A10
Planck pre-launch status: the optical system	Tauber et al.	2010 A&A 520, A2
Planck pre-launch status: the HFI instrument from specification to actual performance	Lamarre et al.	2010 A&A 520, A9
Planck pre-launch status: HFI beam expectations from the optical optimisation of the focal plane	Maffei et al.	2010 A&A 520, A12
Planck pre-launch status: Low Frequency Instrument calibration and expected scientific performance	Mennella et al.	2010 A&A 520, A5
Planck pre-launch status: the optical architecture of the HFI	Ade et al.	2010 A&A 520, A11
Planck pre-launch status: design and description of the Low Frequency Instrument	Bersanelli et al.	2010 A&A 520, A4
Planck pre-launch status: The Planck mission	Tauber et al.	2010 A&A 520, A1
Planck pre-launch status: the Planck-LFI programme	Mandolesi et al.	2010 A&A 520, A3
Planck pre-launch status: Low frequency instrument optics	Sandri et al.	2010 A&A 520, A7
Planck pre-launch status: calibration of the Low Frequency Instrument flight model radiometers	Villa et al.	2010 A&A 520, A6
Planck pre-launch status: expected LFI polarisation capability	Leahy et al.	2010 A&A 520, A8

Plus more than 31 **Planck Technical Papers**

Expected results from simulations

30, 44, 70, 100, 143, 217, 353, 545, 857 GHz – I, Q, U at all channels
Except 545 & 857 GHz

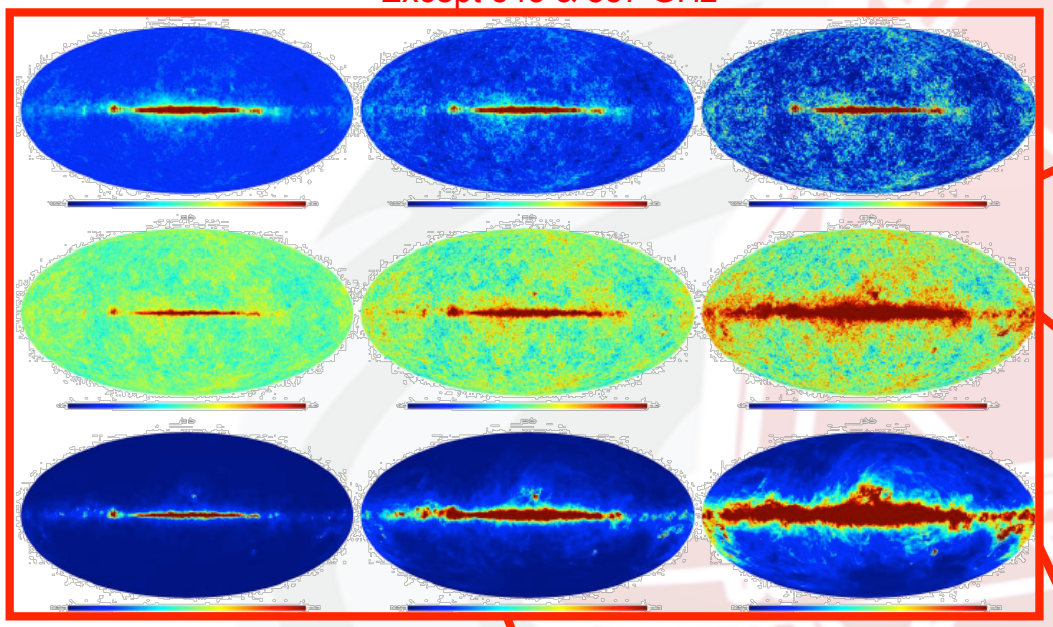

Cosmic Microwave Background

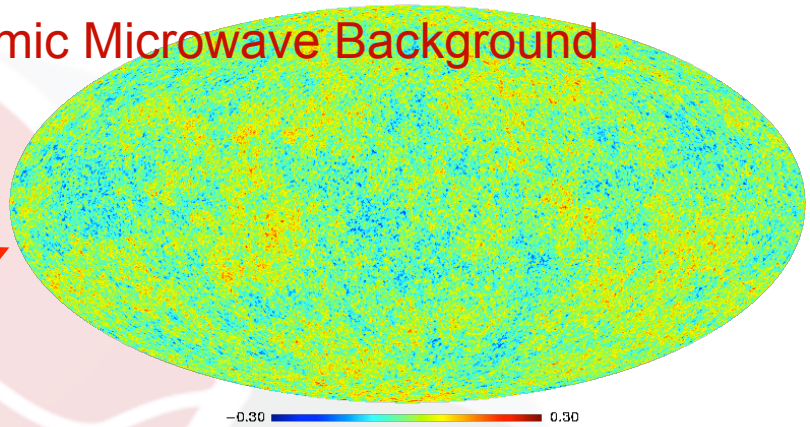

Sunyaev-Zeldovich

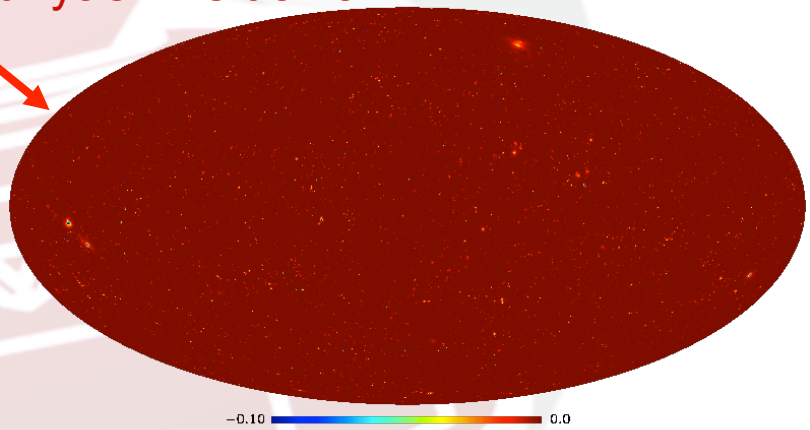

The Milky Way

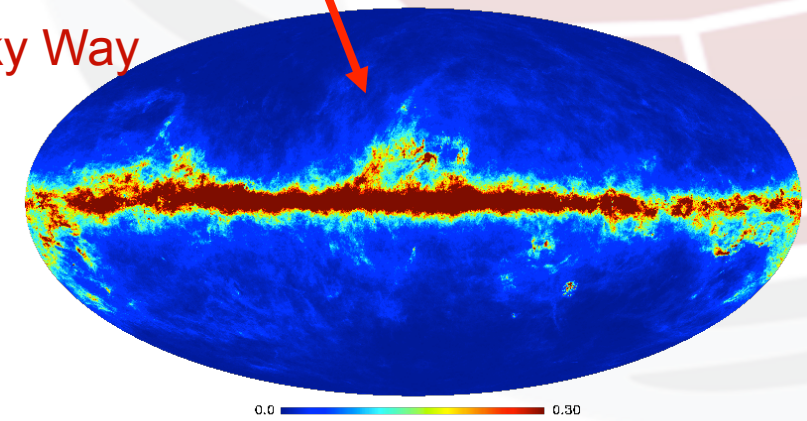

Point & Compact sources

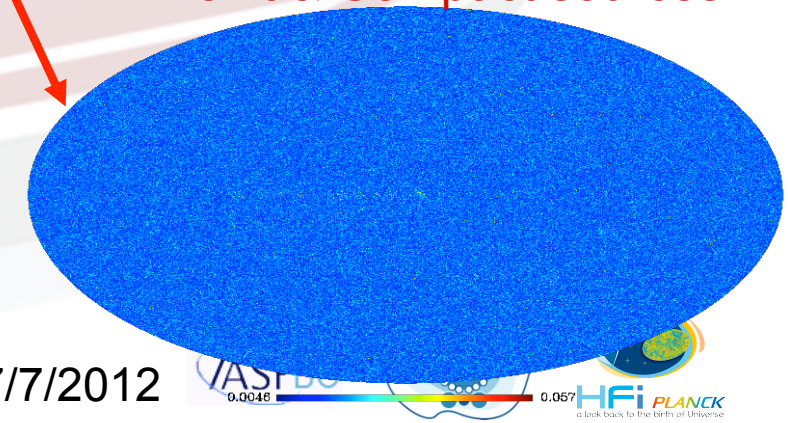

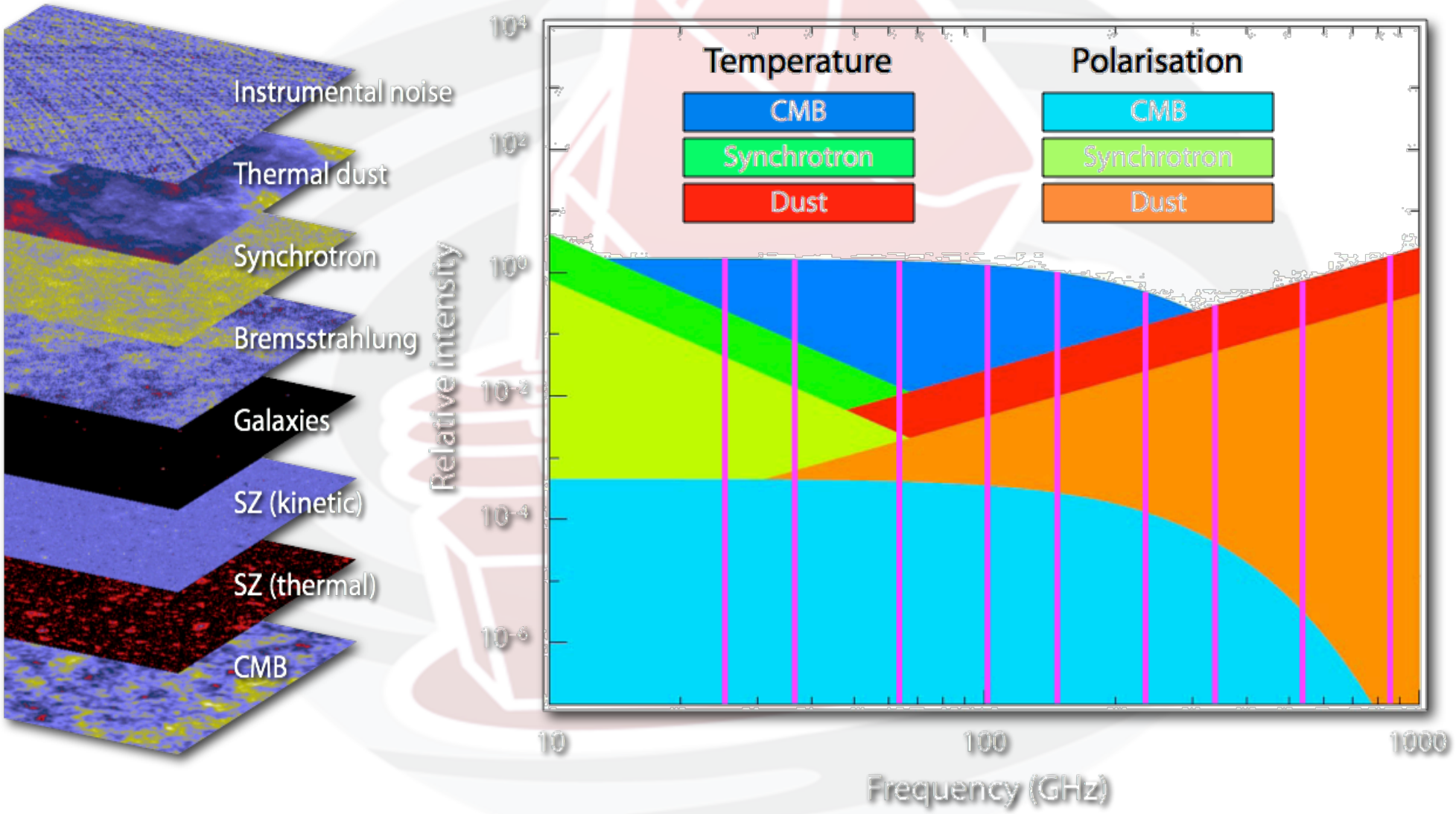
Instrumental noise
Thermal dust
Synchrotron
Bremsstrahlung
Galaxies
SZ (kinetic)
SZ (thermal)
CMB
Temperature
CMB
Synchrotron
Dust
Polarisation
CMB
Synchrotron
Dust
Relative intensity
10
100
1000
Frequency (GHz)

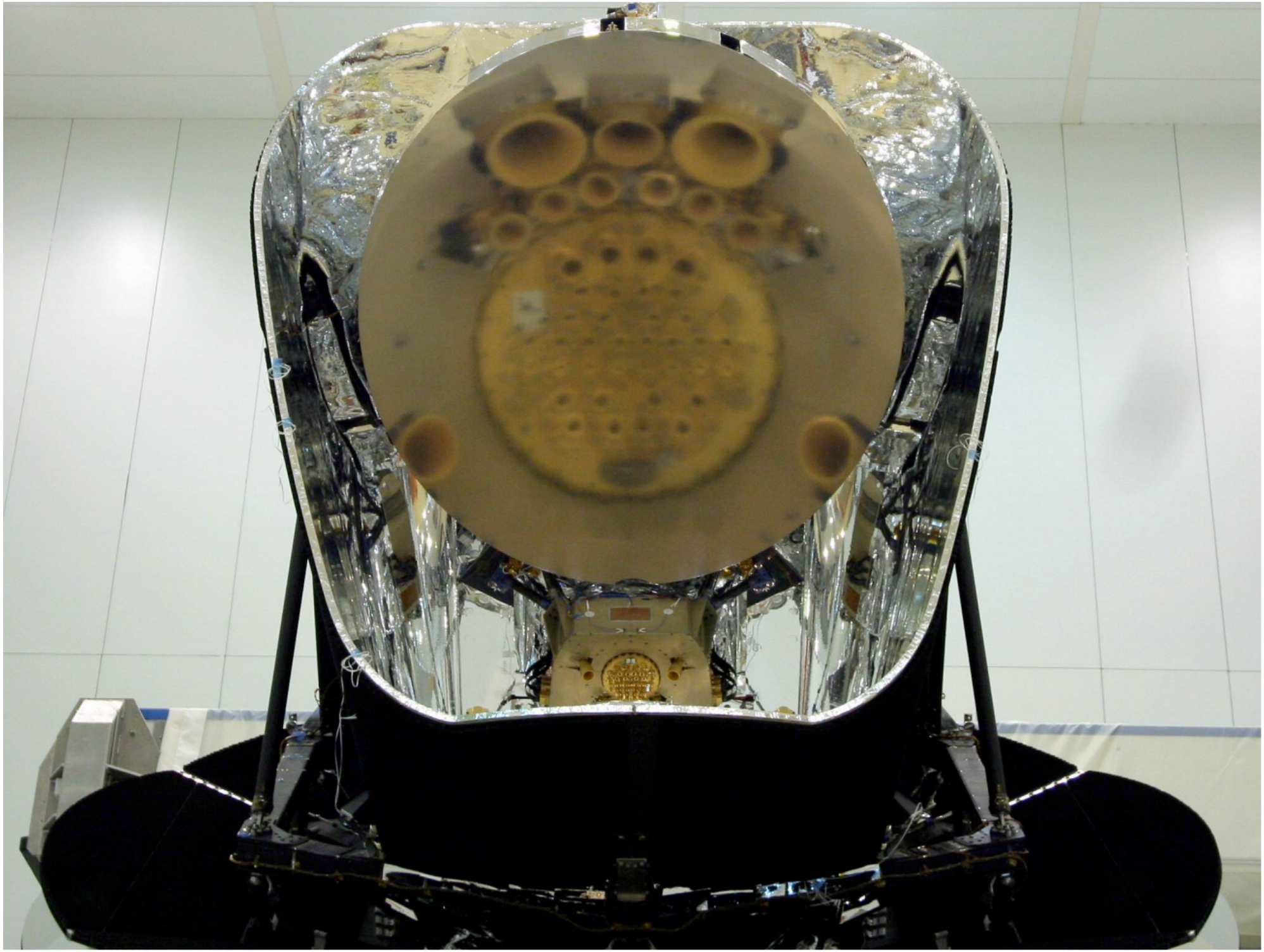

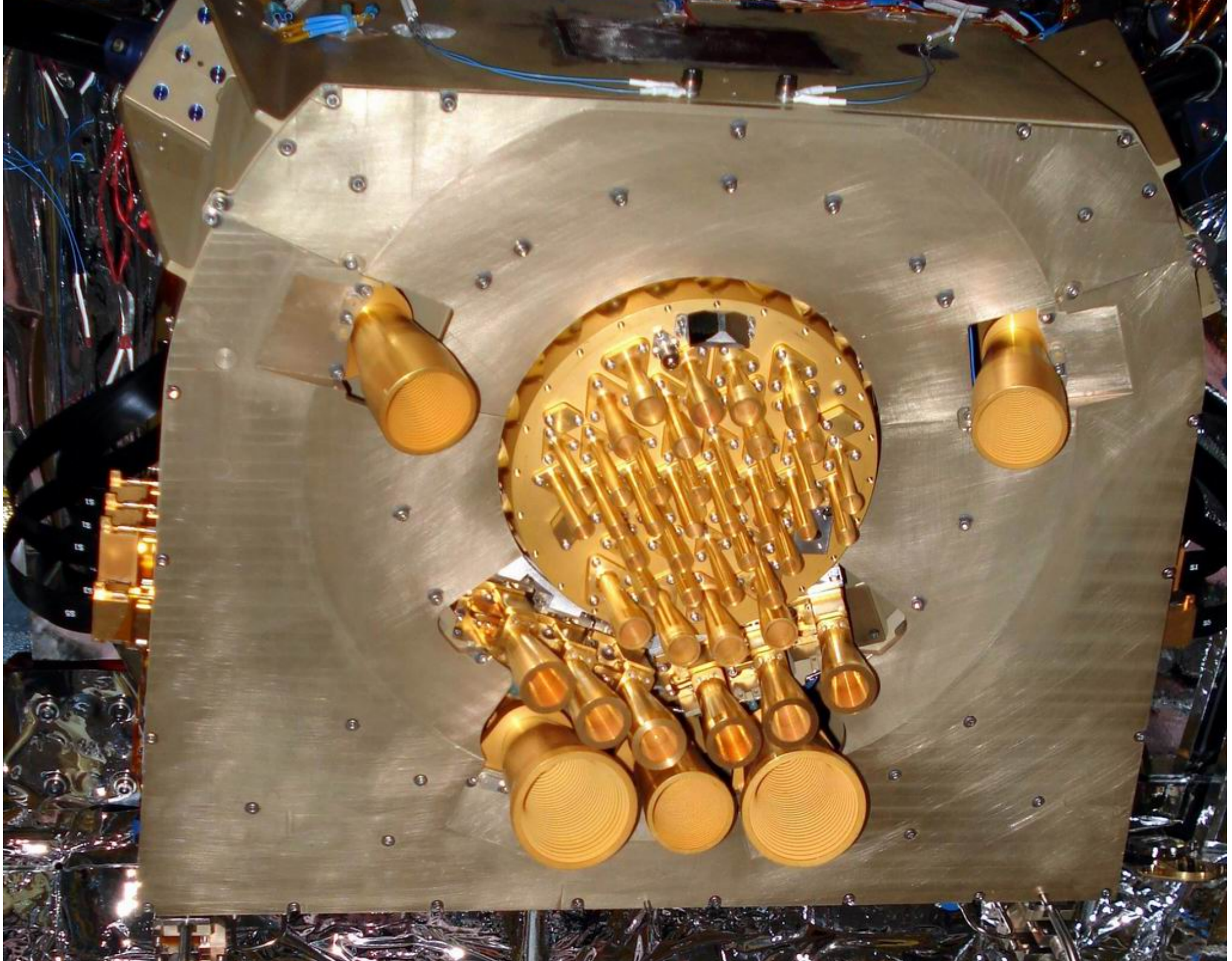

Mission current Status

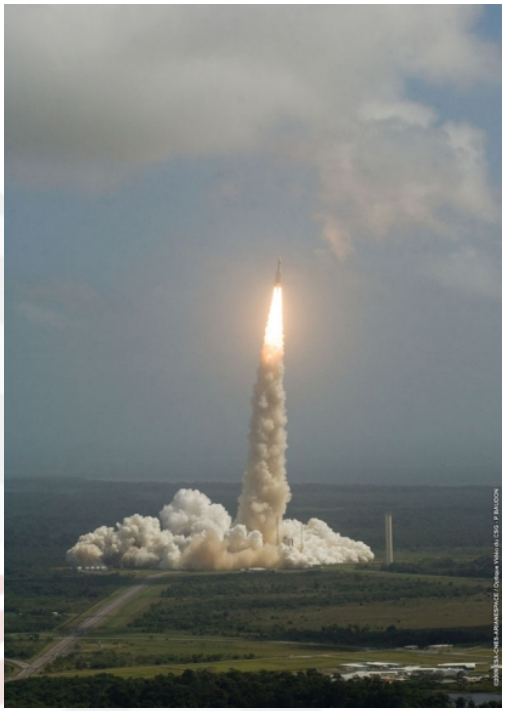

- @ 27 July 2012: 1170 days of operation since launch (14-May-2009 13:12 UT)
- Satellite and instruments worked/working nominally and continuously since start of sky surveys (mid August 2009)
- Sky coverage is 100%
  - **All the sky has been surveyed for about 29.5 months, i.e. about five times with both instruments HFI + LFI, until the end of the cold phase (14 January 2012)**
  - **A further 12 months extension (up to the end of 2012 – beginning of 2013) has been approved (and indeed on-going) with LFI only … maybe will continue during 2013**
  - **Planck-LFI is almost concluding its sixth all-sky survey**

Planck Scanning Strategy

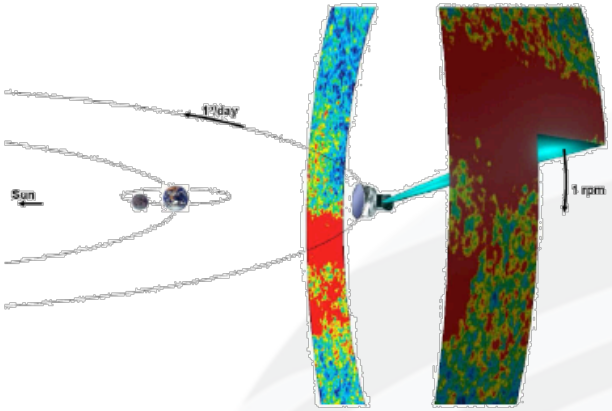

Planck is a survey mission

About 6 months are needed to cover ~95% of the sky.

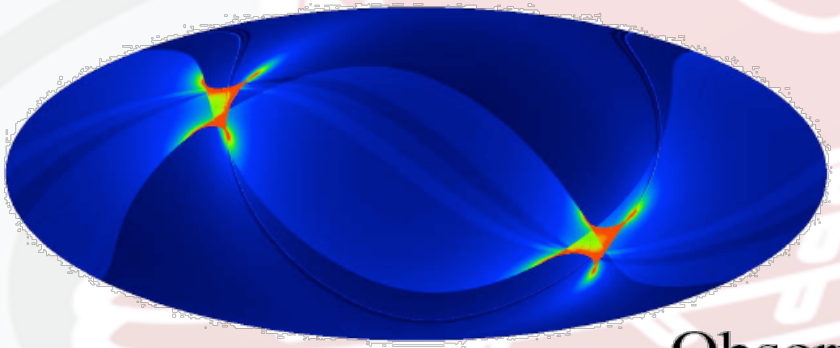

Observing strategy

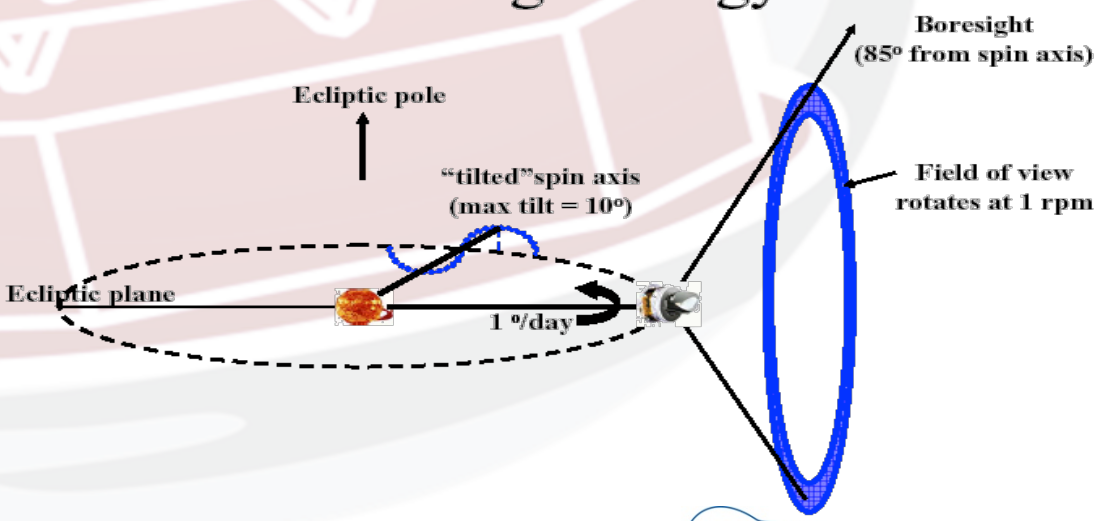

During LFI only phase
Scanning strategy combines standard mode with deep annuli on calibration sources to improve the quality of calibration and systematic effect control

Planck performance "extrapolated" at ≈ final mission

Table 1. *Planck* performances. The average sensitivity, $\delta T/T$, per FWHM^2 resolution element (FWHM is reported in arcmin) is given in CMB temperature units (i.e. equivalent thermodynamic temperature) for for 29.5 (plus 12 for LFI) months of integration.. The white noise (per frequency channel for LFI and per detector for HFI) in 1 sec of integration (NET, in $\mu K \cdot \sqrt{s}$) is also given in CMB temperature units. The other used acronyms are: DT = detector technology, N of R (or B) = number of radiometers (or bolometers), EB = effective bandwidth (in GHz). Adapted from [6, 7].

LFI			
Frequency (GHz)	30	44	70
InP DT	MIC	MIC	MMIC
FWHM	33.34	26.81	13.03
N of R (or feeds)	4 (2)	6 (3)	12 (6)
EB	6	8.8	14
NET	159	197	158
$\delta T/T$ [μK/K] (in T)	2.04	3.14	5.17
$\delta T/T$ [μK/K] (in P)	2.88	4.44	7.32

HFI		
Frequency (GHz)	100	143
FWHM in T (P)	(9.6)	7.1 (6.9)
N of B in T (P)	(8)	4 (8)
EB in T (P)	(33)	43 (46)
NET in T (P)	100 (100)	62 (82)
$\delta T/T$ [μK/K] in T (P)	2.04 (3.31)	1.56 (2.83)

HFI		
Frequency (GHz)	217	353
FWHM in T (P)	4.6 (4.6)	4.7 (4.6)
N of B in T (P)	4 (8)	4 (8)
EB in T (P)	72 (63)	99 (102)
NET in T (P)	91 (132)	277 (404)
$\delta T/T$ [μK/K] in T (P)	3.31 (6.24)	13.7 (26.2)

HFI		
Frequency (GHz)	545	857
FWHM in T	4.7	4.3
N of B in T	4	4
EB in T	169	257
NET in T	2000	91000
$\delta T/T$ [μK/K] in T	103	4134

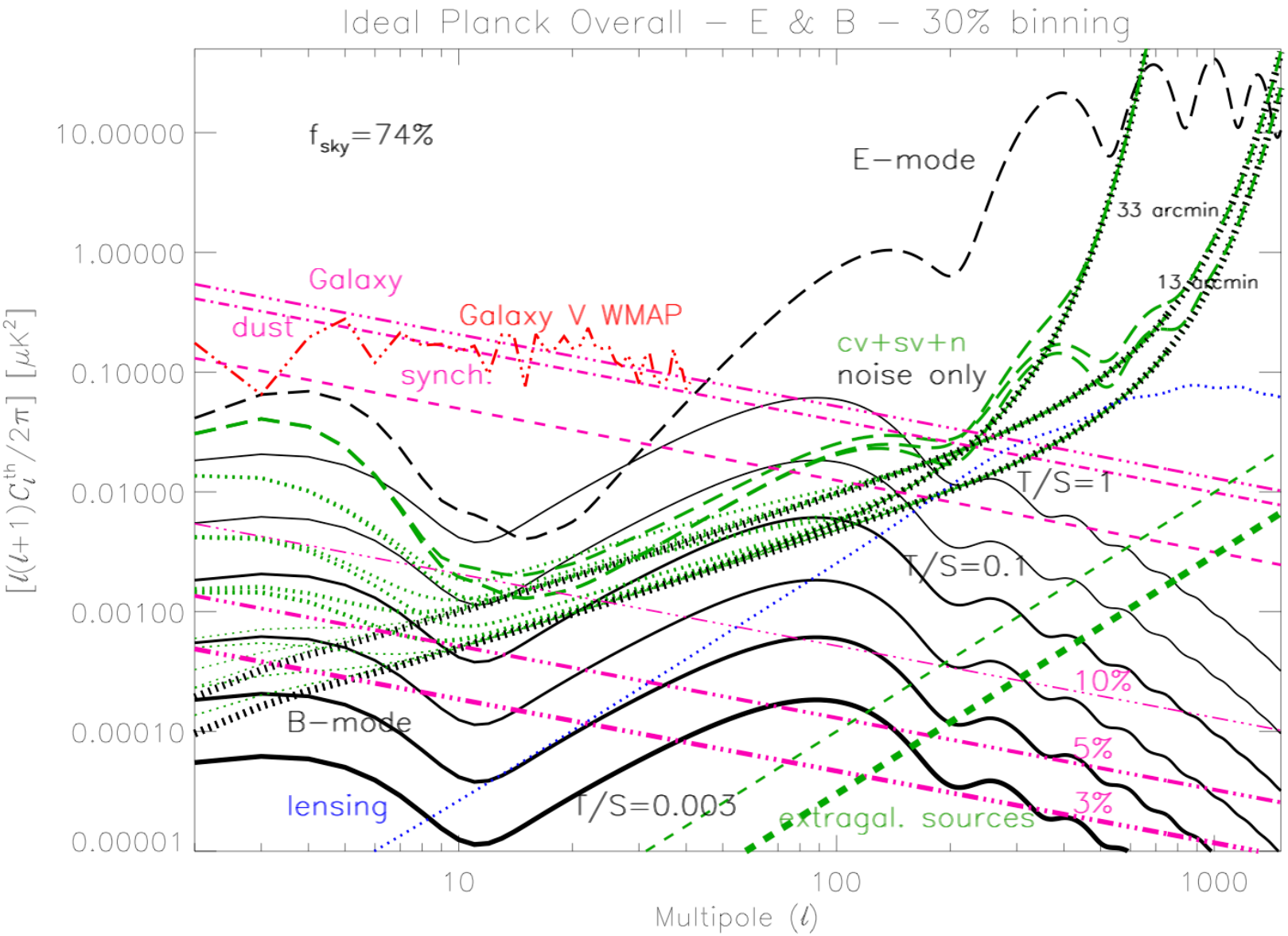

But for now … astrophysics & "cosmology from astrophysics" → ☺ → ☹ → ☺

From simulations to reality!

The Planck view of the sky after almost one year of operations (CMB removed)

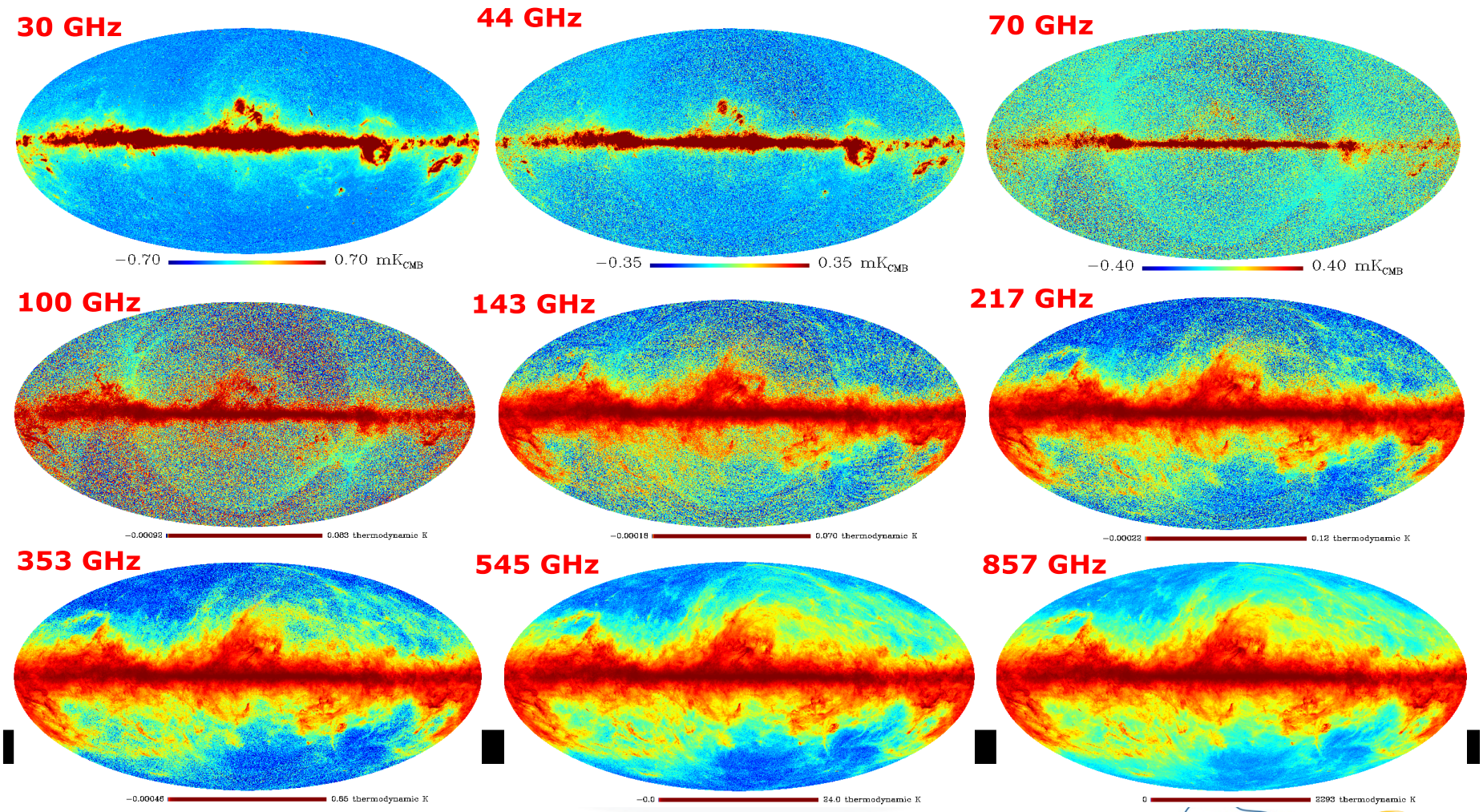

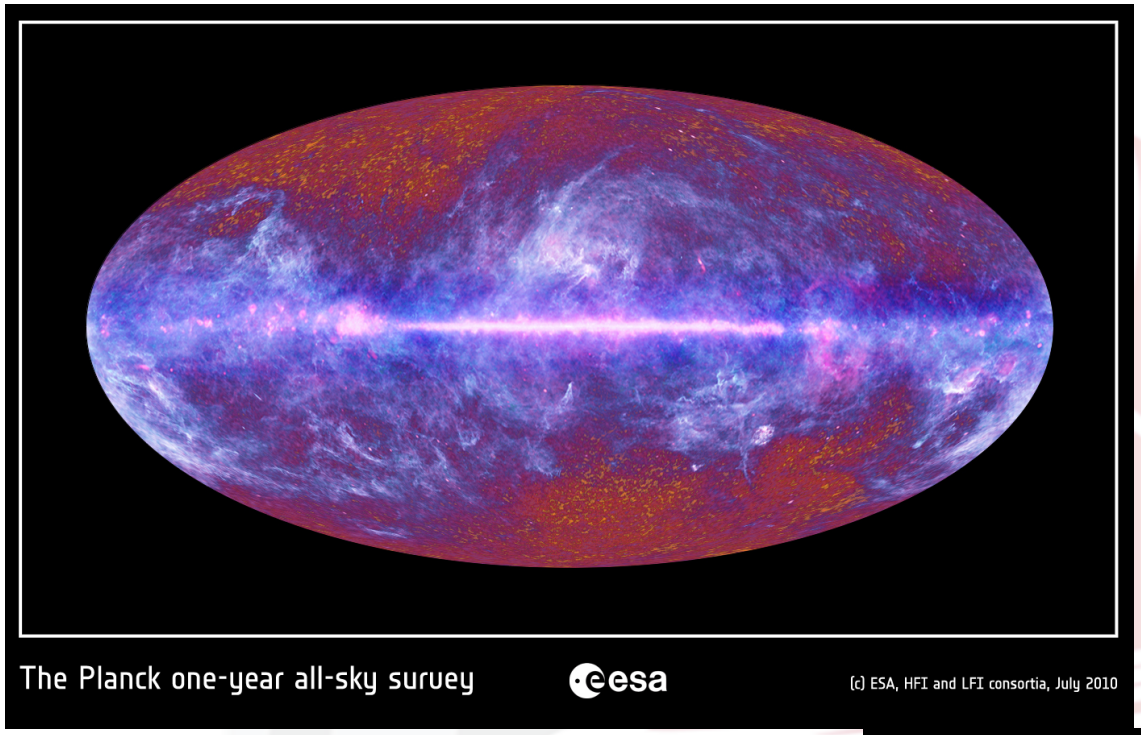

← *View of the sky diffuse emission with Planck*

View of the → sky compact sources with Planck

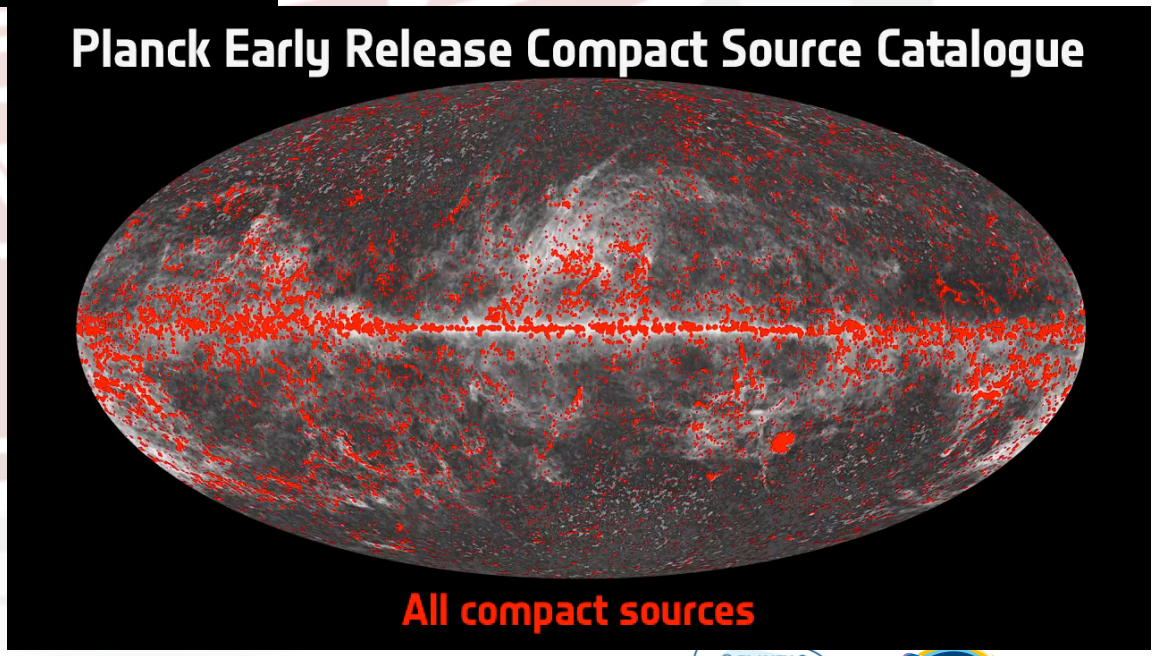

Planck Early Results Papers A&A 536, Dec 2011

These papers are produced by the Planck Collaboration, and are based on data acquired by Planck between 13 August 2009 and 6 June 2010. This set of papers describes the scientific performance of the Planck payload, and presents results on a variety of astrophysical topics related to the sources included in the ERCSC, as well as selected topics on difuse emission. The papers are available online, and links to each are provided below. If you use any of these results for presentations, please acknowledge the corresponding paper, ESA/Planck, and the Planck Collaboration.

Title	Authors	Publication
Planck early results. I. The Planck mission	Planck Collaboration	2011 A&A 536, A1
Planck early results. II. The thermal performance of Planck	Planck Collaboration	2011 A&A 536, A2
Planck early results. III. First assessment of the Low Frequency Instrument in-flight performance	Mennella et al.	2011 A&A 536, A3
Planck early results. IV. First assessment of the High Frequency Instrument in-flight performance	Planck HFI Core Team	2011 A&A 536, A4
Planck early results. V. The Low Frequency Instrument data processing	Zacchei et al.	2011 A&A 536, A5
Planck early results. VI. The High Frequency Instrument data processing	Planck HFI Core Team	2011 A&A 536, A6
Planck early results. VII. The Early Release Compact Source Catalogue	Planck Collaboration	2011 A&A 536, A7
The Explanatory Supplement to the Planck Early Release Compact Source Catalogue	Planck Collaboration	2011 ESA
Planck early results. VIII. The all-sky early Sunyaev-Zeldovich cluster sample	Planck Collaboration	2011 A&A 536, A8
Planck early results. IX. XMM-Newton follow-up for validation of Planck cluster candidates	Planck Collaboration	2011 A&A 536, A9
Planck early results. X. Statistical analysis of Sunyaev-Zeldovich scaling relations for X-ray galaxy clusters	Planck Collaboration	2011 A&A 536, A10
Planck early results. XI. Calibration of the local galaxy cluster Sunyaev-Zeldovich scaling relations	Planck Collaboration	2011 A&A 536, A11
Planck early results. XII. Cluster Sunyaev-Zeldovich optical scaling relations	Planck Collaboration	2011 A&A 536, A12
Planck early results. XIII. Statistical properties of extragalactic radio sources in the Planck Early Release Compact Source Catalogue	Planck Collaboration	2011 A&A 536, A13
Planck early results. XIV. ERCSC validation and extreme radio sources	Planck Collaboration	2011 A&A 536, A14
Planck early results. XV. Spectral energy distributions and radio continuum spectra of northern extragalactic radio sources	Planck Collaboration	2011 A&A 536, A15
Planck early results. XVI. The Planck view of nearby galaxies	Planck Collaboration	2011 A&A 536, A16
Planck early results. XVII. Origin of the submillimetre excess dust emission in the Magellanic Clouds	Planck Collaboration	2011 A&A 536, A17
Planck early results. XVIII. The power spectrum of cosmic infrared background anisotropies	Planck Collaboration	2011 A&A 536, A18
Planck early results. XIX. All-sky temperature and dust optical depth from Planck and IRAS – constraints on the "dark gas" in our Galaxy	Planck Collaboration	2011 A&A 536, A19
Planck early results. XX. New light on anomalous microwave emission from spinning dust grains	Planck Collaboration	2011 A&A 536, A20
Planck early results. XXI. Properties of the interstellar medium in the Galactic plane	Planck Collaboration	2011 A&A 536, A21
Planck early results. XXII. The submillimetre properties of a sample of Galactic cold clumps	Planck Collaboration	2011 A&A 536, A22
Planck early results. XXIII. The first all-sky survey of Galactic cold clumps	Planck Collaboration	2011 A&A 536, A23
Planck early results. XXIV. Dust in the diffuse interstellar medium and the Galactic halo	Planck Collaboration	2011 A&A 536, A24
Planck early results. XXV. Thermal dust in nearby molecular clouds	Planck Collaboration	2011 A&A 536, A25
Planck early results. XXVI. Detection with Planck and confirmation by XMM-Newton of PLCK G266.6-27.3, an exceptionally X-ray luminous and massive galaxy cluster at z~1	Planck Collaboration	2011 A&A 536, A26
Simultaneous Planck, Swift, and Fermi observations of X-ray and gamma-ray selected blazars	Giommi et al.	2012 A&A 541, A160

Current/Next steps

- Intermediate results have been produced almost continuously during 2011/12, with a “first presentation” already done at February 2012 in occasion of the *Planck 2012 Conference in Bologna CNR Area* "***Astrophysics from radio to sub-millimeter wavelengths: the Planck view and other experiments***”

  (Feb 13-17) and then again continuously during 2012 and later.

❖ Planck Intermediate Results. I. Further validation of new Planck clusters with XMM-Newton, arXiv1112.5595P, A&A 543 A102 (2012)

- 2013 – delivery of Planck products & release of cosmological papers based on the first 15 months of data.
- Astrophysical papers will be roughly divided into two wide categories: those mainly based only total intensity data and those requiring well established polarization data; this (but not only of course!) will reflect into readiness/ submission period.

Planck Collaboration "behaviour"

- All papers are/will be reviewed by the (*Planck* Internal) Editorial Board & the *Planck* Science Team.

- Astrophysical projects are carried out by dedicated project teams in the context of *Planck* Working Groups (5 – clusters & secondary anisotropies – 6 – extragalactic sources – 7 – Galactic & solar system science).

- Each project team will prepare one or (typically) more papers.

- We expect several tens of papers in 2012/13.

Planck Intermediate Results Papers

Mid 2012

Intermediate astrophysics results are now being presented in a series of papers based on data taken between 13 August 2009 and 27 November 2010. These recent results are produced by the Planck Collaboration. The papers are available online, and links to each are provided below. If you use any of these results for presentations, please acknowledge the corresponding paper, ESA/Planck, and the Planck Collaboration.

Evolving picture ☺

Title	Authors	Publication
Planck intermediate results. I. Further validation of new Planck clusters with XMM-Newton	Planck Collaboration	2012 A&A 543, A102
Planck intermediate results. II. Comparison of Sunyaev-Zeldovich measurements from Planck and from the Arcminute Microkelvin Imager for 11 galaxy clusters	Planck and AMI Collaborations	2012 Submitted to A&A
Planck intermediate results. III. The relation between galaxy cluster mass and Sunyaev-Zeldovich signal	Planck Collaboration	2012 Submitted to A&A
Planck intermediate results. IV. The XMM-Newton validation programme for new Planck clusters	Planck Collaboration	2012 Submitted to A&A
Planck intermediate results. V. Pressure profiles of galaxy clusters from the Sunyaev-Zeldovich effect	Planck Collaboration	2012 Submitted to A&A
Planck intermediate results. VI: The dynamical structure of PLCKG214.6+37.0, a Planck discovered triple system of galaxy clusters	Planck Collaboration	2012 Submitted to A&A
Planck intermediate results. VII. Statistical properties of infrared and radio extragalactic sources from the Planck Early Release Compact Source Catalogue at frequencies between 100 and 857 GHz	Planck Collaboration	2012 Submitted to A&A

ASTROPHYSICS FROM THE RADIO TO THE SUB-MILLIMETRE

PLANCK AND OTHER EXPERIMENTS IN TEMPERATURE AND POLARIZATION

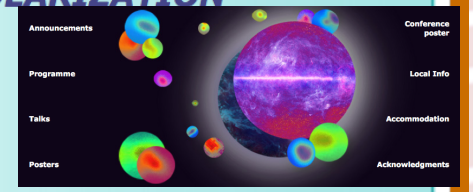

The Conference will focus on the astrophysical sky as seen by Planck and other observatories, and on the potential of Planck astrophysical data and science, including the most recent Planck results. It will include reviews of the state of the art in these areas, and presentation sessions on Galactic and extragalactic science from the radio to the submillimetre (diffuse emission, sources, galaxy clusters, cosmic infrared background, etc.).

The Conference is based on invited plus contributed talks. There will be also a poster session.
A public exhibition with media and public lectures suitable for a general audience will be organized in the context of the Conference.

Bologna, Italy
Area della Ricerca del CNR
February 13th-17th, 2012

Scientific Organizing Committee

Nazzareno Mandolesi (chair)
John Bally
Marco Bersanelli
J. Richard Bond
François R. Bouchet
Carlo Burigana
Richard Davis
George Efstathiou
Paul F. Goldsmith
Matt J. Griffin
Richard E. Hills
Ernst Kreysa
Anne Lähteenmäki
Jean-Michel Lamarre
Charles R. Lawrence
Giuseppe Malaguti
Peter G. Martin
Hans-Ulrik Norgaard-Nielsen
Lyman A. Page
Jean-Loup Puget
Douglas Scott
Rashid A. Sunyaev
Jan A. Tauber
Leonardo Testi
Simon D. M. White
Andrea Zacchei

Local Organizing Committee

Carlo Burigana (chair)
Benedetta Cappellini
Fabio Finelli
Enrico Franceschi
Marco Malaspina
Daniela Paoletti
Sara Ricciardi
Manuela Spiga
Luca Valenziano
Elvio Velardo

Plus already more than 55 non Planck Collaboration Papers which make use of public Planck data

First Planck CMB temperature results: Feb 2013

First Planck CMB polarization results: March 2014

ERCSC papers, A&A 536

- Planck Early Results: The Early Release Compact Source Catalogue 1101.2041
- The Explanatory Supplement to the Planck Early Release Compact Source Catalogue, Planck Collaboration 2011 ESA,

  available @ Planck esa web site http://www.rssd.esa.int/Planck

❖ Revised ERCSC: On 31 Jan 2012, ESA and the Planck Collaboration have released a revised version of the ERCSC

❖ In this new version, some quantities have been updated although there is no change in the number of sources and their flux compared to the previous version of the catalogue

❖ Explanatory Supplement - Version: 6 February 2012

❖ The Early Release Compact Source Catalogue v1.3 can be accessed by the world-wide community from

❖ Planck Legacy Archive

http://www.sciops.esa.int/index.php?project=planck&page=Planck_Legacy_Archive

The Planck ERCSC in brief

Notes. [a] The precise beam values are presented in Planck Collaboration (2011e) and Planck Collaboration (2011f). This table shows the values which were adopted for the ERCSC. [b] Flux density of the median $>10\sigma$ source at $|b| > 30°$ in the ERCSC where σ is the photometric uncertainty of the source. [c] Flux density of the faintest $>10\sigma$ source at $|b| > 30°$ in the ERCSC. [d] Faintest source at $|b| > 30°$ in the ERCSC.

Freq [GHz]	30	44	70	100	143	217	353	545	857
$\lambda(\mu m)$	10000	6818	4286	3000	2098	1382	850	550	350
Sky Coverage (%)	99.96	99.98	99.99	99.97	99.82	99.88	99.88	99.80	99.79
Beam FWHM (′)[a]	32.65	27.00	13.01	9.94	7.04	4.66	4.41	4.47	4.23
# of Sources	705	452	599	1381	1764	5470	6984	7223	8988
# of $\|b\| > 30°$ Sources	307	143	157	332	420	691	1123	2535	4513
$10\sigma^b$ (mJy)	1173	2286	2250	1061	750	807	1613	2074	2961
$10\sigma^c$ (mJy)	487	1023	673	500	328	280	249	471	813
Flux Density Limit[d] (mJy)	480	585	481	344	206	183	198	381	655

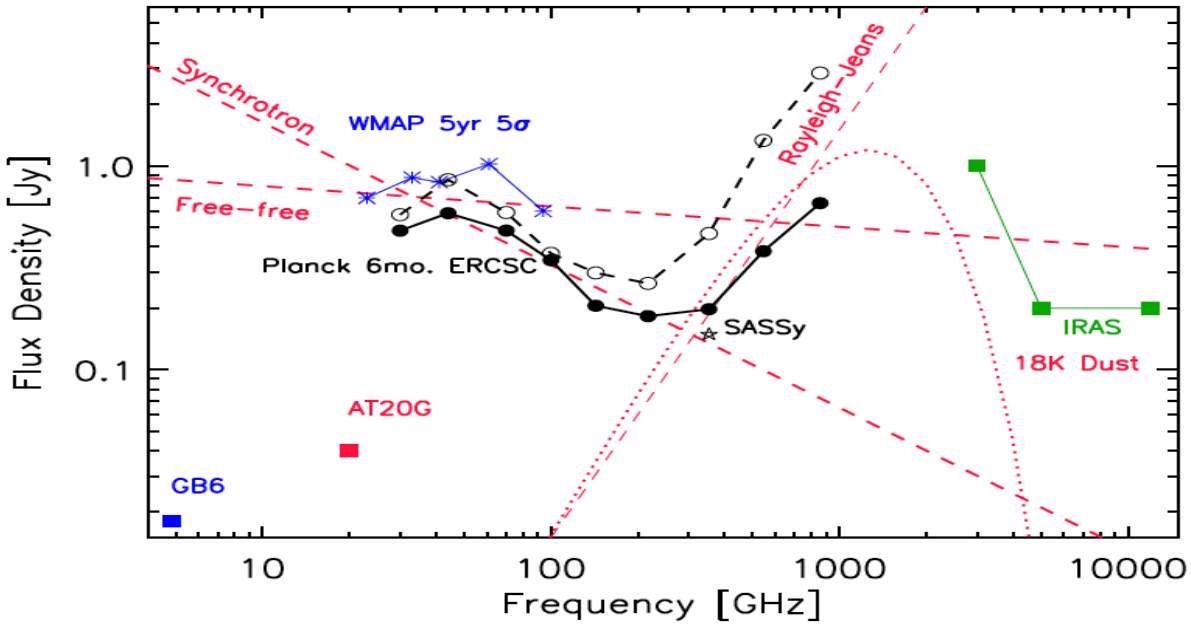

Table 2. ERCSC Catalogue Columns

Column Name	Description
	Identification
NAME	Source name
FLUX	Flux density (mJy)
FLUX_ERR	Flux density error (mJy)
CMBSUBTRACT	Flag indicating detection of source in CMB subtracted maps
EXTENDED	Flag indicating that source is extended
DATESOBS	UTC dates at which this source was observed
NUMOBS	Number of days this source observed
CIRRUS	Cirrus flag based on 857 GHz source counts
	Source Position
GLON	Galactic longitude (deg) based on extraction algorithm
GLAT	Galactic latitude (deg) based on extraction algorithm
POS_ERR	Standard deviation of positional offsets for sources with this SNR (arcminute)
RA	Right Ascension (J2000) in degrees transformed from (GLON,GLAT)
DEC	Declination (J2000) in degrees transformed from (GLON,GLAT)
	Effective beam
BEAM_FWHMMAJ	Elliptical Gaussian beam FWHM along major axis (arcmin)
BEAM_FWHMMIN	Elliptical Gaussian beam FWHM along minor axis (arcmin)
BEAM_THETA	Orientation of Elliptical Gaussian major axis (measured East of Galactic North)
	Morphology
ELONGATION	Ratio of major to minor axis lengths
	Source Extraction Results
FLUXDET	Flux density of source as determined by detection method (mJy)
FLUXDET_ERR	Uncertainty (1 sigma) of FLUXDET (mJy)
MX1	First moment in X (arcmin)
MY1	First moment in Y (arcmin)
MX2	Second moment in X ($arcmin^2$)
MXY	Cross moment in X and Y ($arcmin^2$)
MY2	Second moment in Y ($arcmin^2$)
PSFFLUX	Flux density of source as determined from PSF fitting (mJy)
PSFFLUX_ERR	Uncertainty (1 sigma) of PSFFLUX (mJy)
GAUFLUX	Flux density of source as determined from 2-D Gaussian fitting (mJy)
GAUFLUX_ERR	Uncertainty (1 sigma) of GAUFLUX (mJy)
GAU_FWHMMAJ	Gaussian fit FWHM along major axis (arcmin)
GAU_FWHMMIN	Gaussian fit FWHM along minor axis (arcmin)
GAU_THETA	Orientation of Gaussian fit major axis
	Quality Assurance
RELIABILITY	Fraction of MC sources that are matched and have photometric errors < 30%
RELIABILITY_ERR	Uncertainty (1 sigma) in reliabiliy based on Poisson statistics
MCQA_FLUX_ERR	Standard deviation of photometric error for sources with this SNR
MCQA_FLUX_BIAS	Median photometric error for sources with this SNR
BACKGROUND_RMS	Background point source RMS obtained from threshold maps (mJy)
	Bandfilling (857 GHz catalog only)
BANDFILL217	217 GHz Aperture Photometry Flux Density at 857 GHz Source Position (mJy)
BANDFILL217_ERR	Uncertainty in BANDFILL217
BANDFILL353	353 GHz Aperture Photometry Flux Density at 857 GHz Source Position (mJy)
BANDFILL353_ERR	Uncertainty in BANDFILL353
BANDFILL545	545 GHz Aperture Photometry Flux Density at 857 GHz Source Position (mJy)
BANDFILL54_SERR	Uncertainty in BANDFILL545

ERCSC_f030.fits
ERCSC_f044.fits
ERCSC_f070.fits
ERCSC_f100.fits
ERCSC_f143.fits
ERCSC_f217.fits
ERCSC_f353.fits
ERCSC_f545.fits
ERCSC_f857.fits

ESZ.fits
ECC.fits

Table 6. ESZ Catalogue Columns

Keyword	Type
INDEX	Index of clusters i.e., 1, 2, 3...
NAME	*Planck* name of cluster candidate
GLON	Galactic Longitude from *Planck* (deg)
GLAT	Galactic Latitude from *Planck* (deg)
RA	Right Ascension (deg) from *Planck* (J2000)
DEC	Declination (deg) from *Planck* (J2000)
SNR	Signal-to-noise ratio returned by the matched multi-filter (MMF3)
ID	External identifier of cluster e.g., Coma, Abell etc.
REDSHIFT	Redshift of cluster from the MCXC X-ray cluster compilation (Piffaretti et al. 2010) unless stated otherwise in the notes
GLON_X	Galactic Longitude of the associated X-ray cluster (deg)
GLAT_X	Galactic Latitude of the associated X-ray cluster (deg)
RA_X	Right Ascension (deg) of the associated X-ray cluster (J2000)
DEC_X	Declination (deg) of the associated X-ray cluster (J2000)
THETA_X	Angular size (arcmin) at 5R500 from X-ray data.
Y_PSX	Integrated Compton-Y ($arcmin^2$) at X-ray position and within 5R500 (THETA_X)
Y_PSX_ERR	Uncertainty in Y_PSX
THETA	Estimated angular size (arcmin) from matched multi-filter (MMF3)
THETA_ERR	Uncertainty in THETA
Y	Integrated Compton-Y ($arcmin^2$) at *Planck* position and within THETA from matched multi-filter (MMF3)
Y_ERR	Uncertainty in Y

Table 7. ECC Catalogue Columns

Keyword	Type
NAME	Source name
SNR	Signal to Noise ratio of detection
GLON	Galactic longitude (deg) based on bandmerge algorithm
GLAT	Galactic latitude (deg) based on bandmerge algorithm
RA	Right Ascension in degrees (J2000)
DEC	Declination in degrees (J2000)
APFLUX353	Aperture flux density at 353 GHz (mJy)
APFLUX545	Aperture flux density at 545 GHz (mJy)
APFLUX857	Aperture flux density at 857 GHz (mJy)
APFLUX3000	Aperture flux density at 3000 GHz (mJy)
APFLUX353_ERR	Uncertainty (1 sigma) in APFLUX353
APFLUX545_ERR	Uncertainty (1 sigma) in APFLUX545
APFLUX857_ERR	Uncertainty (1 sigma) in APFLUX857
APFLUX3000_ERR	Uncertainty (1 sigma) in APFLUX3000
TEMPERATURE	Temperature from greybody fit (K)
BETA	Emissivity index from greybody fit
S857	Flux density at 857 GHz from greybody fit (mJy)
TEMPERATURE_ERR	Uncertainty (1 sigma) in TEMPERATURE (K)
BETA_ERR	Uncertainty (1 sigma) in BETA
S857_ERR	Uncertainty (1 sigma) in S857
BESTNORM	Summed squared residuals for best fit (mJy^2)
TEMPERATURE_CORE	Core Temperature from greybody fit to cold residual emission (K)
BETA_CORE	Emissivity index from greybody fit to cold residual emission
MAJ_AXIS_FWHM_CORE	Ellipse major axis of cold residual emission (arcmin)
MIN_AXIS_FWHM_CORE	Ellipse minor axis of cold residual emission (arcmin)
TEMPERATURE_CORE_ERR	Uncertainty (1 sigma) TEMPERATURE_CORE (K)
BETA_CORE_ERR	Uncertainty (1 sigma) BETA_CORE
MAJ_AXIS_FWHM_CORE_ERR	Uncertainty (1 sigma) MAJ_AXIS_FWHM_CORE
MIN_AXIS_FWHM_CORE_ERR	Uncertainty (1 sigma) MIN_AXIS_FWHM_CORE

Planck Early Release Compact Source Catalogue

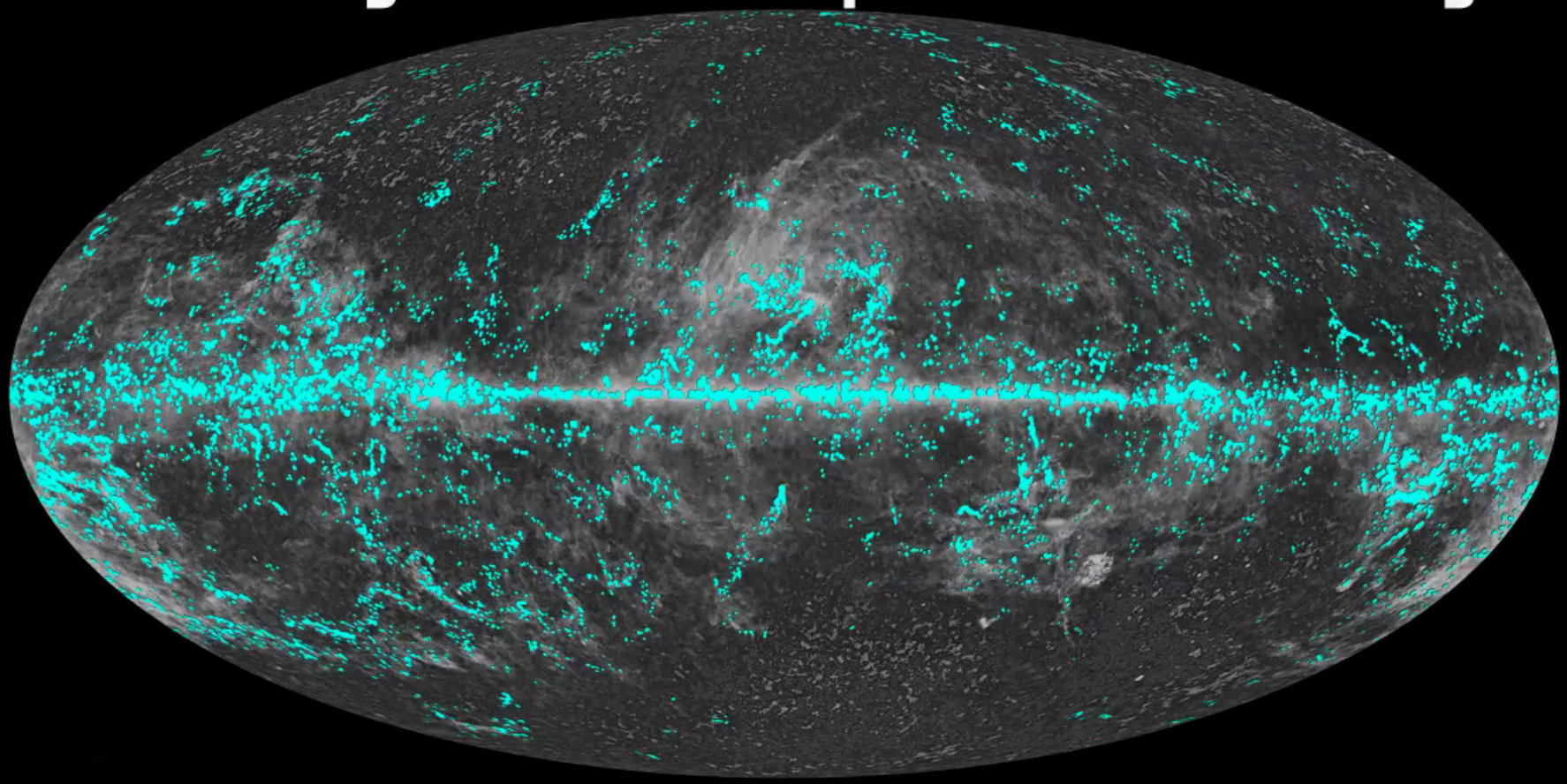

Galactic sources

Planck Early Release Compact Source Catalogue

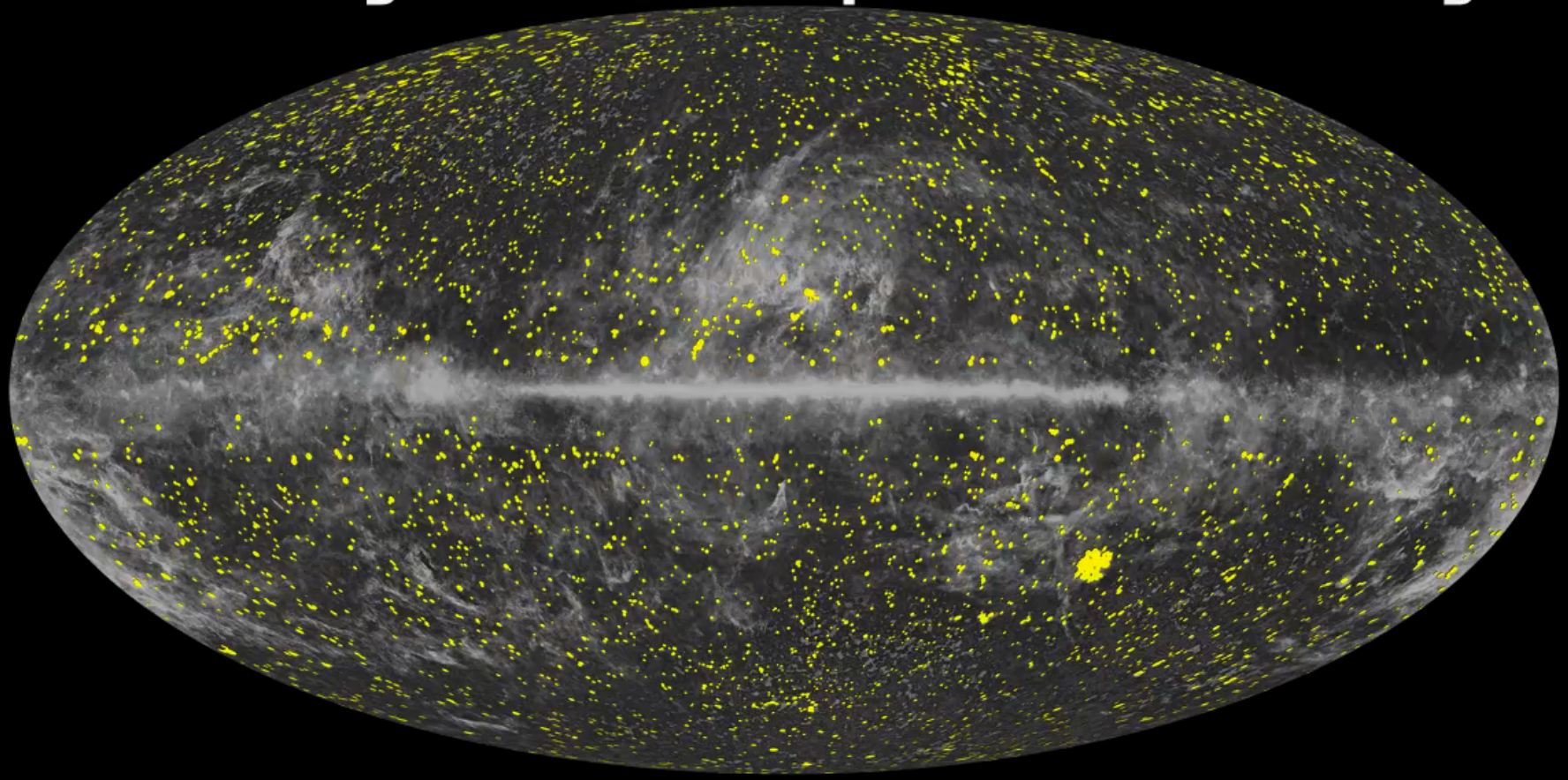

Extragalactic sources

Planck Early Release Compact Source Catalogue

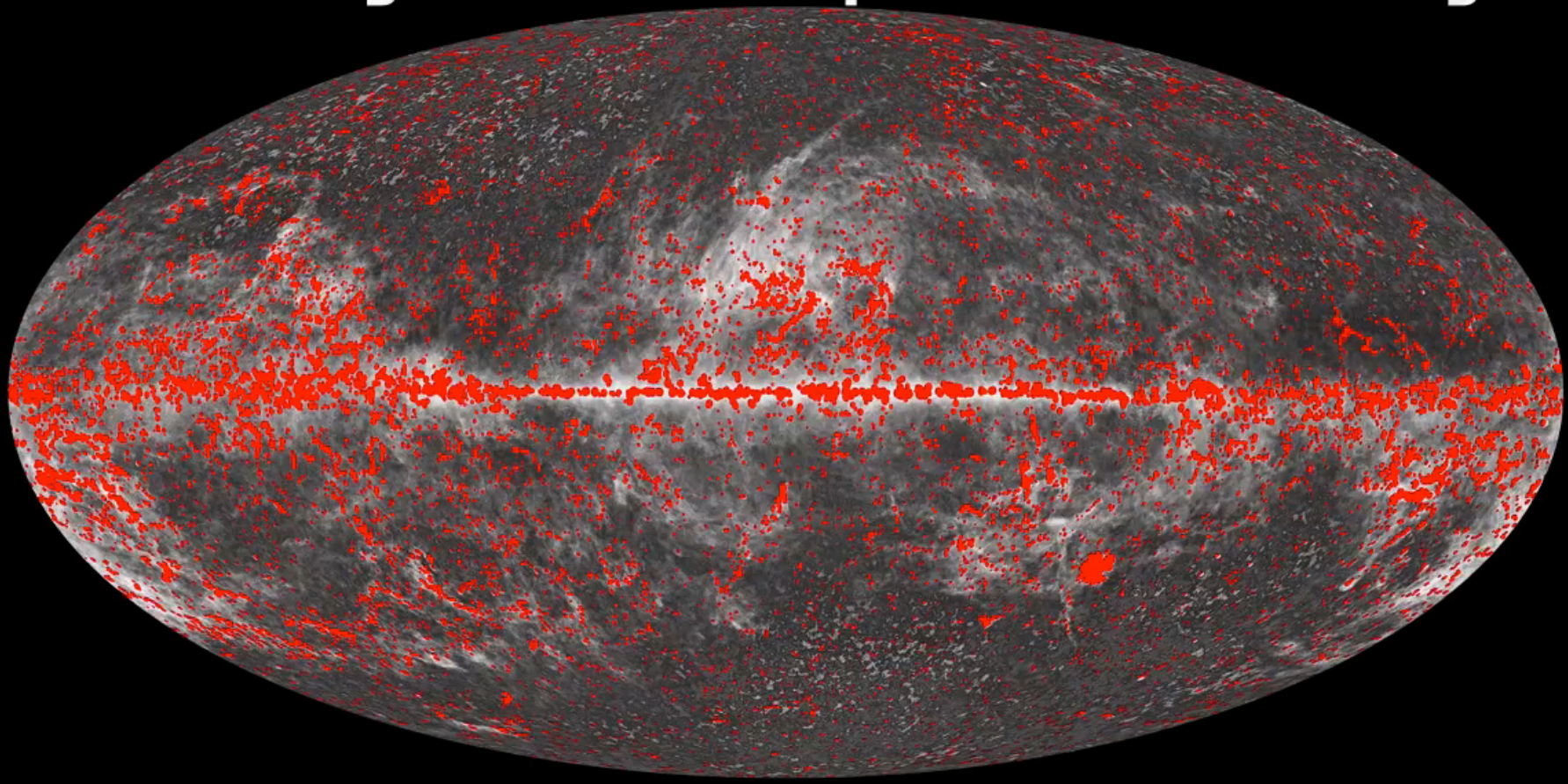

All compact sources

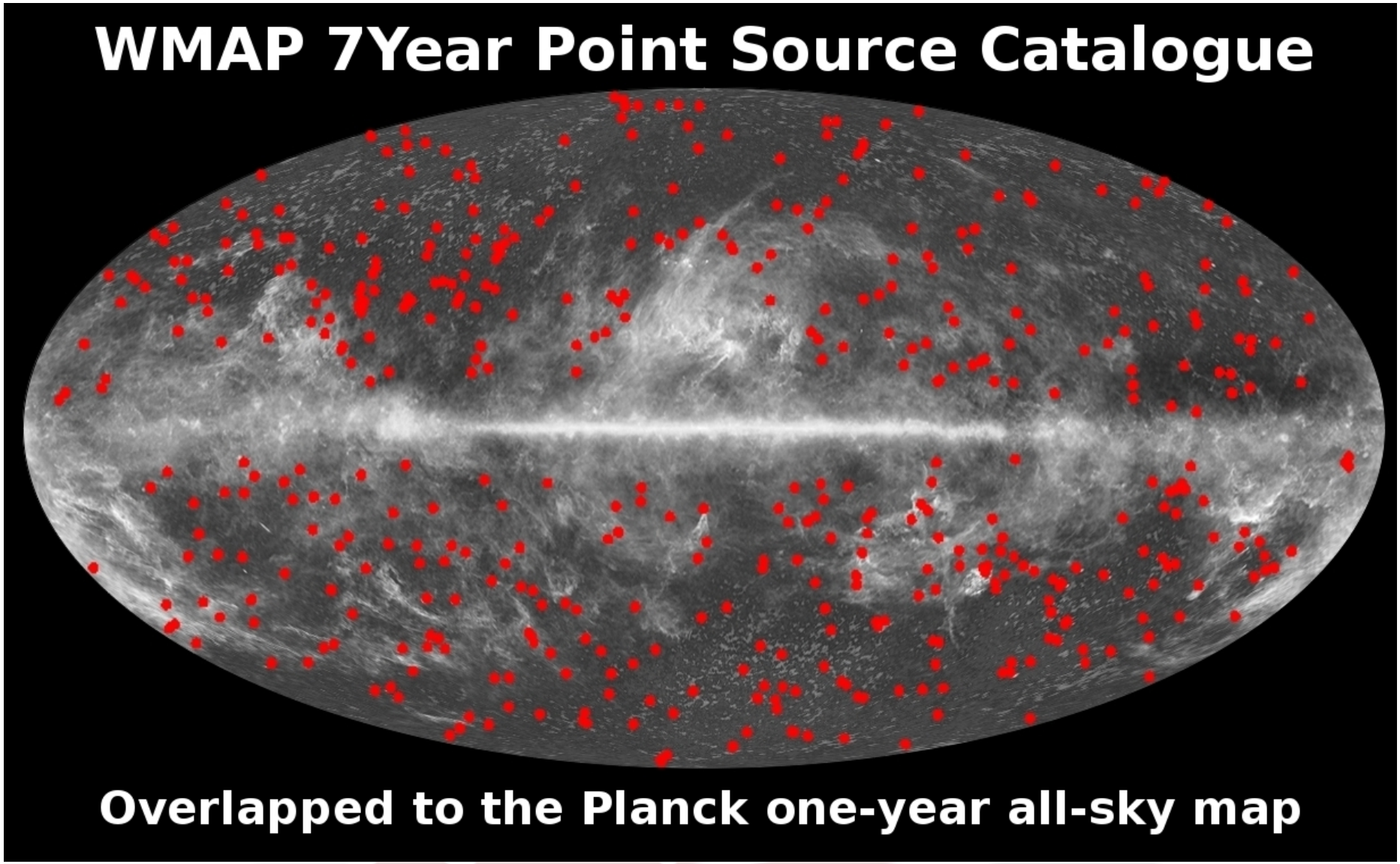
WMAP 7Year Point Source Catalogue
Overlapped to the Planck one-year all-sky map

Clusters (WG5)

Sunyaev-Zeldovich effect: basics

It is a secondary anisotropy predicted in 1972 due to inverse Compton Scattering between CMB photons (~0.3 meV) and free electrons (~ few KeV) of the hot Intra-Cluster Medium. CMB photons acquire energy!

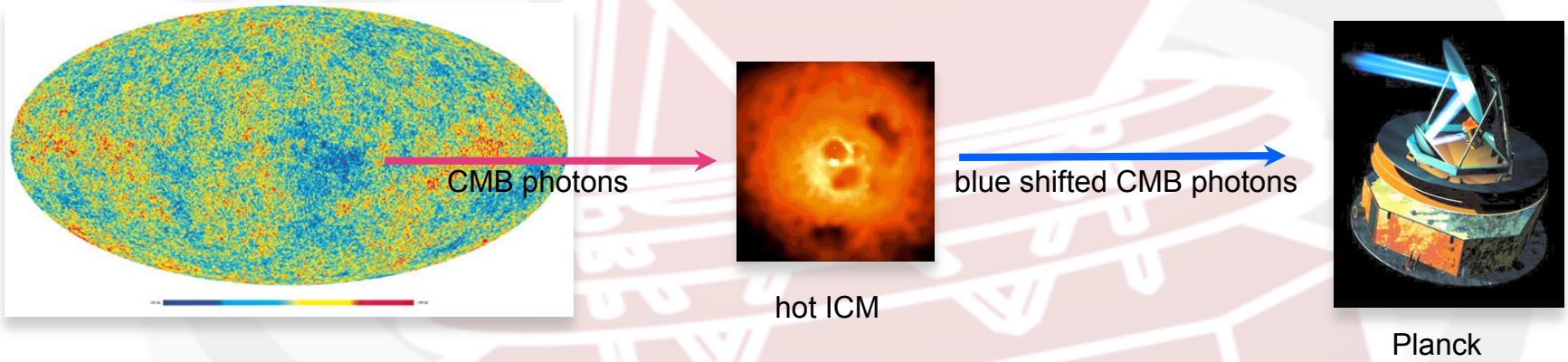

- Thermal SZ : CMB photons are scattered by random motion of thermal electrons
- Kinetic SZ : CMB photons are scattered by bulk motion of electrons

Sunyaev-Zeldovich effect: properties

$$\frac{\Delta T_{SZ}}{T_{CMB}} = f(x)\, y$$

$$y = \int_{los} n_e \sigma_T \frac{kT_e}{m_e c^2} d\ell$$ y-Compton parameter

$f(x)$ provides the frequency dependence $x = \frac{h\nu}{kT_{CMB}}$

$$Y = \int_{cluster} y\, d\Omega \qquad Y\, D_A^2 = \frac{\sigma_T}{m_e c^2} \int P\, dV$$

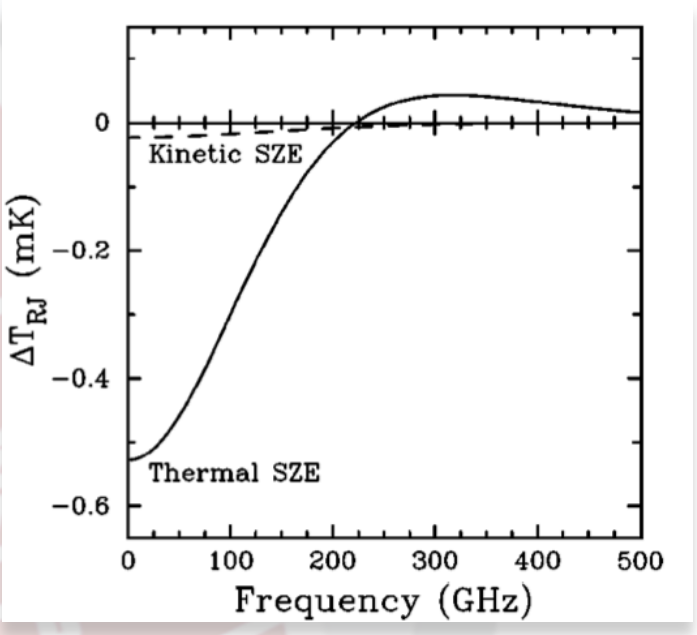

Carlstrom, Holder and Reese 2002

- SZ effect does not depend on z;
- y-Compton gives the amplitude of the effect (~ 1 mK)
- SZ vanishes for ~217 GHz (signature of the effect; one of the Planck channels is centered @ 217 GHz specifically to identify the zero transition of TSZ);
- Y is the integrated Compton that is proportional to the temperature-weighted mass of the cluster divided by the angular diameter distance D_A which is the only term depending on z (weakly). This is an useful relation for extracting cosmological information (that are in D_A) when combined with other observations (X-ray typically).

The Early SZ (ESZ) cluster sample from Planck

ESZ is made of 189 SZ clusters or candidates detected over the whole sky during the first ten months of CMB temperature observation.

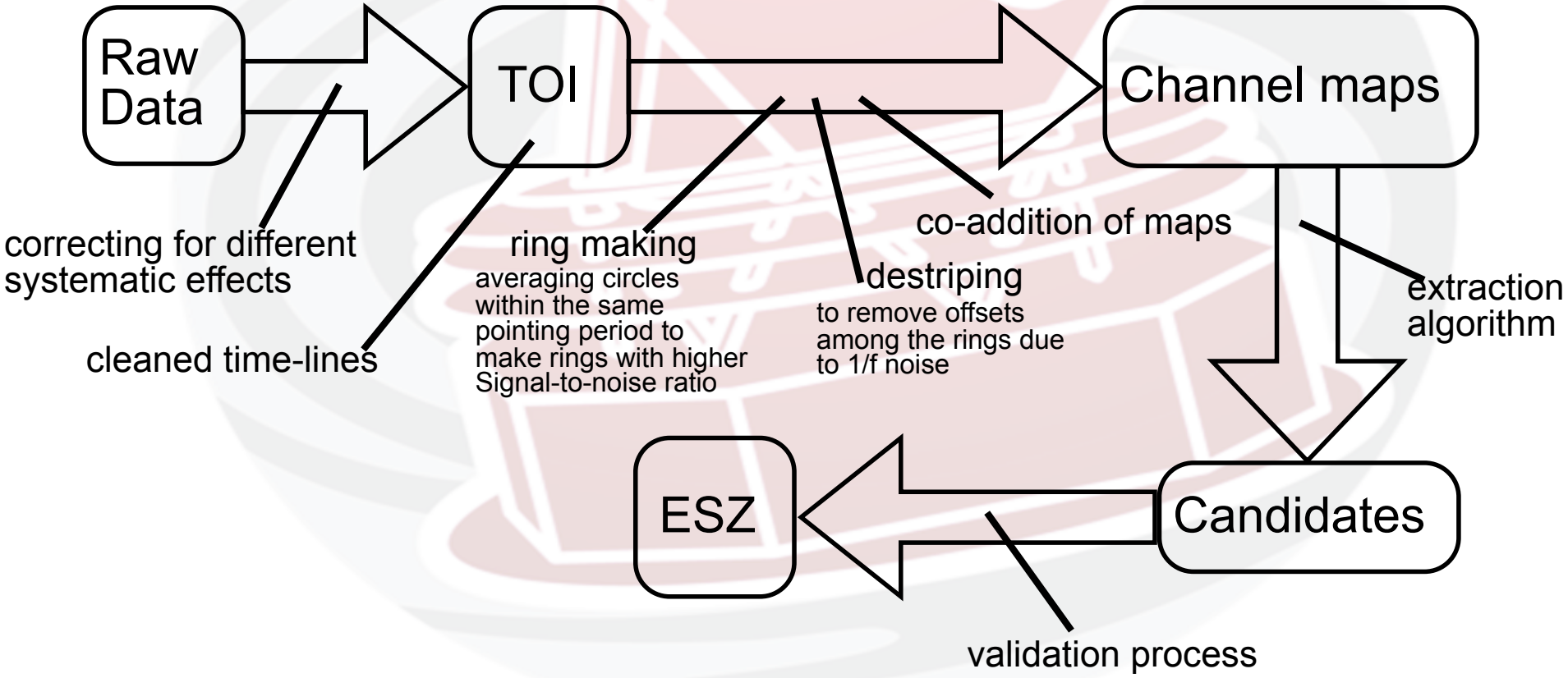

SZ Detection in *Planck*

Several slides comes from courtesy of M. Douspis

multi-matched filter

(MMF, *Melin et al. 09*)

- Uses known EM spectrum
  - SZ without relativistic effect
- Use known spatial profile
  - Universal spherical profile from X-rays observations

- Applied on the full sky

  → candidates list

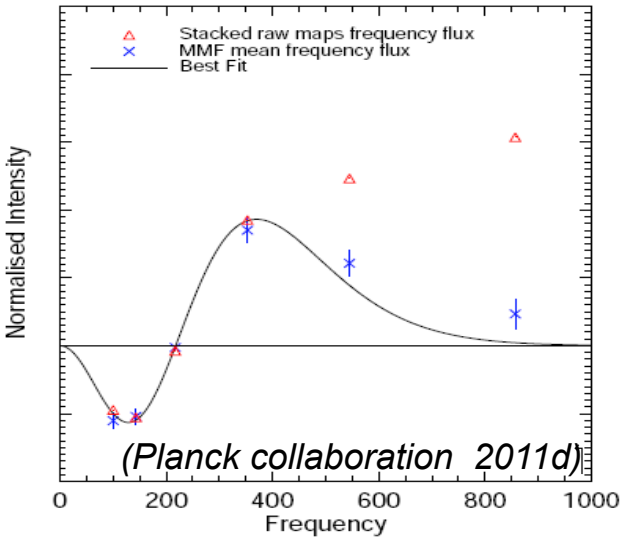

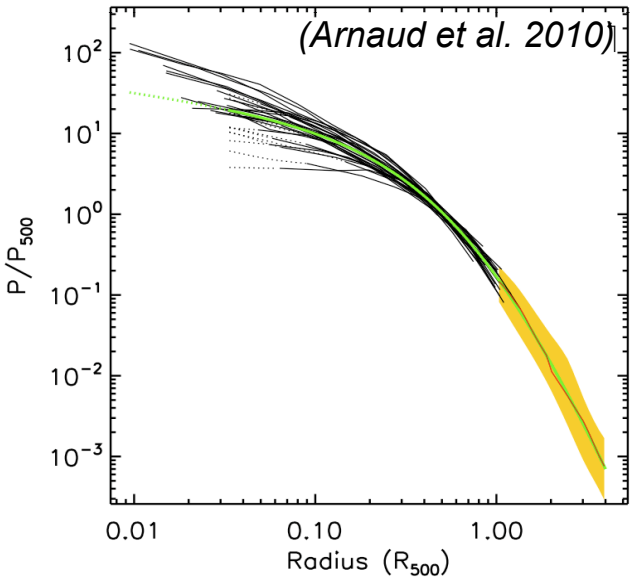

Validation of candidates

Cross-checks in *Planck* (CC, SSO)

Cross-correlation with existing catalogues

Search in logs & databases

Search in data (RASS, SDSS)

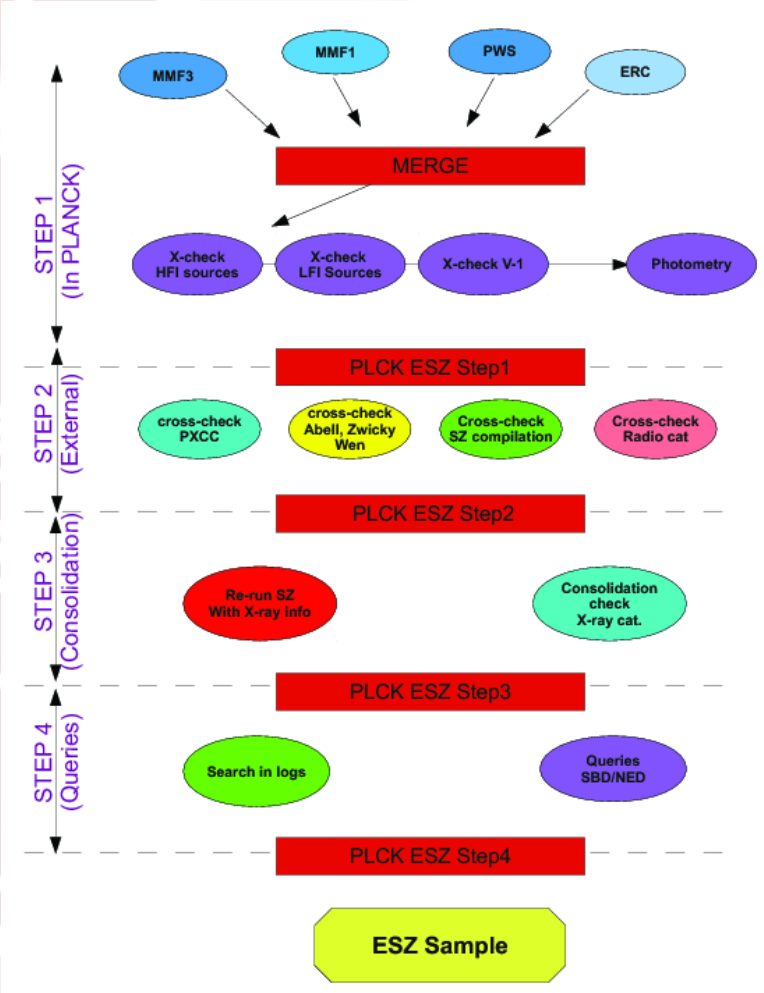

Confirmation of clusters

- In optical (ENO/INT-WHT-TNG, ESO/MPG-NTT RTT, NOT, NOAO,...) + *redshift*

  In SZ (AMI)

  X-rays (XMM) + *redshift*

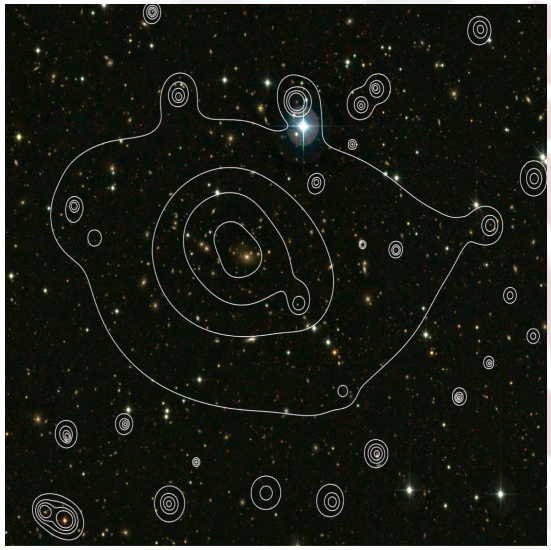

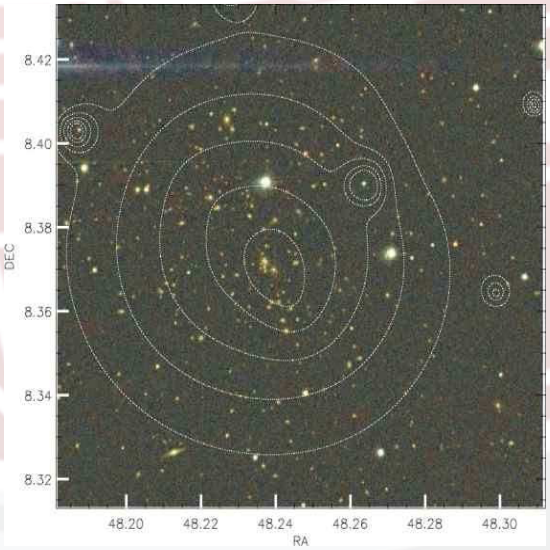

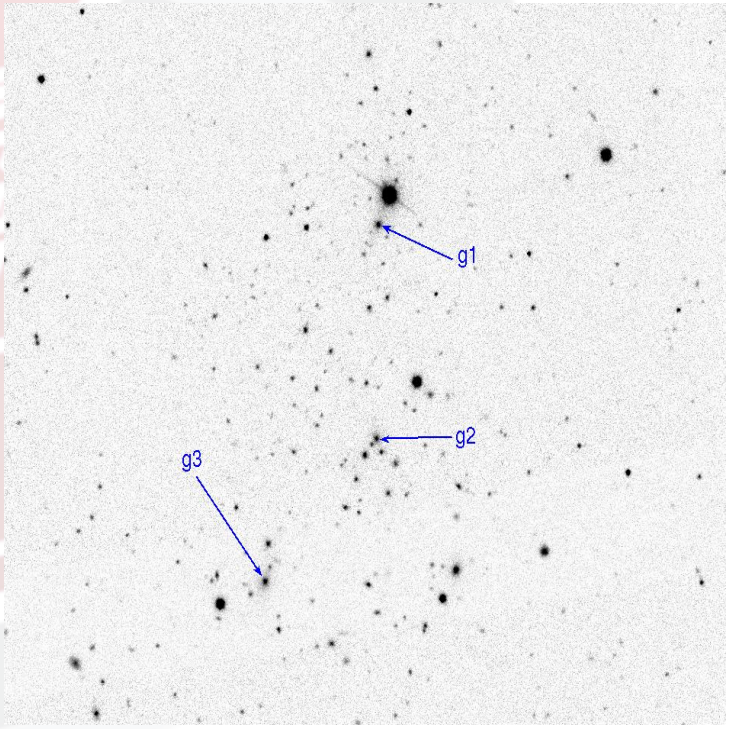

ESO/MPG ENO/IAC80 RTT

Confirmation of clusters

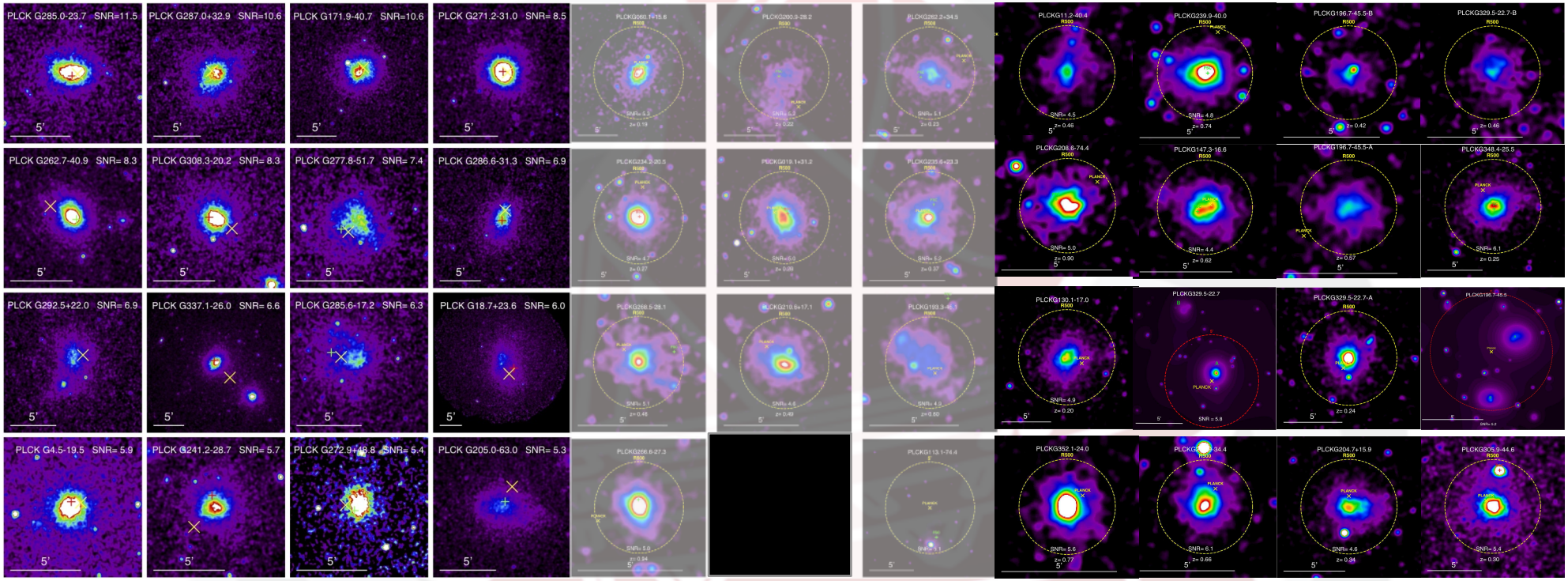

XMM-Newton DDT program

- short snapshot exposures (10ksec)
- high success rate (>85%)
- 43 *Planck* SZ candidates confirmed
- 51 new clusters confirmed with XMM-Newton
- ~ 14% of multiple systems

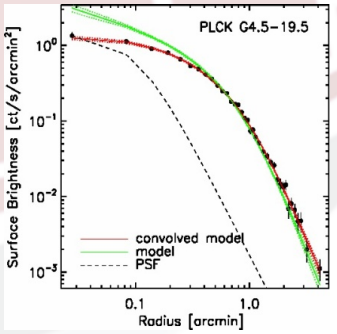

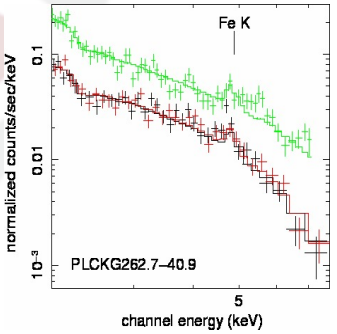

The *Planck* ESZ

189 clusters with S/N>6 (b>14deg)

- 169 known in X+optical+SZ
- 20 new
  - 11 confirmed with XMM
  - 9 unconfirmed* (@ 11/01/2011)
    - 7 confirmed by SPT+AMI since

10 New confirmed by XMM @ S/N<6

Since ESZ → 26 new published

Planck Coll., Early 08 & 26, Planck Coll. Intermediate 1 & 4

The ESZ

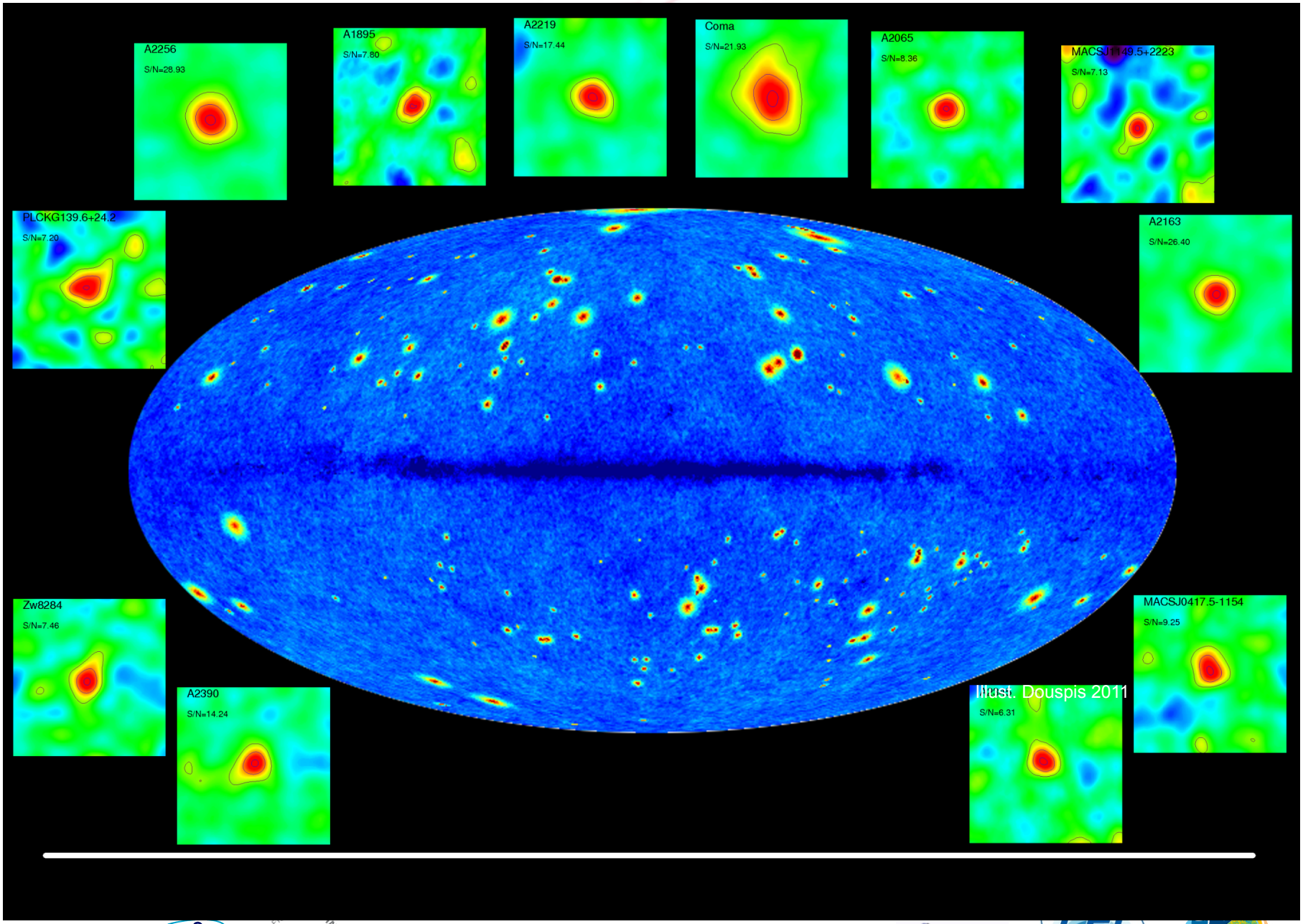
A2256
S/N=28.93
A1895
S/N=7.80
A2219
S/N=17.44
Coma
S/N=21.93
A2065
S/N=8.36
MACSJ1149.5+2223
S/N=7.13
PLCKG139.6+24.2
S/N=7.20
A2163
S/N=26.40
Zw8284
S/N=7.46
A2390
S/N=14.24
Illust. Douspis 2011
S/N=6.31
MACSJ0417.5-1154
S/N=9.25

The Early SZ (ESZ) cluster sample from Planck

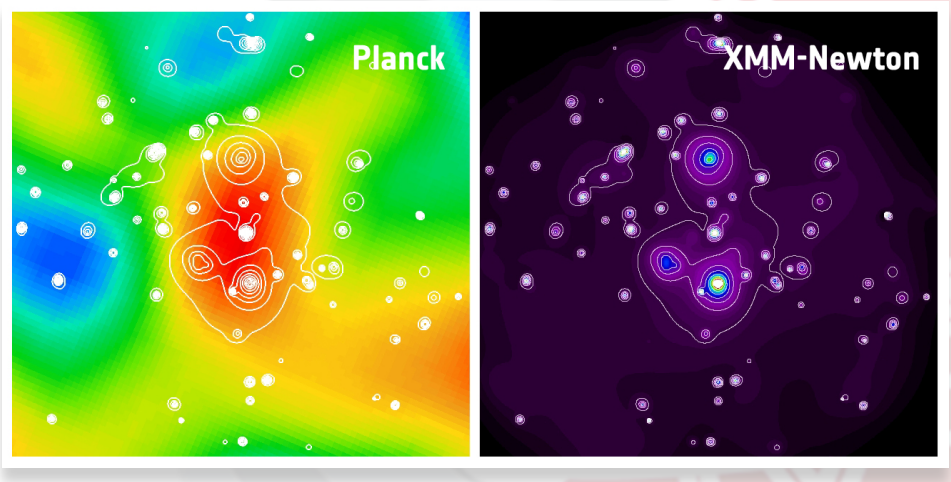

newly discovered supercluster, PLCK G214.6+37,
Planck (left) and XMM-Newton (right panel)

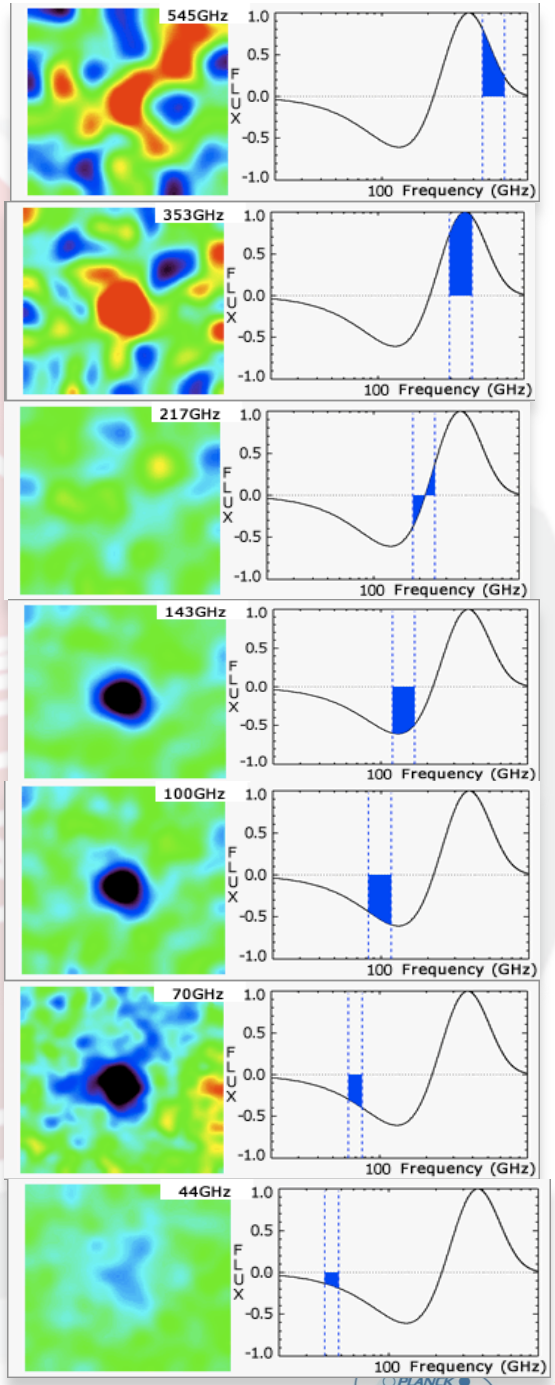

Abell 2319

At the end of the mission it will be delivered the Planck SZ cluster catalogue containing many hundreds of clusters at z~1.

The previous all-sky catalogue is RASS (Rosat All Sky Survey) but at much lower depth (i.e. z~0.1)

ESZ properties

Planck ESZ are relatively close

→ (86% @ z<0.3)

Masses span a decade → 1.5×10^{15} M_{sol}

90% of RASS X-ray clusters with masses $M > 9 \times 10^{14}$ M_{sol} are **blindly** detected by *Planck* and are in the ESZ

25% of new Planck clusters confirmed by XMM have masses $> 9 \times 10^{14}$ M_{sol}.

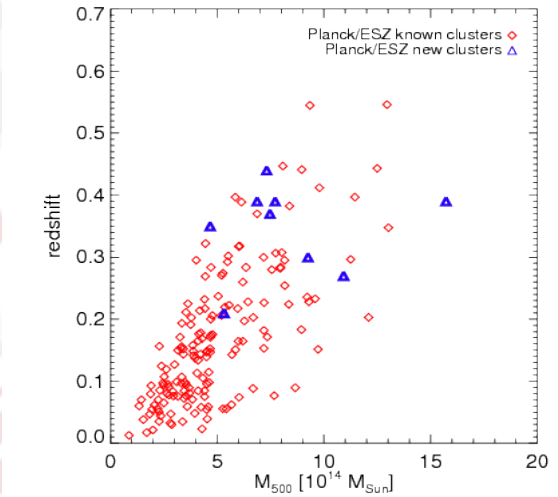

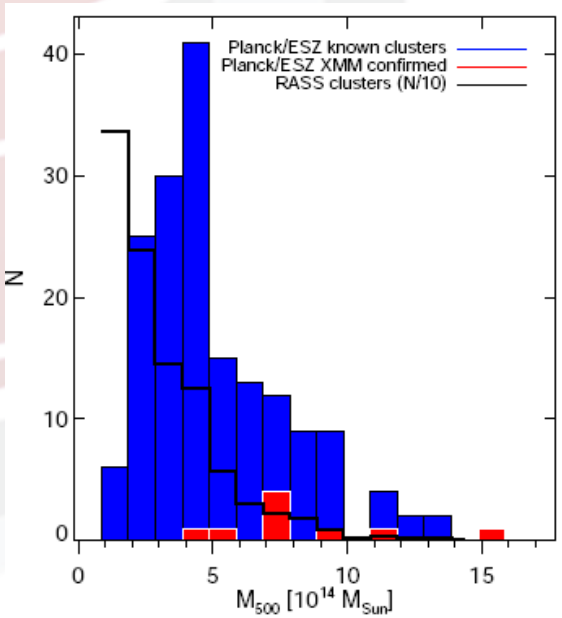

Planck has the unique ability to detect the rarest and most massive clusters on the entire sky

ESZ and other surveys

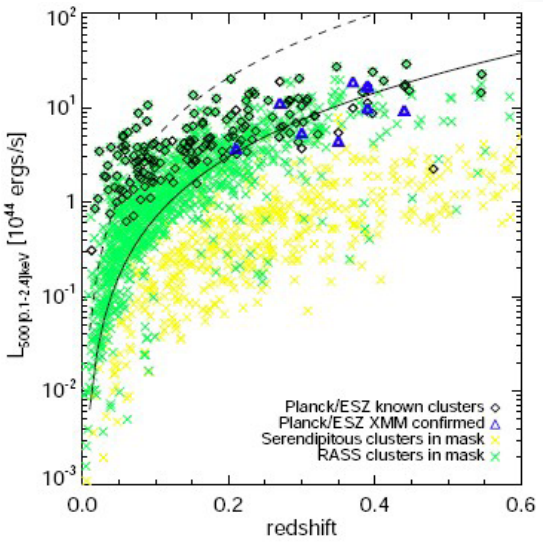

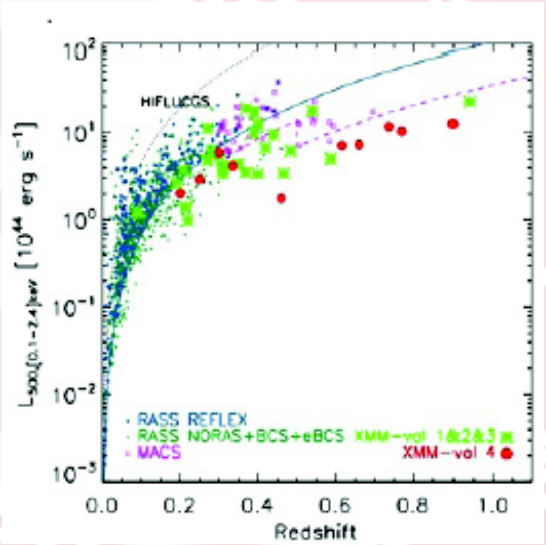

The ESZ completes the high M-z region sparsely populated by RASS clusters (massive dynamically perturbed systems)

The ESZ is a reference sample for z<0.5 massive clusters complementary to high-z SPT sample

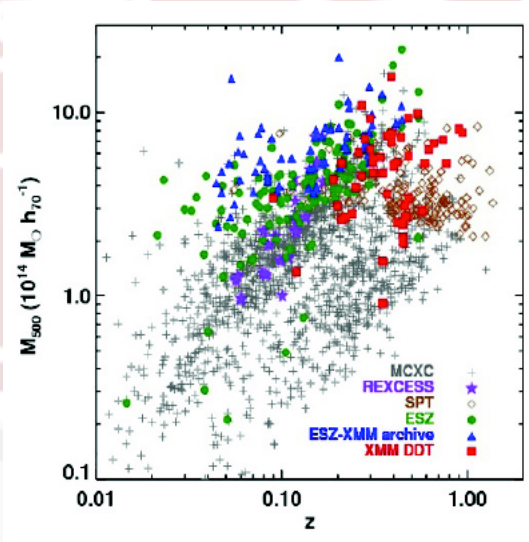

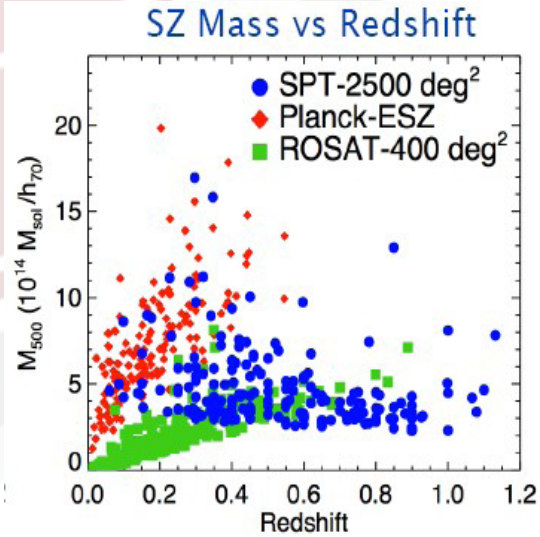

SZ clusters

clusters = Dark matter + Hot gas + stars

Link between these components ?

New detected clusters

not detected in X or optical, why ?

Cosmological probe

Need for masses and redshifts !

z possible from optical/x-ray follow ups

- Masses from X: hot gas scaling relation Lx-M-Y
- Masses from optical: # of galaxies (stars) → Richness-M-Y
- Masses from optical: WL (dark matter) relation Y-M

Planck Coll. Early 10,11,12 Intermediate 3

See talk from Pointecouteau on baryons in *Planck* SZ clusters

X-ray properties of new clusters

Morphologically complex compared to X-ray clusters

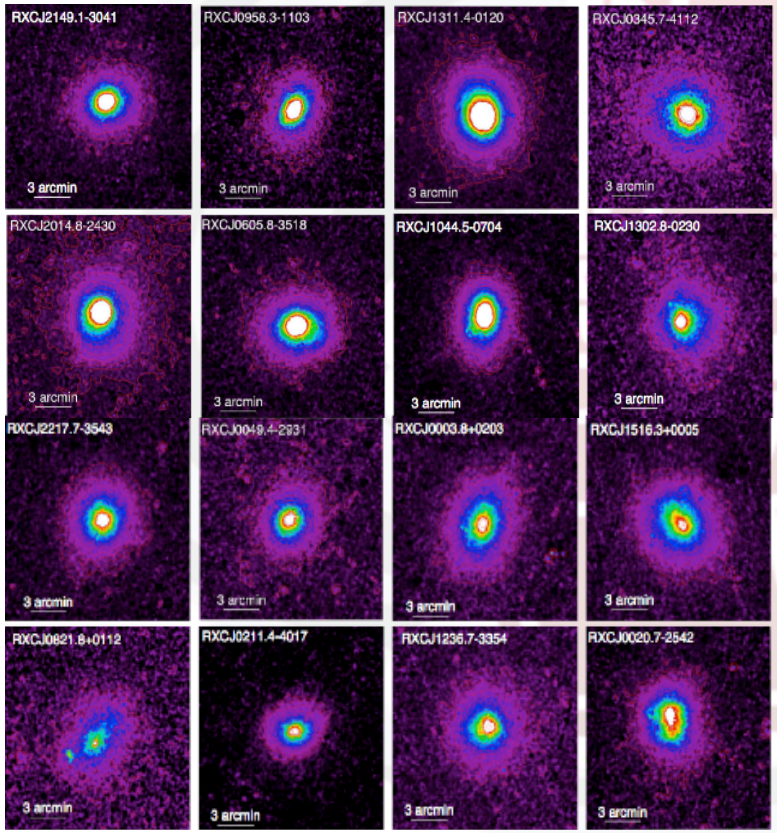

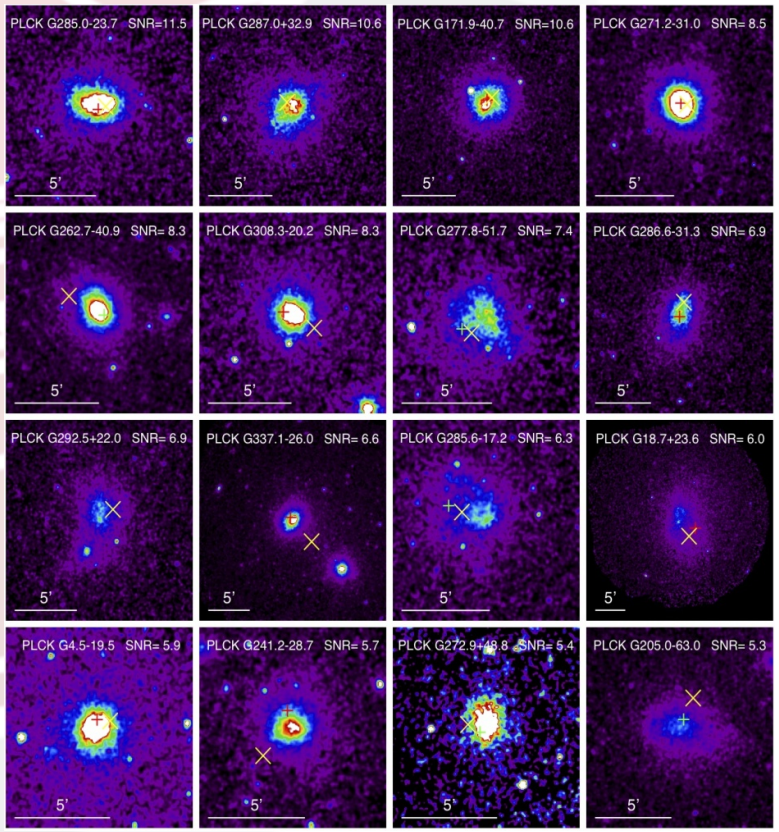

X-ray properties of new clusters

Morphologically complex compared to X-ray clusters

Under-luminous in Xray given their mass

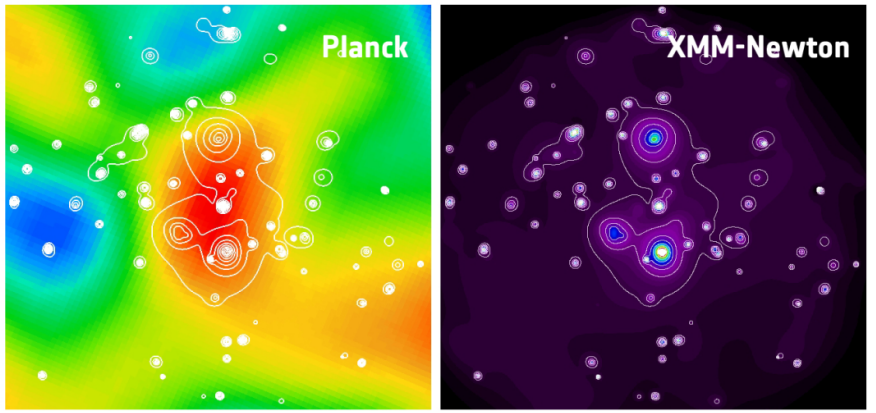

Density profiles of Planck new clusters shallower than Xray clusters of similar masses (REXCESS or EXCPRES)

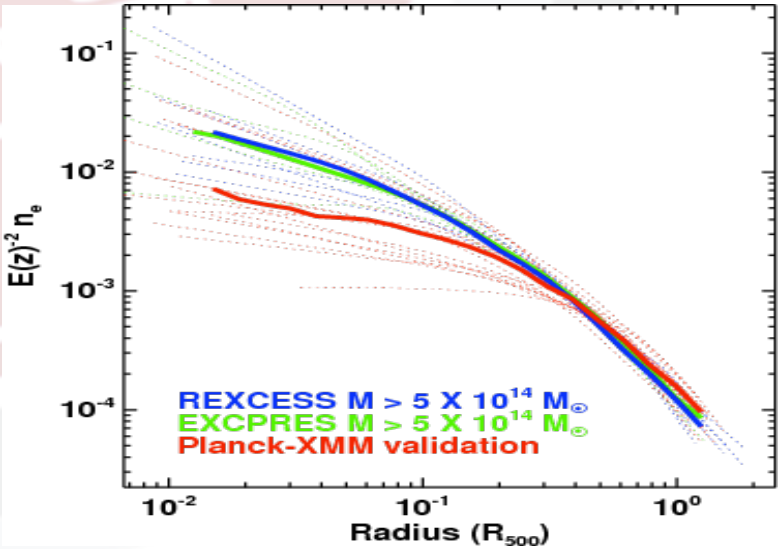

Multiple systems: double, triple systems

→ First superclusters in SZ

X-ray properties of new clusters

Planck in opening a new window on the understanding of the formation and evolution of clusters

Complementarity of observations: SZ, X, radio, Optical ...

eg. PLCKG287.0+32.9 *(Bagchy et al. 2011)*

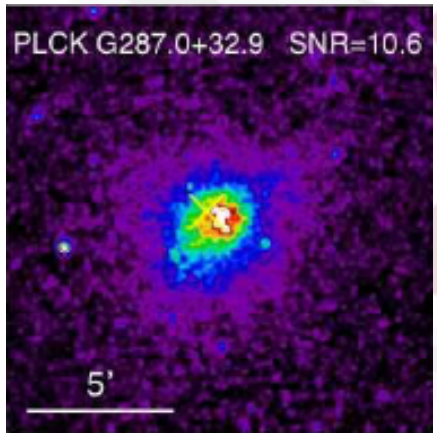

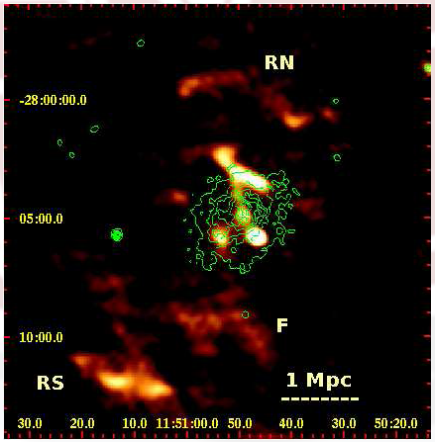

Observations of radio arcs, revealing possible shocks and mergers.

Summary on clusters with Planck

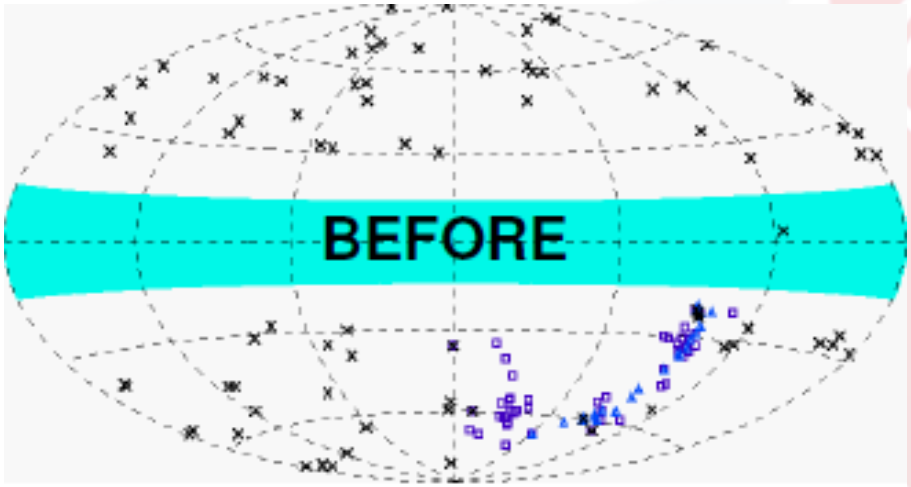

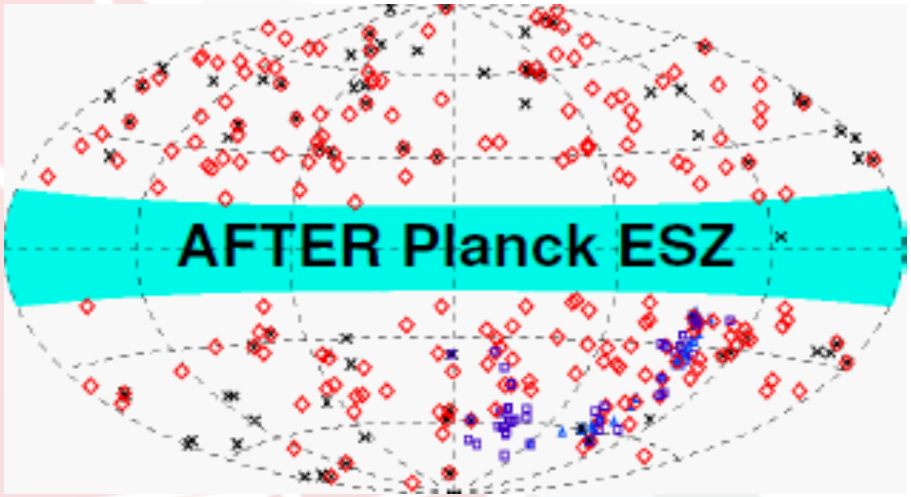

***Planck* has released a unique all sky sample**

of 199 (+26) clusters

Most homogeneous and complete sample all sky of massive z<0.5 clusters

First SZ measure for 80% of known clusters of the ESZ

Equivalent number and complementary sample wrt SPT 2012

Implications/Argument

Several slides comes from courtesy of E. Pointecouteau

We want to measure SZ scaling relations:

- **Astrophysics**
  - **ratio between gas mass weighted and X-ray spectroscopic weighted temperature depends on cluster thermodynamics**
  - **X-ray predictions for pressure signal vs SZ**
- **Cosmology**
  - **robust constraint on relationship between global observable (YSZ) and mass (via low-dispersion mass proxy, YX)**
  - **baseline for further evolution studies, cosmology…**

→ investigate correlations between: YSZ and M, TX, LX, Mgas...

THREE COMPLEMENTARY STUDIES

1. Statistical approach

- 1882 X-ray selected clusters (MCXC, Piffaretti +11), with homogenised L_{500}, z

2. Planck ESZ clusters

- 62 high SNR clusters
- clusters with good XMM archive data

3. New Planck clusters, XMM confirmed

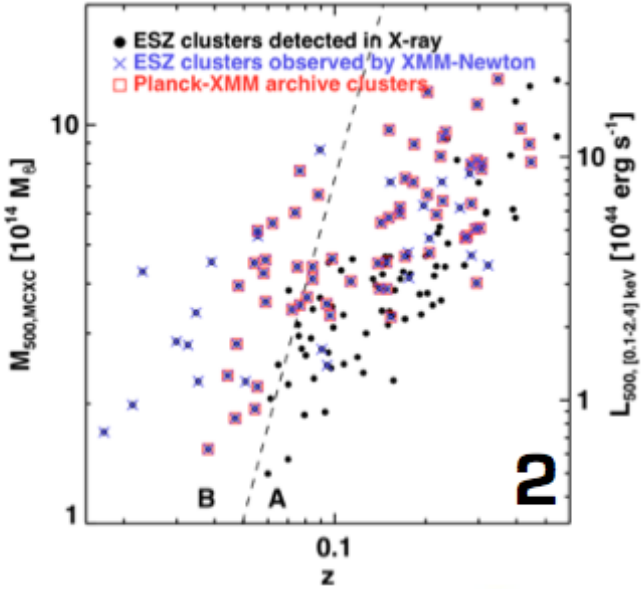

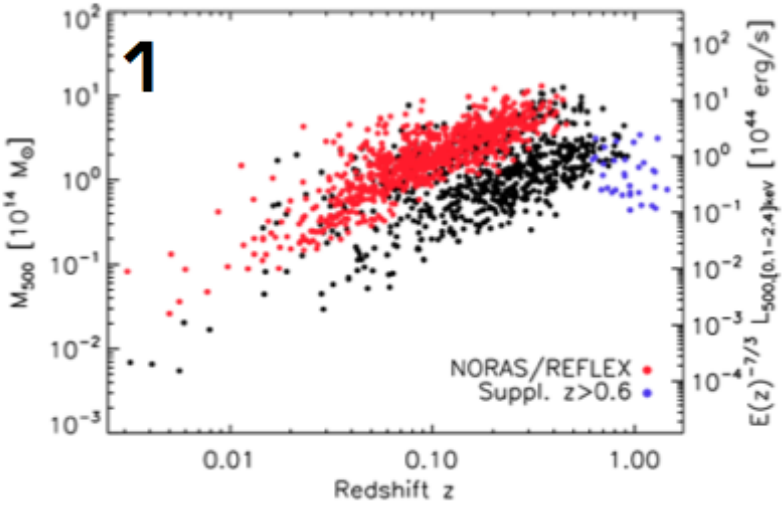

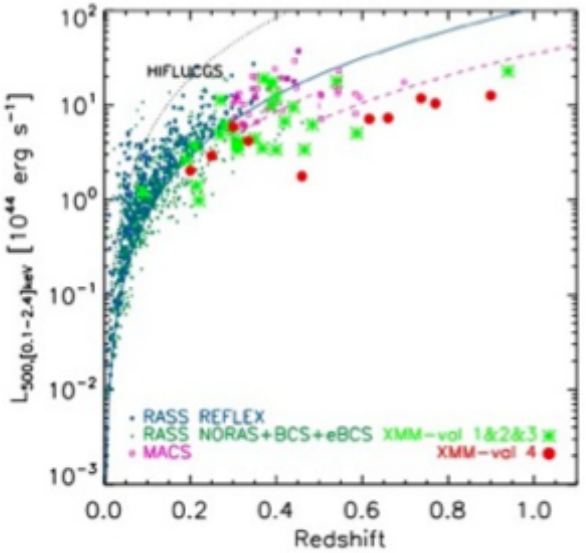

SZ - X SCALING RELATIONS

Y_{SZ} - L_X relation

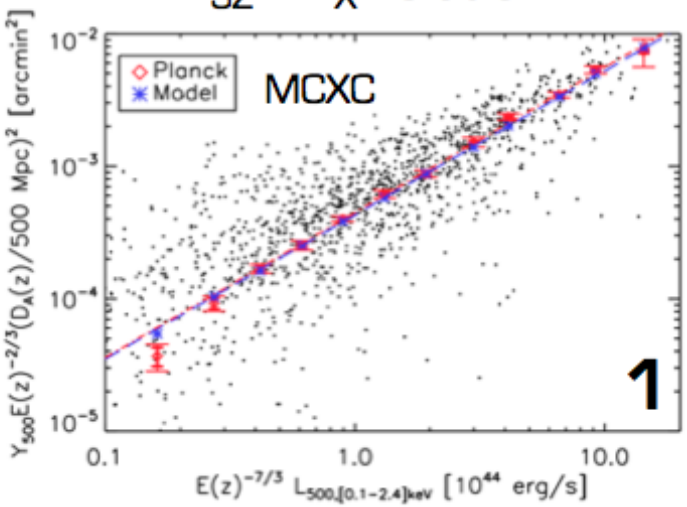

Y_{SZ} - Y_X relation

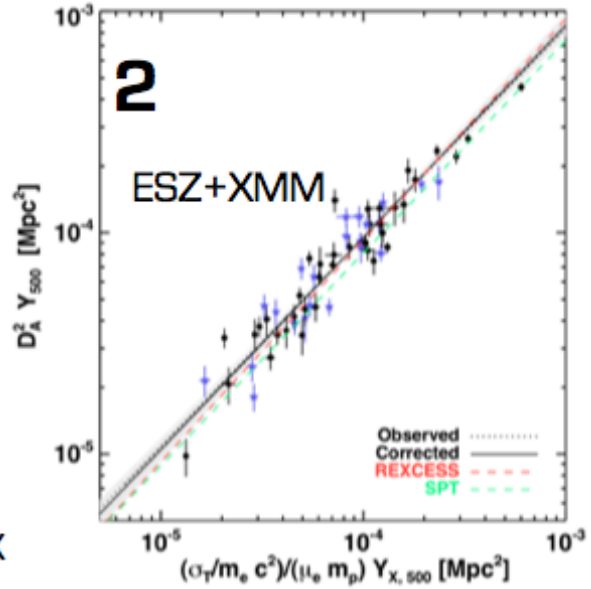

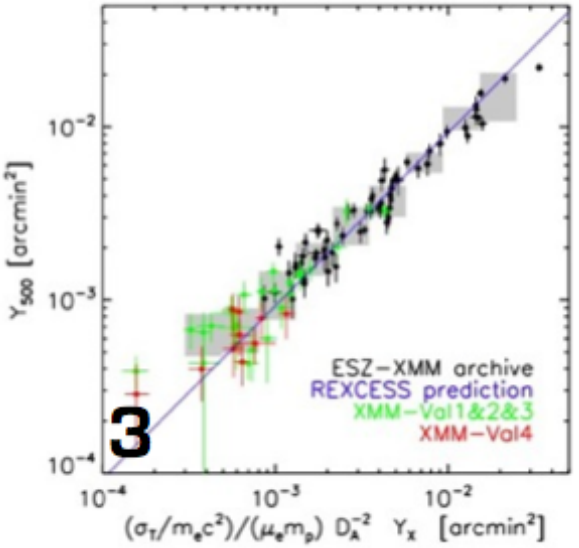

- SZ data and X-ray based prediction are consistent

NO MISSING HOT BARYONS
(at least within R_{500})

SZ - X SCALING RELATIONS

- Homogenous results from pre/post-Planck studies

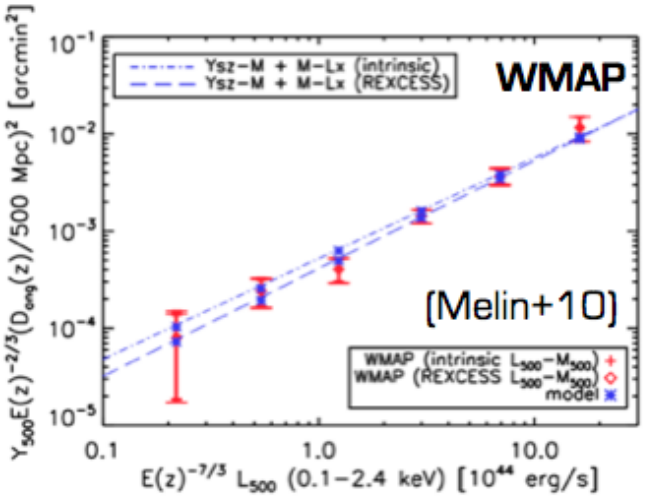

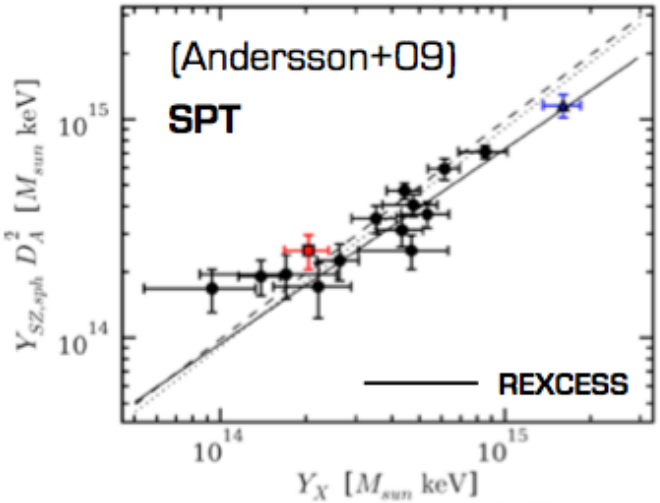

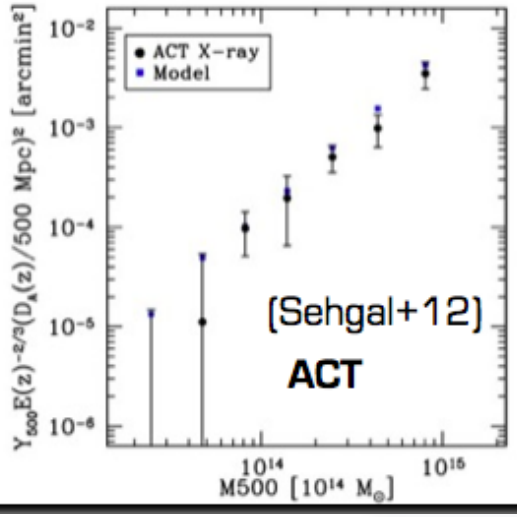

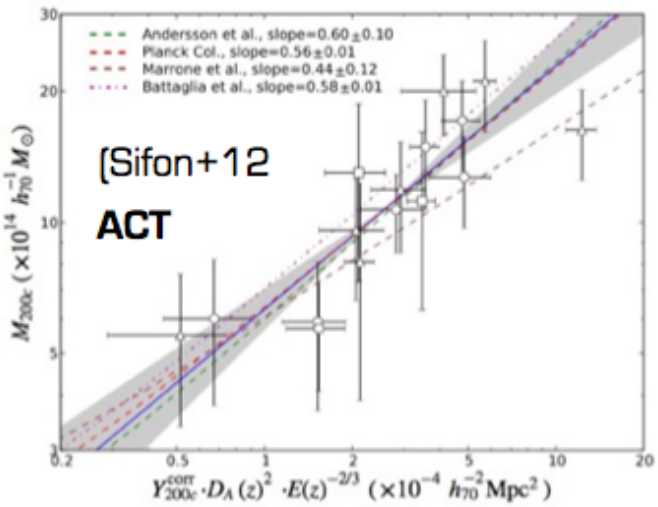

SZ - OPTICAL SCALING RELATIONS

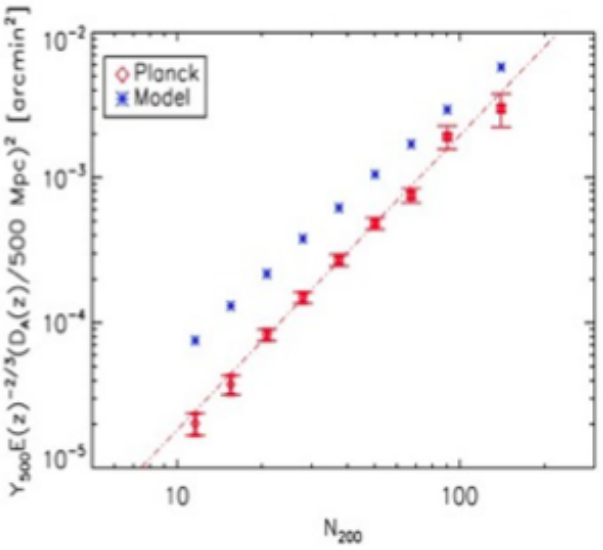

PC+11

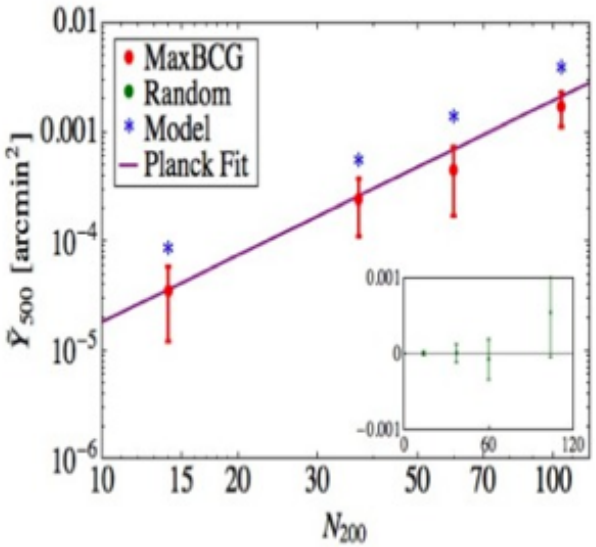

Draper+11

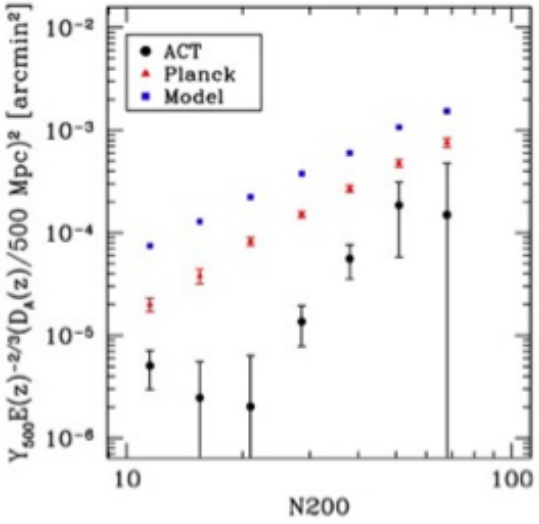

Sehgal+12

- Selection effect (X-ray vs optically selected samples)?
- SZ not an adequate proxy for halos?
- systematic biases?
- use N_{opt} - M_{wl} instead of N_{opt} - Lx?

AN OPEN QUESTION

Survey biases

- volume effect, Malmquist bias
- complex dynamical structures
- orientation, projection, miscentering
- foreground and background contamination

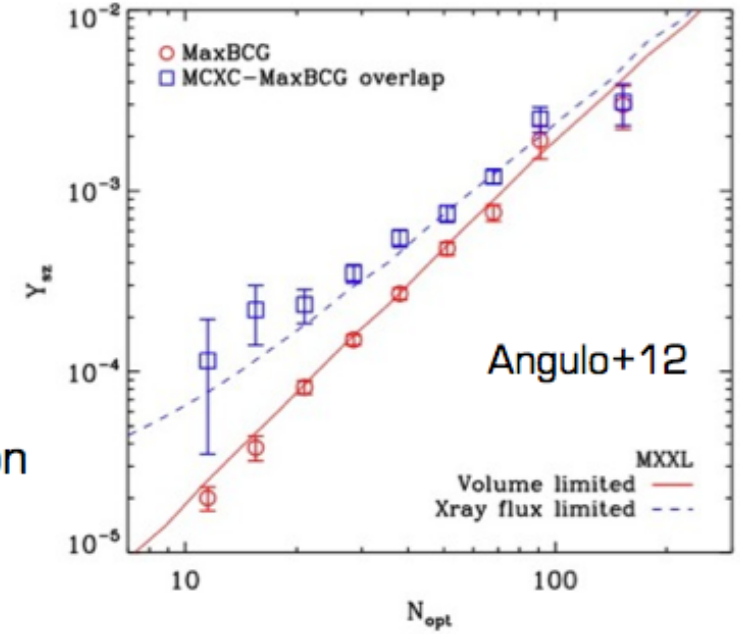

Observable biases

- residual uncertainties on absolute calibration (X, SZ, optical,...)
- systematics on mass estimation (HE, lensing masses, richness)
- covariance between observables
- lack of constraints on the evolution
- complex physics

→ **affect slope, normalisation and intrinsic scatter**

CLUSTER MASSES AND SZ SIGNAL

Determine Y_{SZ}-M_{HE} and Y_{SZ}-M_{WL} relationships

- Investigate scatter and dependence on mass measurement method
- Try to give a 'holistic' view of clusters through X-ray, SZ and lensing
- Relationship between M_X and M_{WL} is a test of non-thermal pressure support (expect ~10% HE mass bias)

- Previous work: either SZ+WL or X-rays+WL

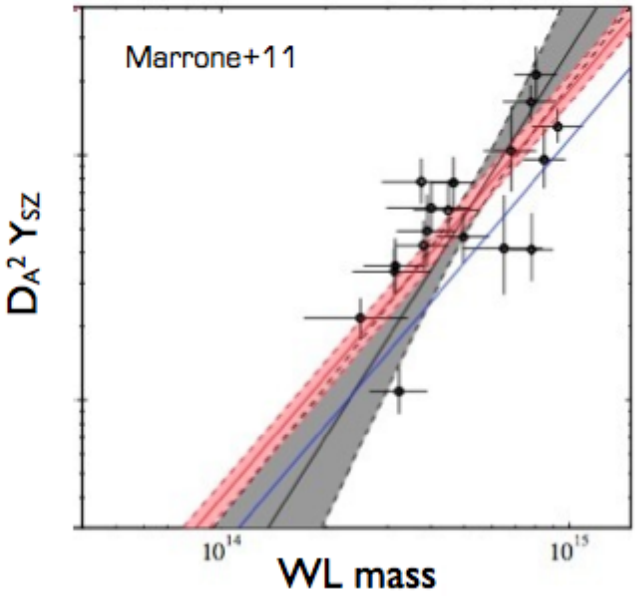

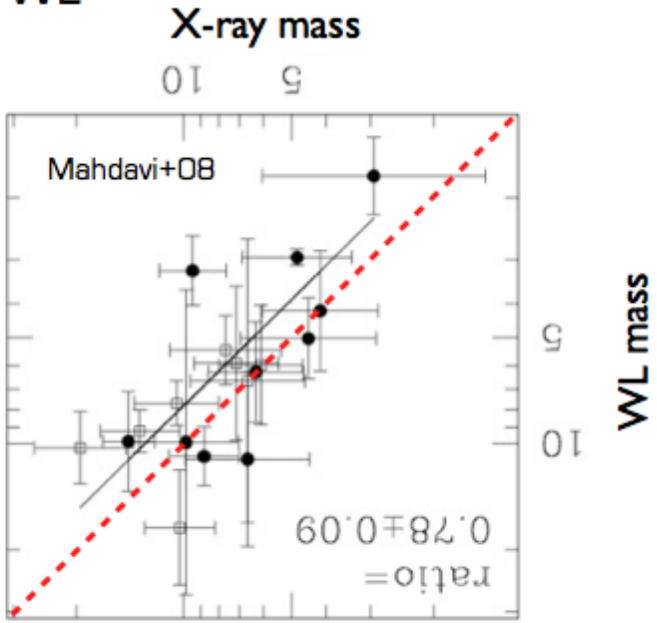

THE Y_{SZ}-M_{WL} RELATION

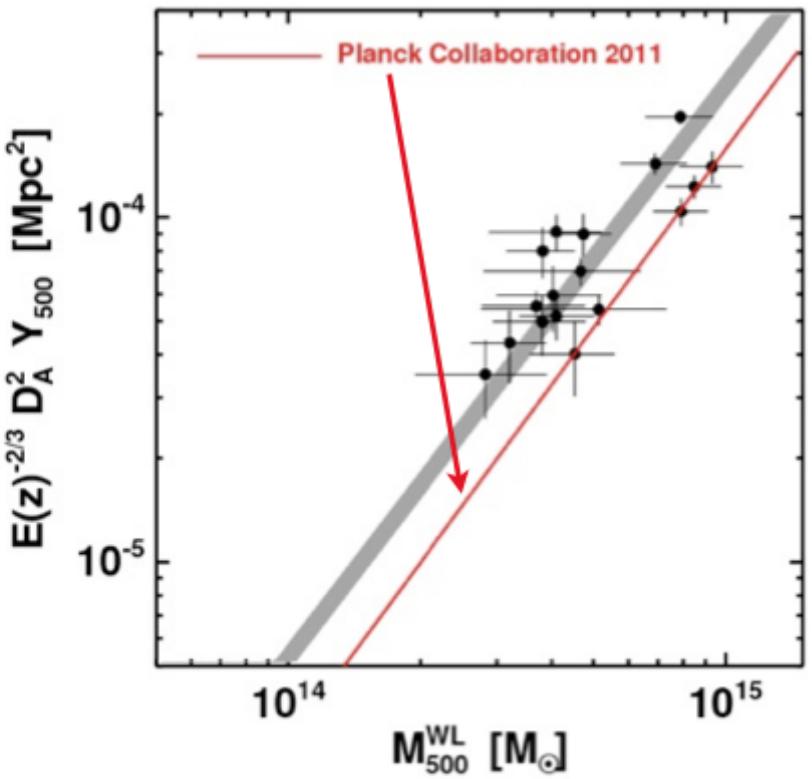

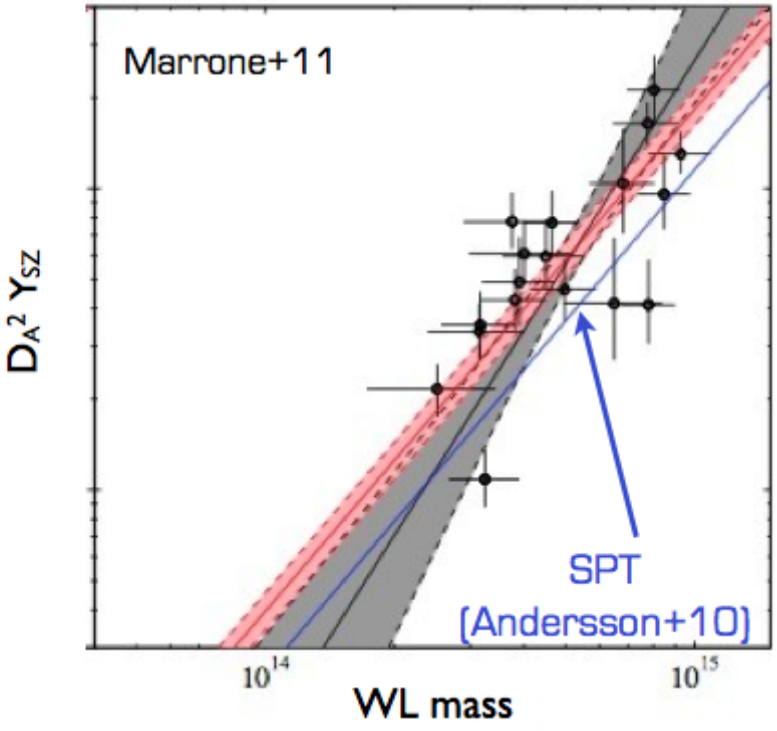

Good constraints on Y-M relation using WL masses

CLUSTER MASSES AND SZ SIGNAL

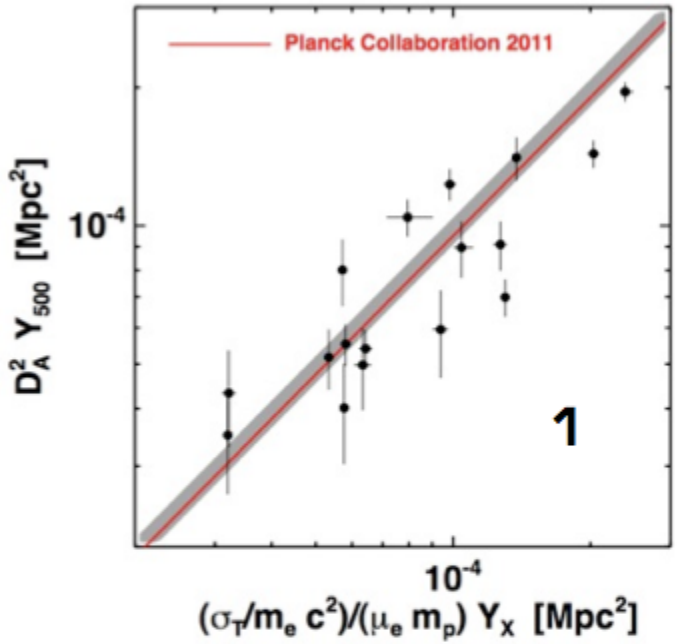

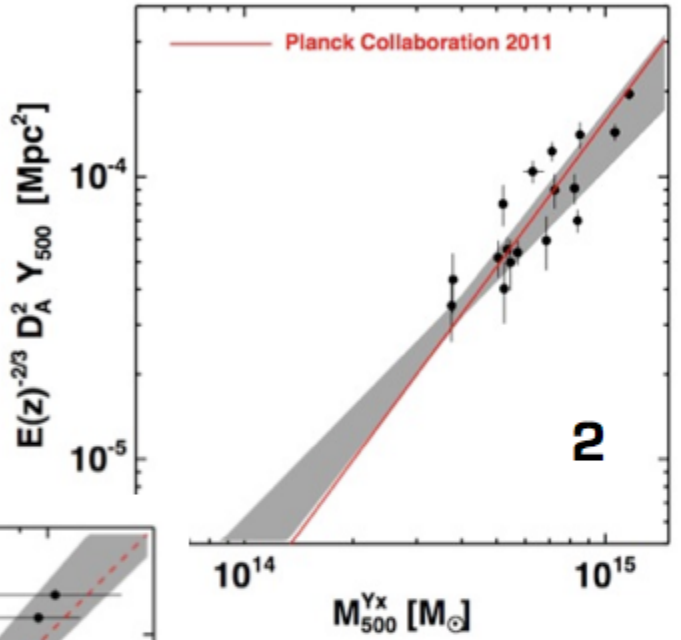

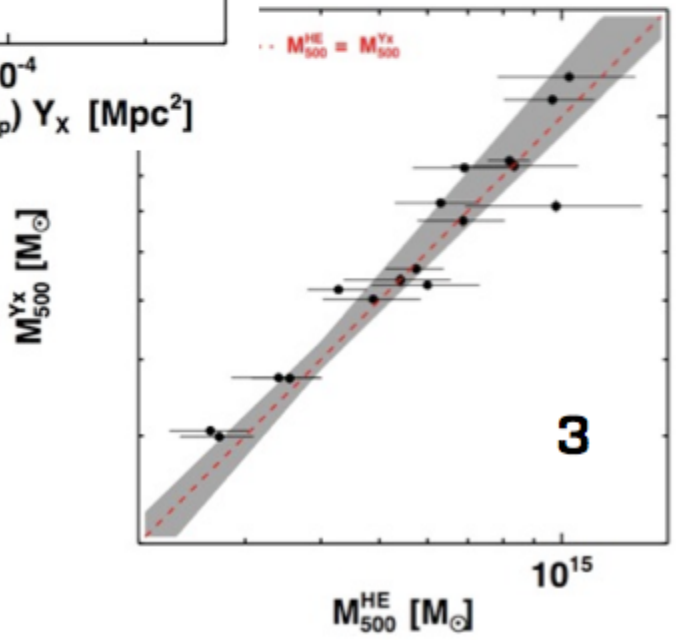

SZ fluxes and HE X-ray masses agree with previous Planck results!

ETIENNE POINTECOULTEAU, 1
irap

CLUSTER MASSES AND SZ SIGNAL

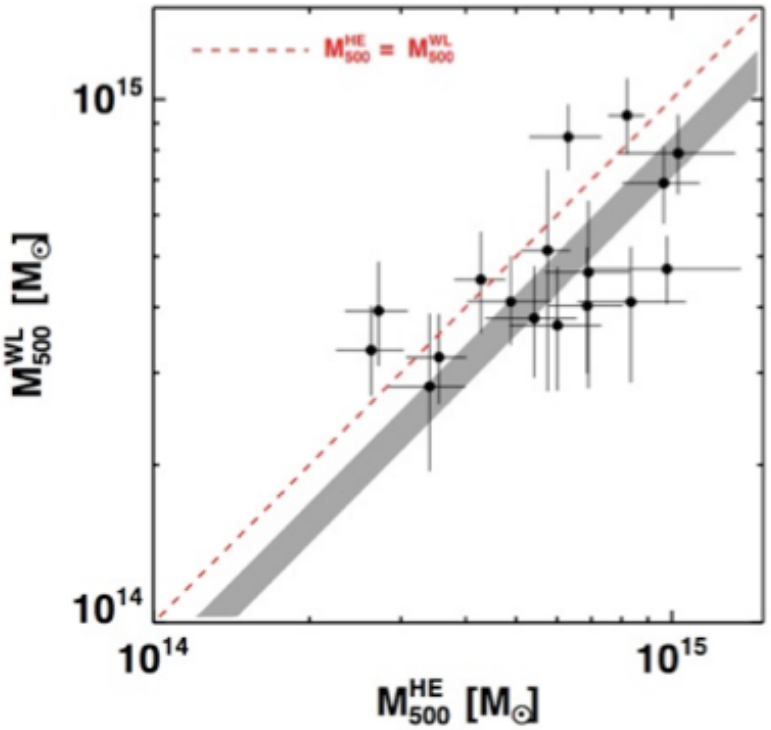

HSE X-ray masses ≠ WL masses

→ convergence between observable/methods required to tackle the ~10-20% differences in mass proxies

SZ mass proxy: YSZ - M

- SZ fluxes and HE X-ray masses agree

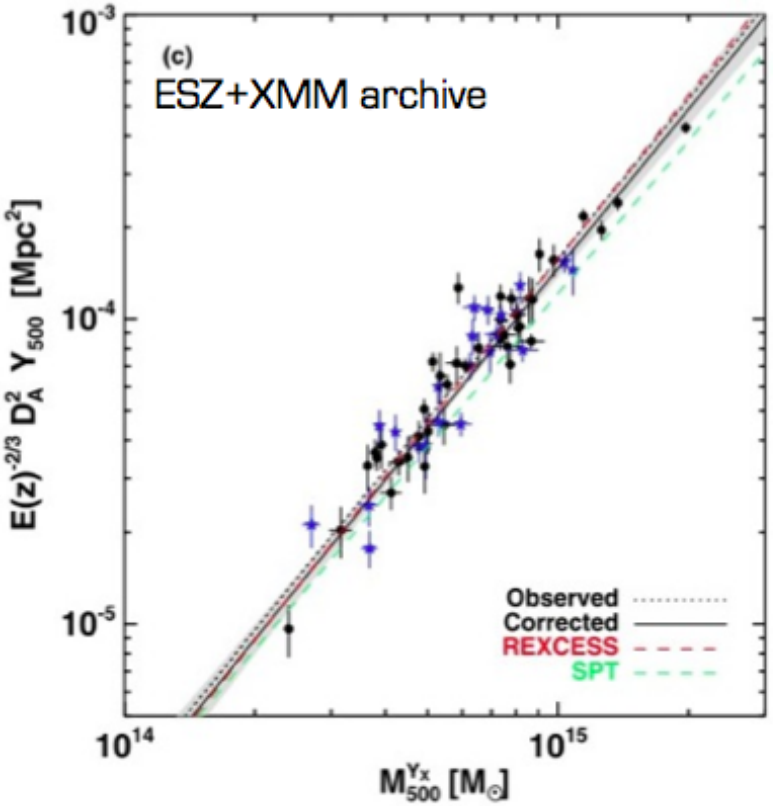

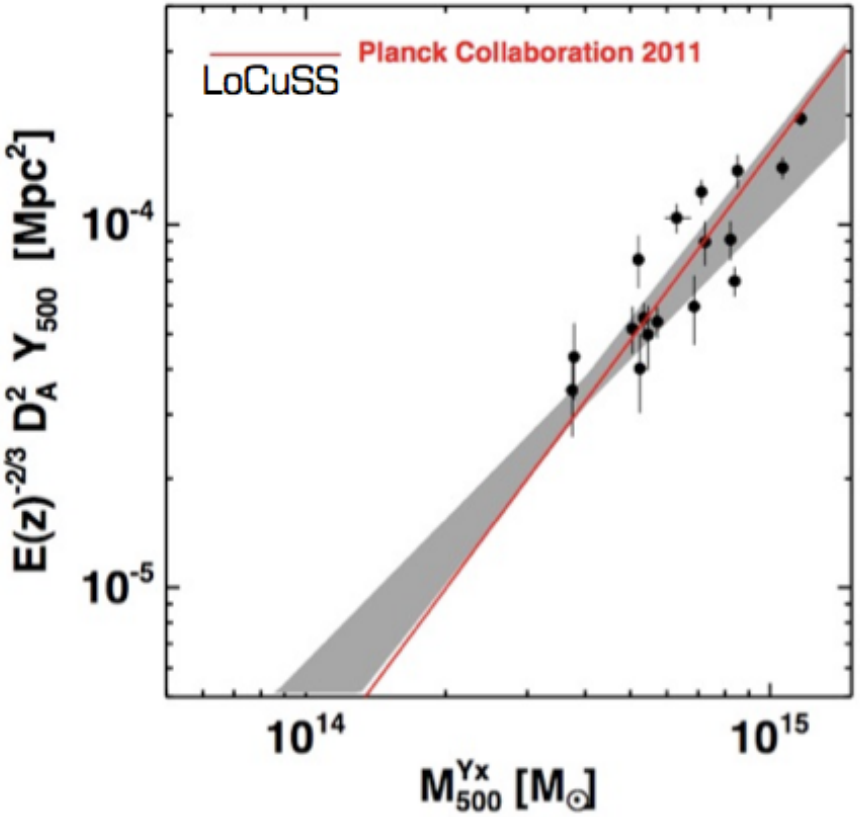

Planck Collaboration+11+12

Conclusions on Clusters

- ✓ **Strenghten our overall view of ICM properties and mass content of clusters**
  - ❖ Close long standing issue of the « missing hot baryons » from excellent agreement between observed Y_{SZ} and X-ray-based predictions
  - ❖ High precision calibration of the SZ scaling relation (Y_{SZ} – M)
  - ❖ Agreement between the present results, ground-based results and X-ray predictions augurs well for our understanding of cluster astrophysics

- ✓ **Further convergence of mass proxies (within R_{500}) is needed**
  - ❖ SZ, X-rays, lensing, optical, …

- ✓ **Promising for the use of SZ (Planck) clusters for precision cosmology**

Extragalactic sources & Far-IR background (WG6)

C. Burigana, Paris, 25-27/7/2012

Planck Early Results:
Validation and Extreme Radio Sources in the ERCSC

The ERCSC contains hundreds of extragalactic radio sources, many with SEDs extending to frequencies 143 GHz or higher. The Planck observations are complemented by approximately simultaneous ground-based observations at frequencies below and overlapping Planck frequency bands. The flux density scales of the ground-based and Planck observations are found to be consistent.

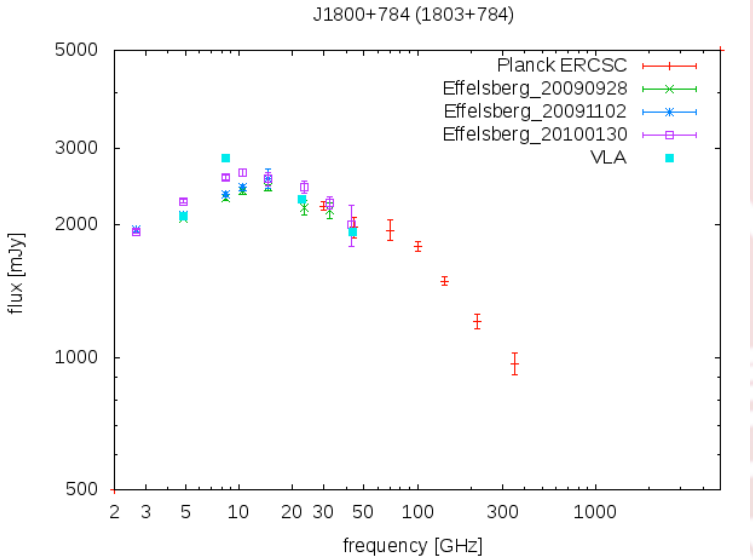

Effelsberg, VLA and Planck measurements of a true GPS quasar: J1800+784 flaring during the Planck observations

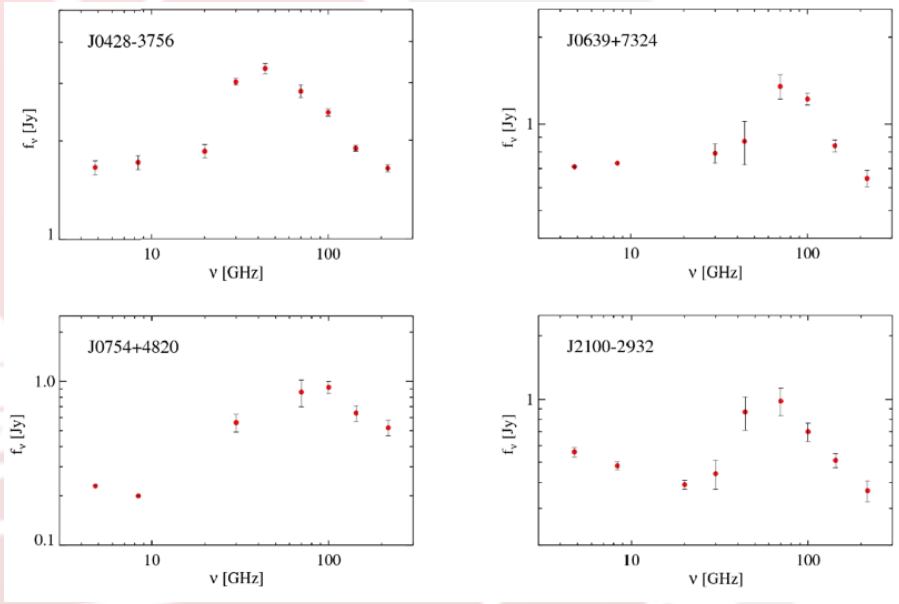

SEDs of possible new GPS candidates emerged when combining the Planck data with the low frequency archival data.

- Planck has demonstrated that the high frequency counts (at least for frequencies ≤ 143 GHz) of bright extragalactic sources are dominated at the bright end by synchrotron emitters, not dusty galaxies;

- In many cases, the spectra can reasonably be fit with a single power law, as expected for one component synchrotron emission. In some cases, such as J1800+784, the quality of the data permits us to clearly see the expected spectra break of ~ -0.5 expected from the aging of the synchrotron-producing electrons;

- In the case of some of the apparently flat spectrum sources, we find clear evidence that the nominally flat spectrum is made up of two or more peaked components.

Planck Early Results: Spectral energy distributions and radio continuum spectra of Northern extragalactic radio sources

The nine Planck frequencies, from 30 to 857 GHz, are complemented by a set of simultaneous observations ranging from radio to gamma-rays.

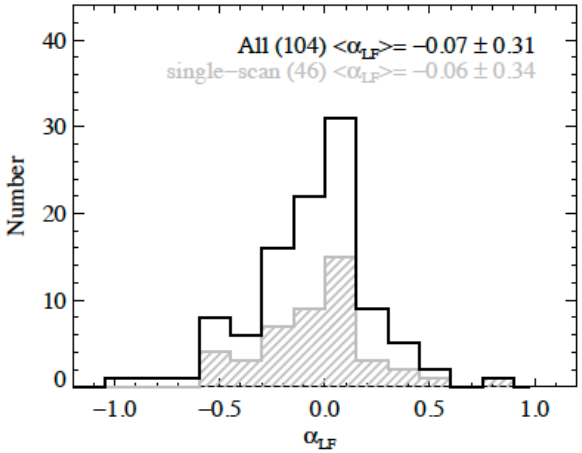

Distribution of LF spectral indices for the whole sample (104 sources).

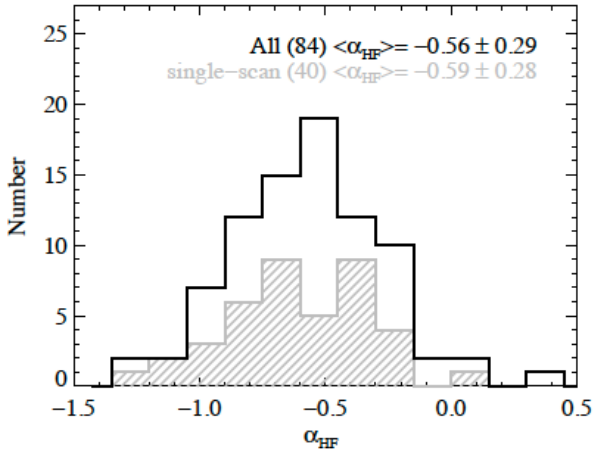

Distribution of HF spectral indices for the 84 sources that had three or more data points. The sources that have only been scanned once by Planck are shown hatched (40 sources).

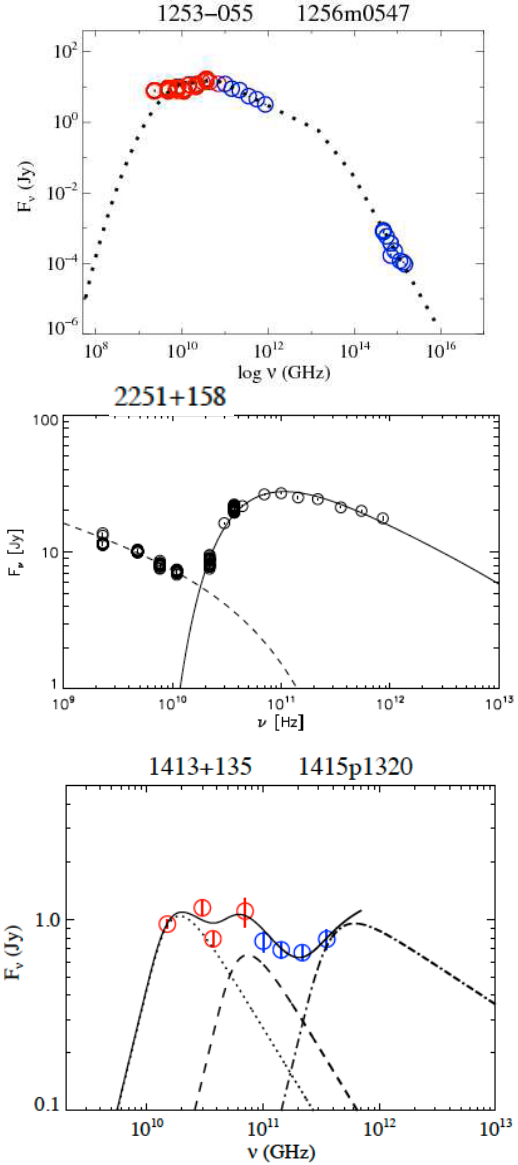

- The 104 SEDs, supplemented with archival data, demonstrate the usefulness of *Planck* data in determining the SED peak frequencies and fluxes and in modelling the spectral energy distributions in greater detail.

- The data demonstrate that the synchrotron spectrum contains contributions from several physically distinct AGN components;

- We have presented some examples of total flux density monitoring to demonstrate in how different activity stages sources have been observed during Planck scans.

SEDs and radio spectra using Planck ERCSC data

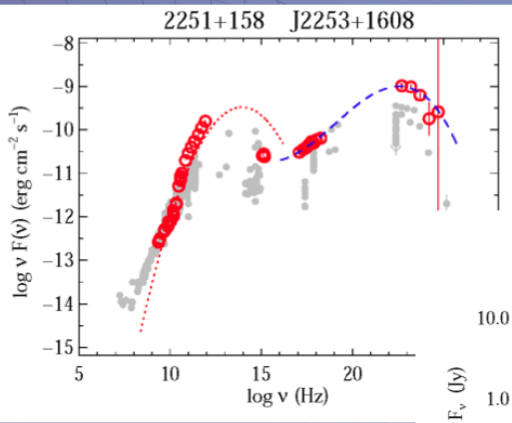

For this source, the data are from a single scan, for many others in the early paper, from averaged scans.

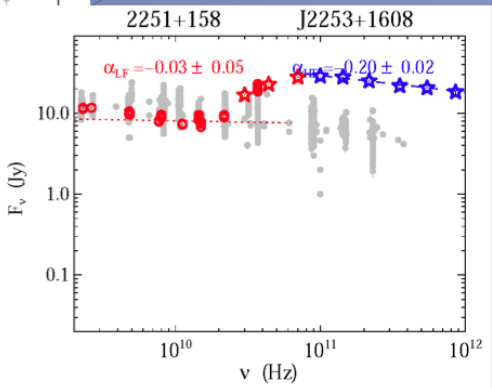

Modelling and understanding the synchrotron spectra of blazars

Spectral energy distributions, SEDs

- Contemporary models fit the high-energy inverse Compton (IC) part rather nicely, but (still) almost completely ignore the synchrotron (=radio) part which most likely is the source for the high-energy emission

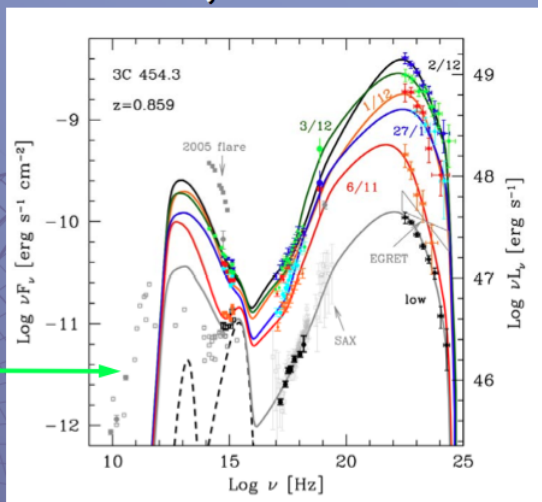

Bonnoli et al. 2010

The physics determining SED shapes in blazars

Planck Early Results: Statistical properties of extragalactic radio sources in the Planck Early Release Compact Source Catalogue

First estimate of the Early Release Compact Source Catalogue at 100, 143, and 217 GHz counts of extragalactic radio sources at bright flux density levels.

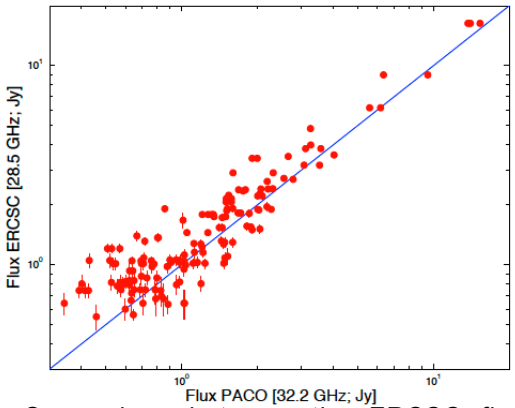

Comparison between the ERCSC flux densities at 30 GHz and at 44 GHz with the almost simultaneous ATCA measurements (PACO project) at 32.2 and 39.7 GHz, respectively. No correction for the slightly different frequencies has been applied.

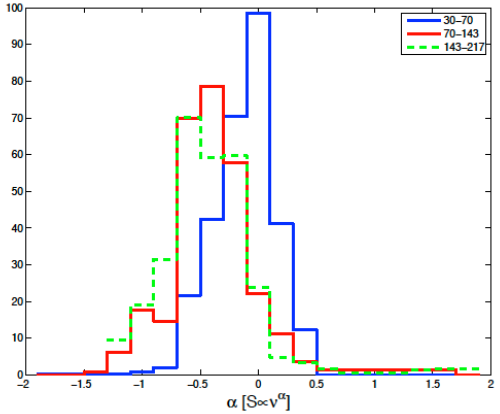

Spectral index distributions for different frequency interval calculated by taking into account all sources selected at 30 GHz with Sv > 1 Jy. There is clear evidence for a steepening above 70 GHz.

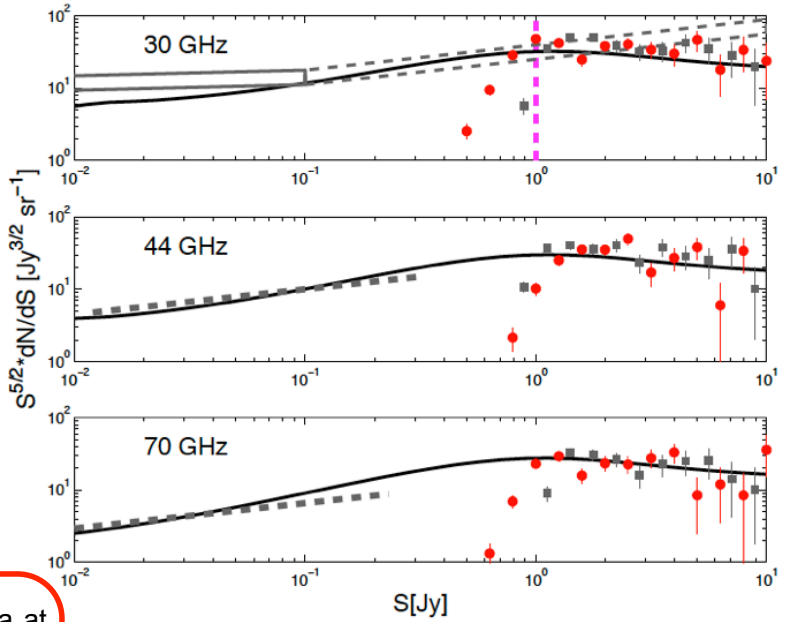

Euclidean normalized differential number counts at the LFI frequencies: red circles show the counts of sources with counterparts in our reference 30 GHz sample; solid curves show the total number counts of extragalactic radio sources predicted by the de Zotti et al. (2005) model. Also shown are: the counts at 31 GHz from DASI (grey dashed box); at 33 GHz from the VSA (grey box); counts from WMAP 5-yr survey (grey squares); counts estimated by Waldram et al. (2007) (grey dashed line); dashed magenta line in the upper panel indicates the flux completeness limit, 1.0 Jy.

- Counts at 30, 44, and 70 GHz in good agreement with those derived from WMAP data at nearby frequencies;

- The completeness limit of the ERCSC is somewhat deeper than that of WMAP at 30 and 70 GHz and somewhat shallower at 44 GHz;

- At higher frequencies the ERCSC has allowed us to obtain the first estimate of the differential number counts at bright flux density levels.

- At 30, 143 and 217 GHz, the present counts join smoothly to those from deeper surveys over small fractions of the sky.

- An analysis of source spectra finds clear evidence of a steepening of the mean spectral index above ≃ 70GHz: the contamination of the CMB power spectrum by radio sources below the detection limit is significantly lower than previously estimated.

Radiosource number counts - 1

- It has also been shown by that differential number counts at 30, 44, and 70 GHz are in good agreement with those derived from WMAP data at nearby frequencies.
- The model is consistent with the present counts at frequencies up to 70 GHz, but over-predicts the counts at higher frequencies by a factor of about 2.0 at 143 GHz and about 2.6 at 217 GHz.
- The analysis of the spectral index distribution over different frequency intervals, within the uniquely broad range covered by Planck in the mm and sub-mm domain, has highlighted an average steepening of source spectra above about 70 GHz.
- This steepening accounts for the discrepancy between the model predictions and the observed differential number counts at HFI frequencies.

Radiosource number counts - 2

- In the fall of 2011, a successful explanation of the change detected in the spectral behavior of ERCSC extragalactic radio sources at frequencies above 70-80 GHz has been proposed by Tucci et al. 533, A57:1-21.
- → First attempt at constraining the most relevant physical parameters that characterize the emission of blazar sources by using the number counts and the spectral properties of ERS estimated from high–frequency radio surveys. A relevant steepening in blazar spectra with emerging spectral indices in the interval between −0.5 and −1.2, is commonly observed at mm/ sub-mm wavelengths.
- This spectral behavior is caused, at least partially, by the transition from the optically–thick to the optically–thin regime in the observed synchrotron emission of AGN jets.
- Indeed, a “break” in the synchrotron spectrum of blazars above which the spectrum becomes “‘steep” is predicted by models of synchrotron emission from inhomogeneous unresolved relativistic jets. Based on these models, Tucci et al. evaluated the frequency at which the break occurs on the basis of the ERS flux densities measured at 5 GHz and of the most typical values for the relevant physical parameters of AGNs.

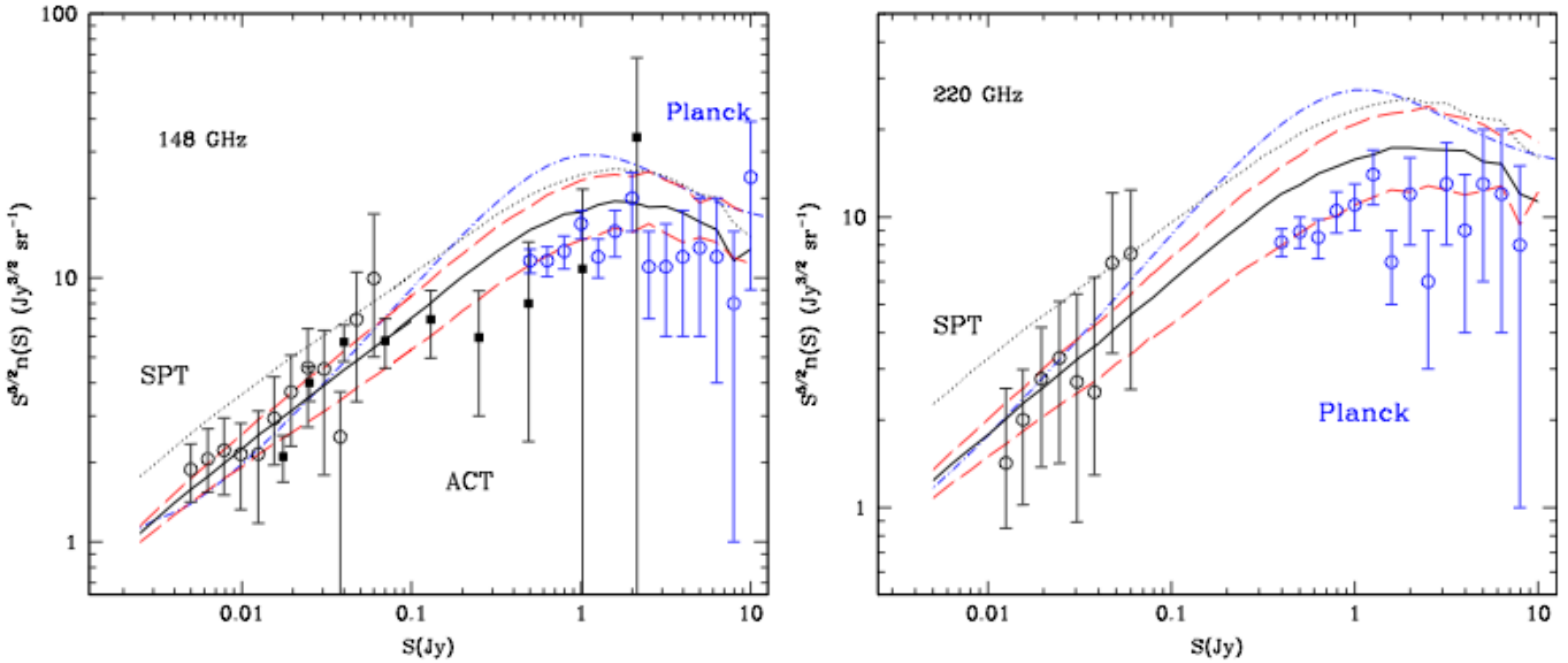

Comparison between predicted and observed differential number counts at 148 GHz (left panel) and at 220 GHz (right panel). Filled circles: ACT data; open black circles: SPT data; open blue circles: Planck ERCSC counts at 143 GHz (left panel) and 217 GHz (right panel). The plotted lines indicates predictions of different models, as follows: C0(dotted lines), C1 (thick continuous lines), C2Ex (lower red long–dashed lines) and C2Co (upper red long–dashed lines) and the model by de Zotti et al 2005, A&A 431:893-903 (blue dash–dotted line). From Tucci et al., A&A, Vol. 533, A57, 2011.

Radiosource number counts - 3

- High frequency (v ≥ 100 GHz) data on source number counts are the most powerful for distinguishing among different models.
- These most recent data on number counts require spectral "breaks" in blazars' spectra and clearly favor the model C2Ex.
- According to this, most of the FSRQs (which are the dominant population at low frequencies and at Jy flux densities), differently from BL Lacs, should bend their flat spectrum before or around 100 GHz.
- The C2Ex model also predicts a substantial increase of the BL Lac fraction at high frequencies and bright flux densities.
- On the whole, the parameter rM should be of parsec–scales, at least for FSRQs, in agreement with theoretical predictions (Marscher & Gear 1985, ApJ 298:114-127), whereas values of rM≪1pc should be only typical of BLLacobjects or of rare quasar sources.

Radiosource number counts - 4

- The two most relevant models of, i.e. C2Co and C2Ex, assume different distributions of rM for BL Lacs and FSRQs, with the former objects that generate, in general, the synchrotron emission from more compact regions, implying higher values of ν_M (above 100GHz for bright objects).
- These two models differ only in the r_M distributions for FSRQs: in the C2Co model the emitting regions are more compact, implying values of ν_M partially overlapping with those for BL Lacs, whereas in the C2Ex model they are more extended, thus predicting very different values of ν_M for FSRQs and BL Lacs.
- This is indeed observed: a clear dichotomy between FSRQs and BL Lac objects has been found in the Planck ERCSC. Almost all radio sources show very flat spectral indices at LFI frequencies, i.e. $\alpha_{LFI} - 0.2$, whereas at HFI frequencies, BL Lacs keep flat spectra, i.e. $\alpha_{HFI} - 0.5$, and a high fraction of FSRQs show steeper spectra, i.e. $\alpha_{HFI} < -0.5$.

Planck Early Results: The Planck View of Nearby Galaxies

ERCSC provides an unsurpassed survey of galaxies at sub-millimeter wavelengths, representing a major improvement in the numbers of galaxies detected, as well as the range of far-IR/submm wavelengths over which they have been observed.

ERCSC catalogue has been matched to *IRAS*-detected galaxies in the Imperial *IRAS* Faint Source Redshift Catalogue (IIFSCz)

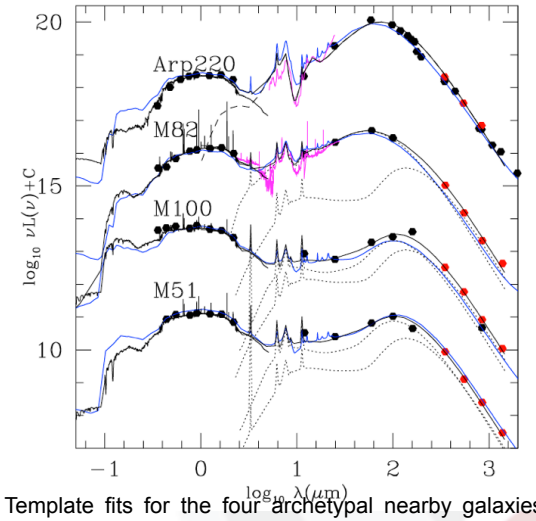

Template fits for the four archetypal nearby galaxies, M51, M100, M82 and Arp 220. Black curves: fits with Efstathiou and Rowan-Robinson templates (black dotted lines), blue curves: Silva et al. (1998) models. *Planck* ERCSC data shown as red filled hexagrams. *ISO*-SWS mid-infrared spectroscopy data are shown in magenta.

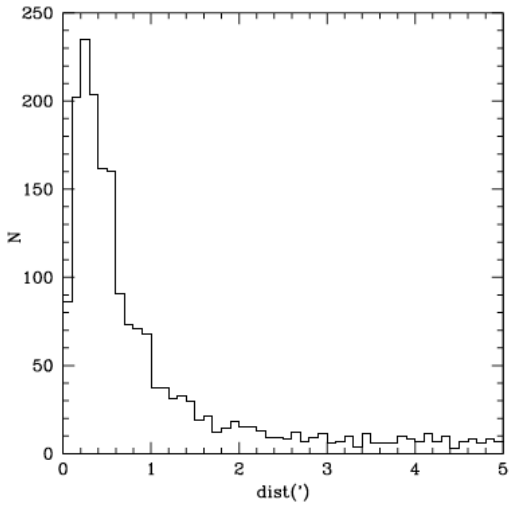

Histogram of offsets between ERCSC and IIFSCz positions.

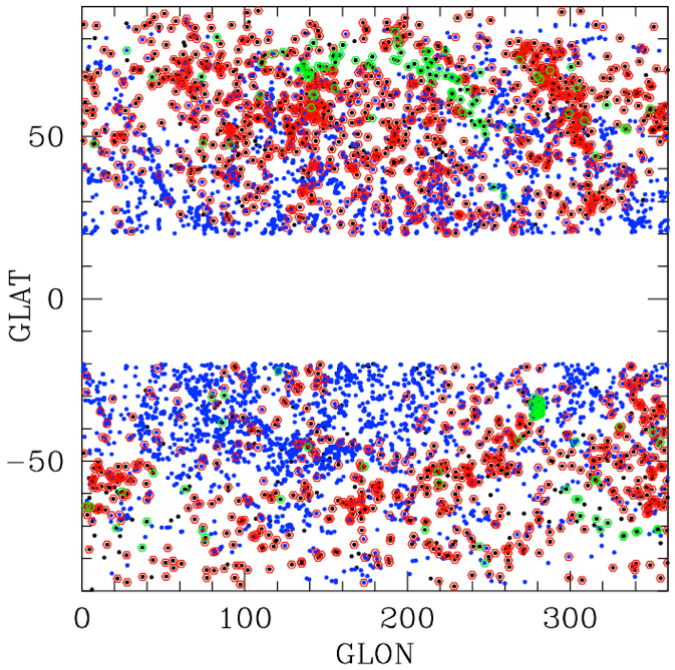

Sky plot of ERCSC sources in galactic coordinates. Black filled hexagons are ERCSC point-sources and blue filled hexagons are ERCSC sources flagged as extended. Red hexagons are sources associated with IIFSCz *IRAS* FSC galaxies, after scrutinising suspect categories with NED (and excluding some, as described in the text). Green hexagons are ERCSC sources not associated with IIFSCz, but associated with bright galaxies in NED (only for $|b| > 60^\circ$ for extended sources).

- Our studies of nearby galaxies detected by Planck have shown evidence for colder dust than has previously been found in local galaxies. This suggests that previous studies of dust in local galaxies have been biased away from such luminous cool objects;

- We also find that the dust SEDs in most galaxies are better described by parametric models containing two dust components, one warm and one cold, with the cold component reaching temperatures as low as 10K.

Planck Early Results:
Origin of the submm excess dust emission in the Magellanic Clouds

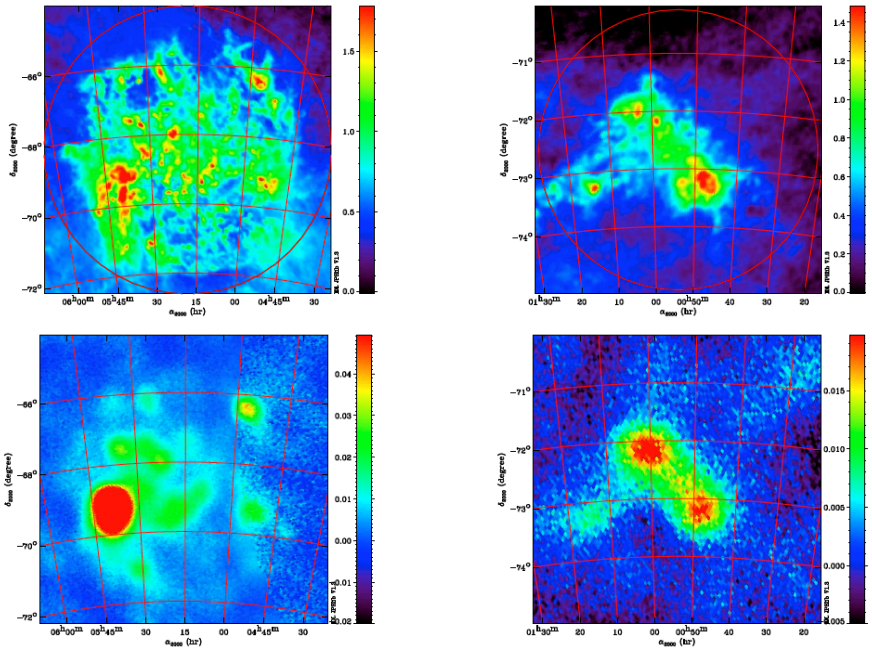

Planck Data for the LMC (Left) and SMC (right) at 857 (top) and 28.5 GHz (bottom) at full resolution. The upper panels are shown in log scale. The circle shows the region used to extract average SEDs.

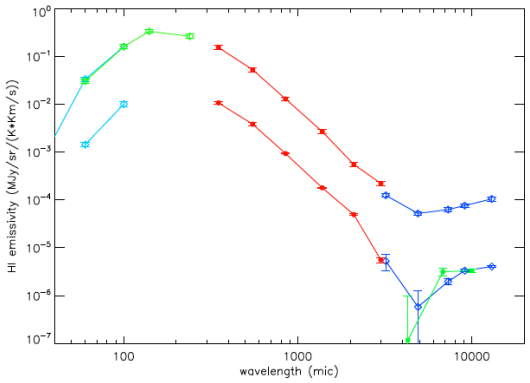

Average foreground SED toward the LMC and SMC including DIRBE , IRAS-IRIS , Planck-HFI , Planck-LFI and WMAP (lower curve) compared to the SED of the high latitude low column-density SED, scaled up by a factor of 10 for clarity (upper curve).

- We assessed the existence and investigated origin of millimeter excess emission in the LMC and the SMC using the Planck data.

- The LMC temperature map shows the presence of a warm inner arm already found with the Spitzer data, but also shows the existence of a previously unidentified cold outer arm.

- We show that the excess previously reported in the LMC can be fully explained by CMB fluctuations.

- Possible interpretation of the SMC excess employs the Two-Level-System (TLS) model developed by Meny et al. (2007) combined with spinning dust.

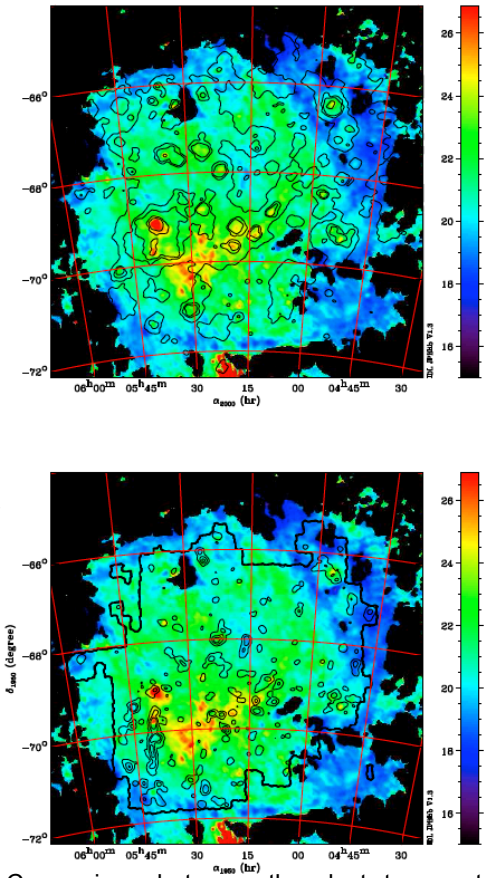

Comparison between the dust temperature map of the LMC with H_alfa (Top) and CO emission (Bottom). The CO contours are at 0.5, 2., 4 and 10 Kkm/s. H_alfa contours are at 1, 10, 50, 100, 500 and 1000 Rayleigh. The thick line shows the edge of the available CO surveys.

The University of Manchester
Jodrell Bank Observatory

MANCHESTER 1824

Morphology

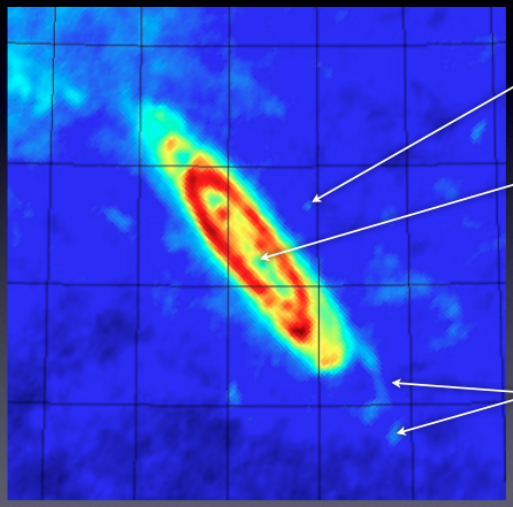

Planck 857GHz (log), DX5

The University of Manchester
Jodrell Bank Observatory

MANCHESTER 1824

Herschel (HELGA)

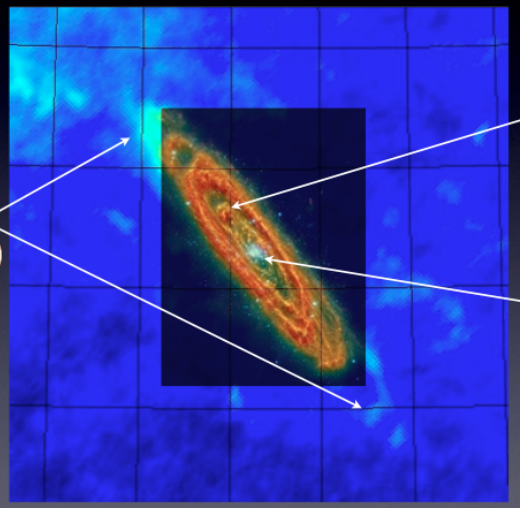

NB: using press release image Includes XMM

Data will become public later this year

Planck 857GHz (log), DX5

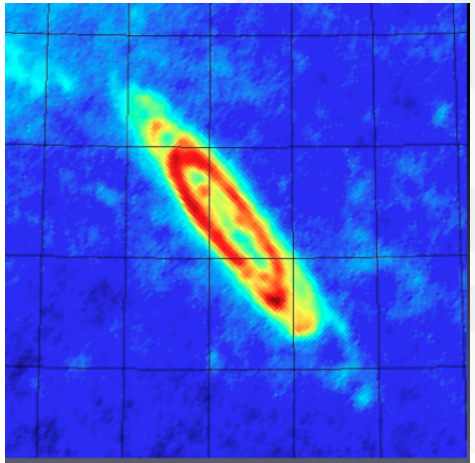

Planck 545GHz (log), DX5

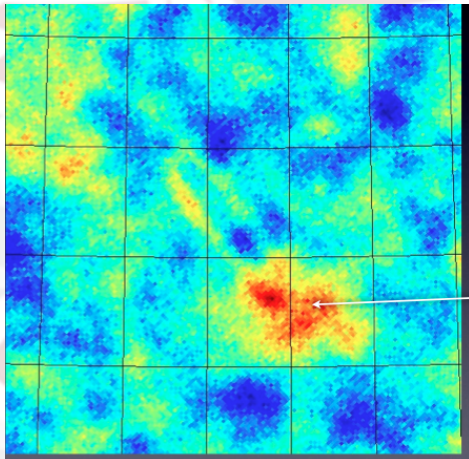

Planck 143GHz, DX5

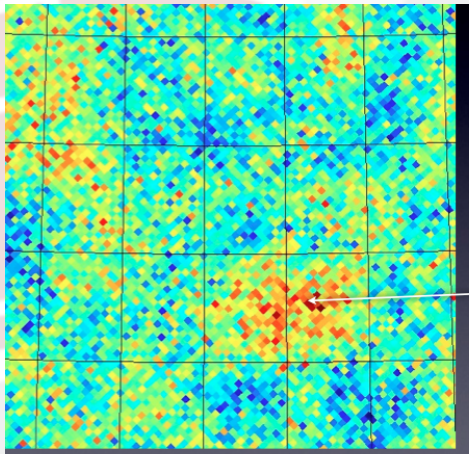

Planck 70.3GHz, DX5

The case of NGC 205

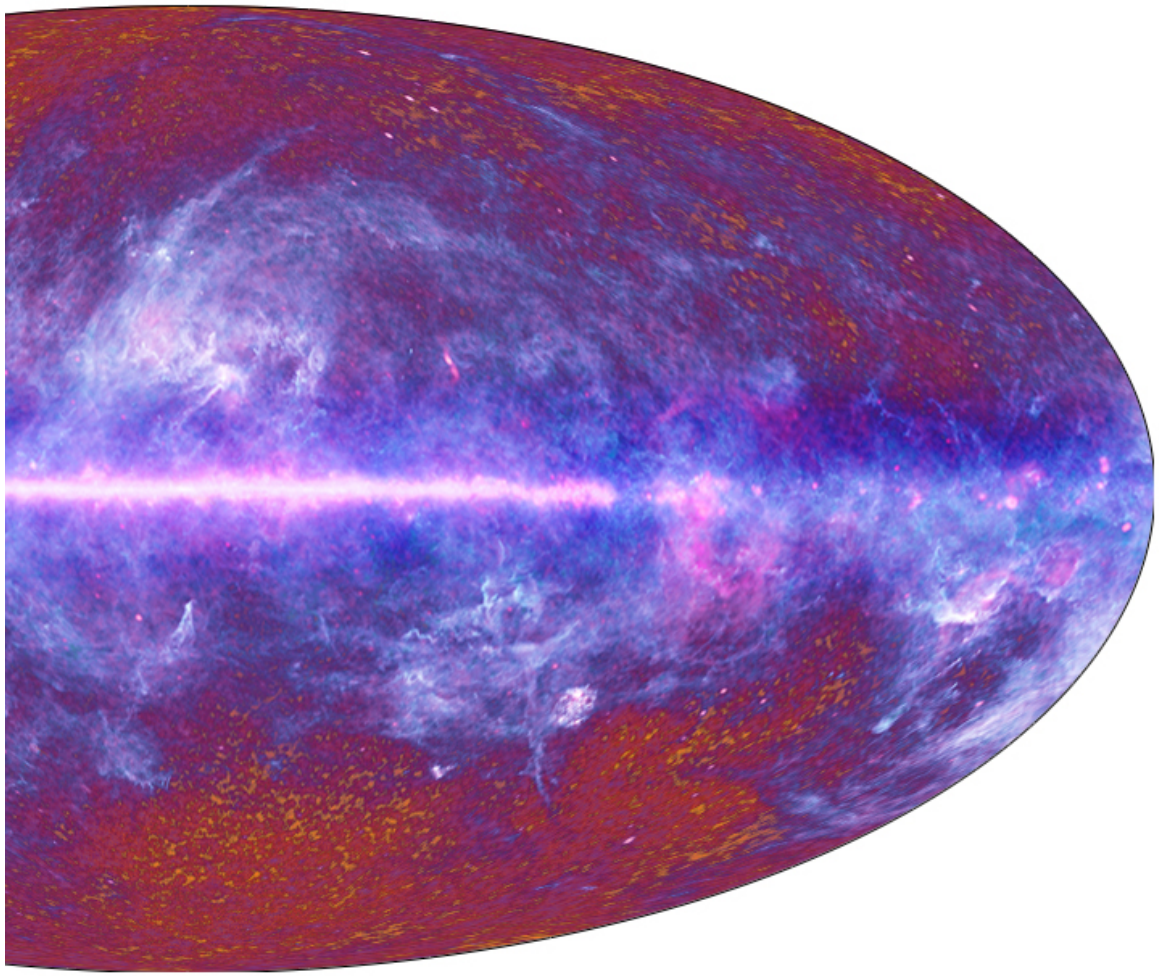

Several slides comes
from courtesy of
G. Lagache

CIB anisotropies in Planck/HFI: component separation and measurements

(Planck Early results, XVIII, A&A 536, 18)

Angular power spectrum of CIB anisotropies with Planck/HFI

- Planck: all sky but…
  - a lot of diffuse Galactic cirrus contamination
  - the CMB is there… It is our noise.

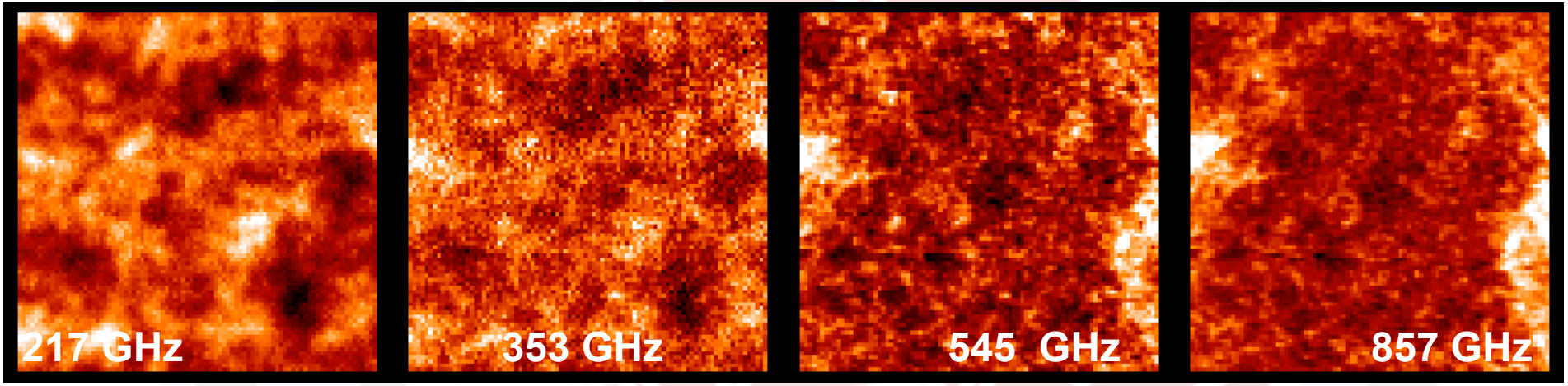

  - First analysis:
    - Six high-Galactic latitude fields for a total of 140 Sq. Deg.
    - Very low dust contamination - <N(HI)>= 0.7 – 1.8 10^{20} at/cm^2

- Component separation based on templates removal
  - *Planck*/HFI 143 GHz map for the CMB (wiener-filtered)
  - HI GBT data for Galactic dust *(Martin+2011)*

Removing Galactic dust: why not using FDS99 maps?

- Why not using the Finkbeiner et al. 1999 extrapolation?
  - Because of CIB anisotropies in the IRAS map at 100 microns (see Pénin et al. 2012) !

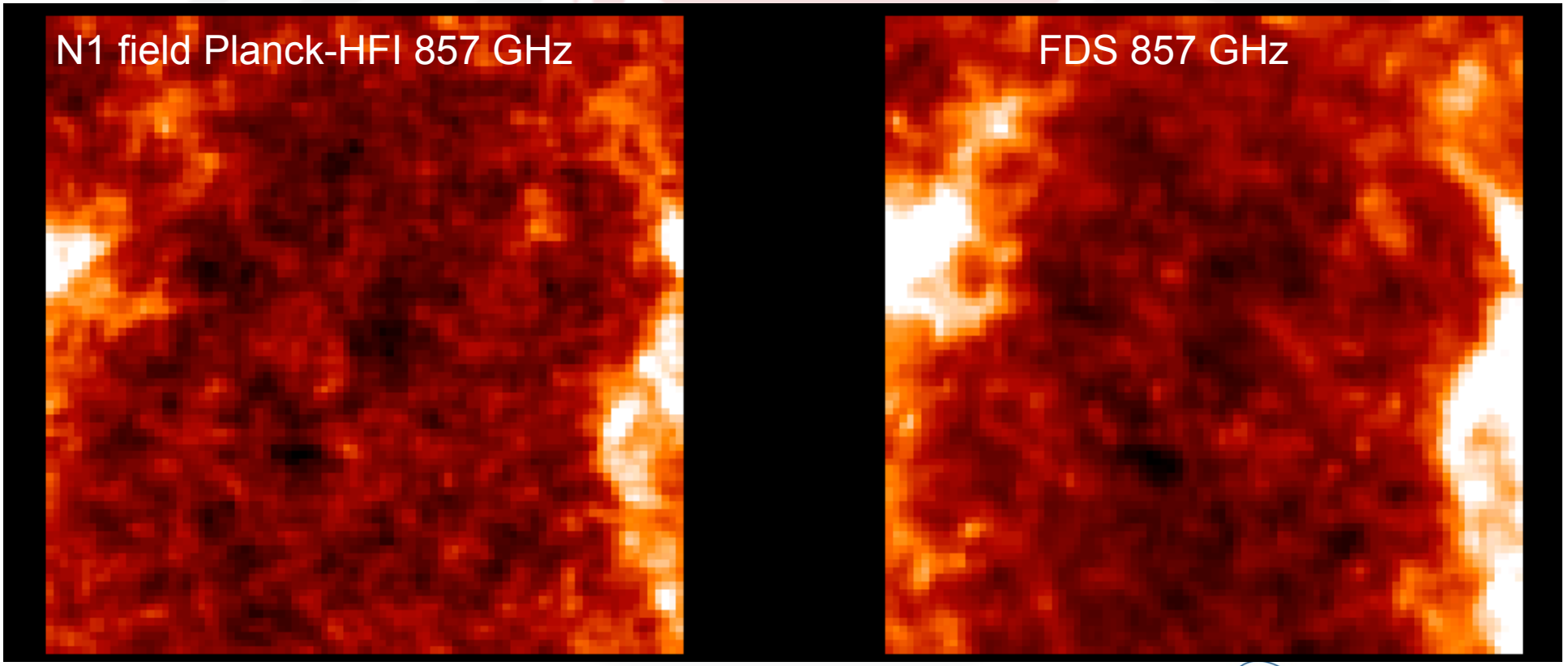

Component separation: removing Galactic dust

HI: best tracer of dust emission in the diffuse sky

- HI data in each field: different velocity components (local, IVC, HVC)

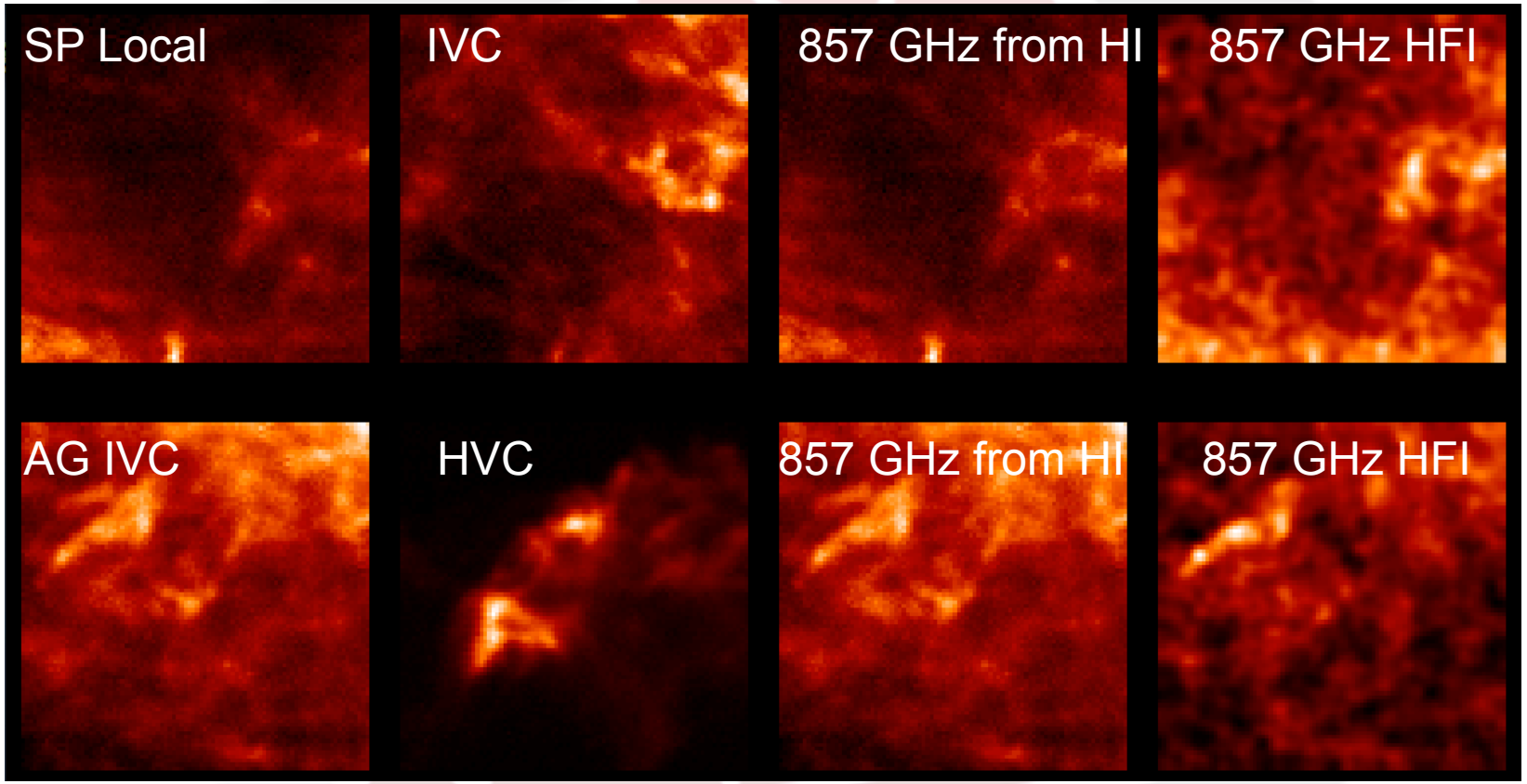

(See astroph 1101.2036)

- Model: *Planck*/HFI at each ν

$$I_\nu(x,y) = \sum_i \alpha_\nu^i N_{HI}^i(x,y) + C_\nu(x,y)$$

Component separation: removing CMB

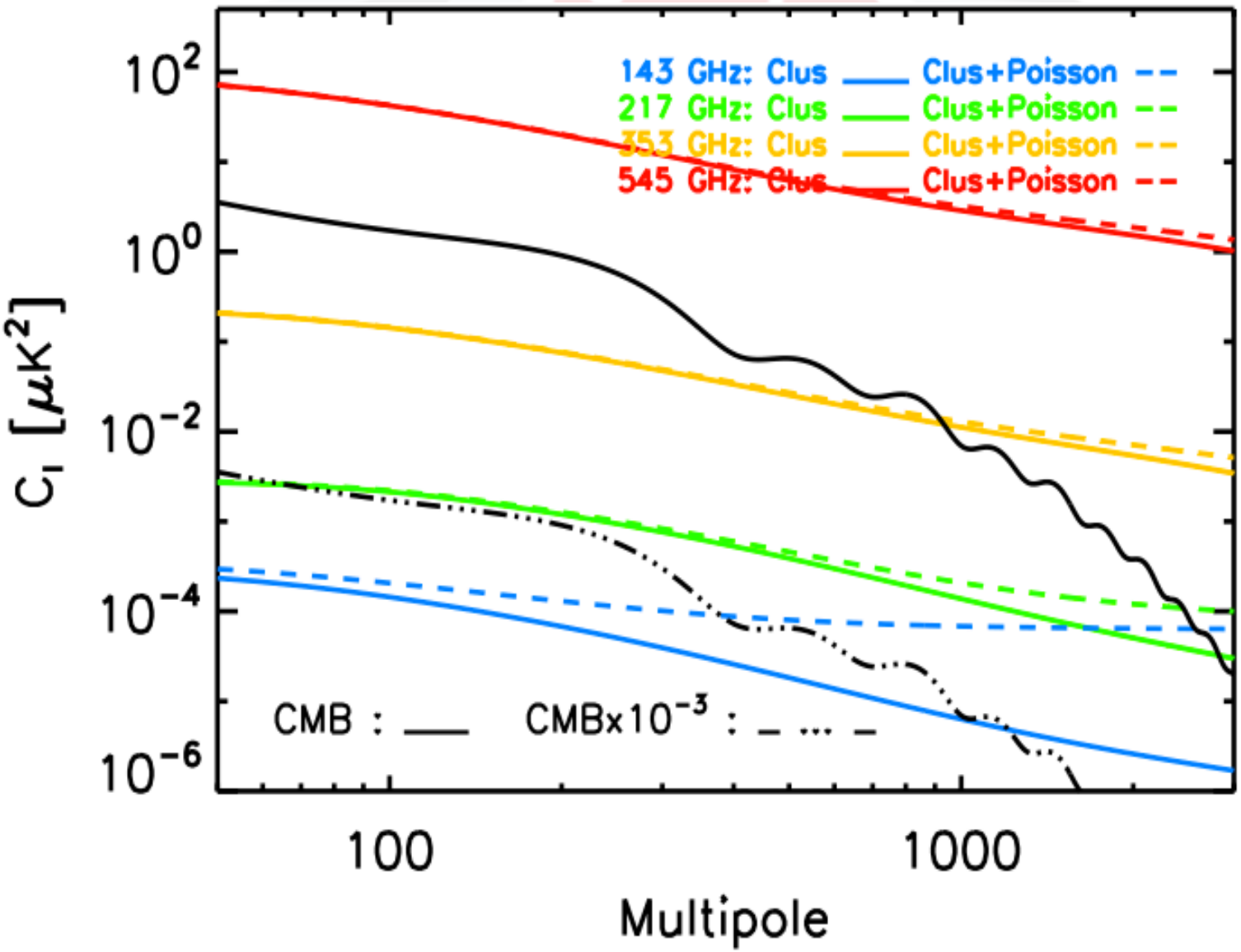

Component separation: removing CMB

- Whatever the component separation method:
  - Problem of « decontamination » (CIB leakage in CMB map)
  - Need a CIB model to decontaminate but this is what we want to measure….

- To avoid CIB leakage: use much lower frequencies (example: CMB map from component separation using only 30-40-70-100 GHz) but low angular resolution.

- The simplest: template CMB map (wiener filtering)
  - 143 GHz frequency maps wiener filtered for 217 and 353 GHz
    - CIB contamination of about 10% at 217 GHz (M. Remazeille)
  - 100 GHz frequency maps wiener filtered for 143 GHz (but low S/N)

Component separation: residual maps

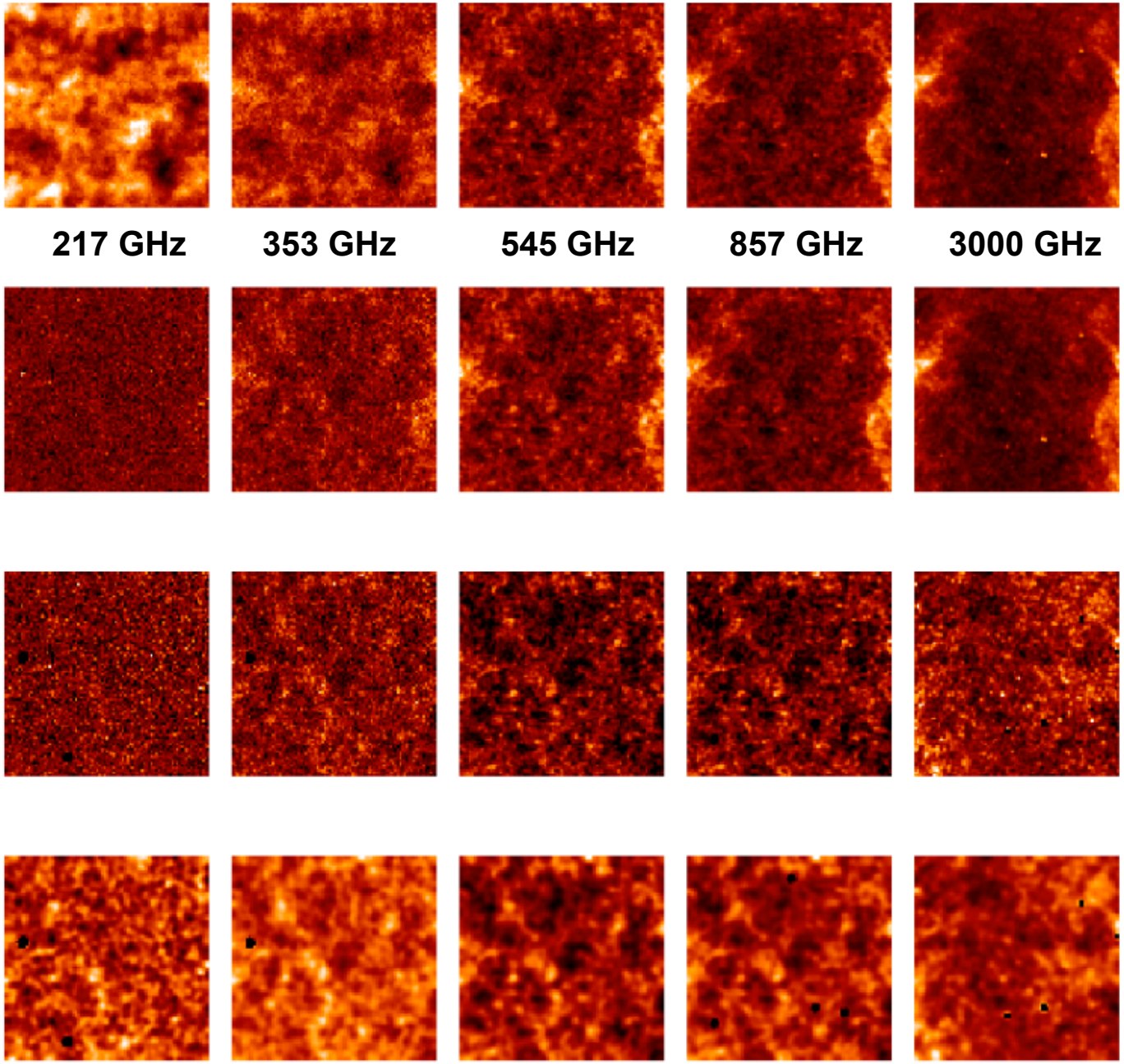

HFI « raw » maps
26.4 Sq. Deg.

Raw maps
– CMB

CIB maps
= Raw maps
– CMB
– Galactic dust
(PS mask)

CIB maps @
10 arcmin

Component separation: residual power spectra

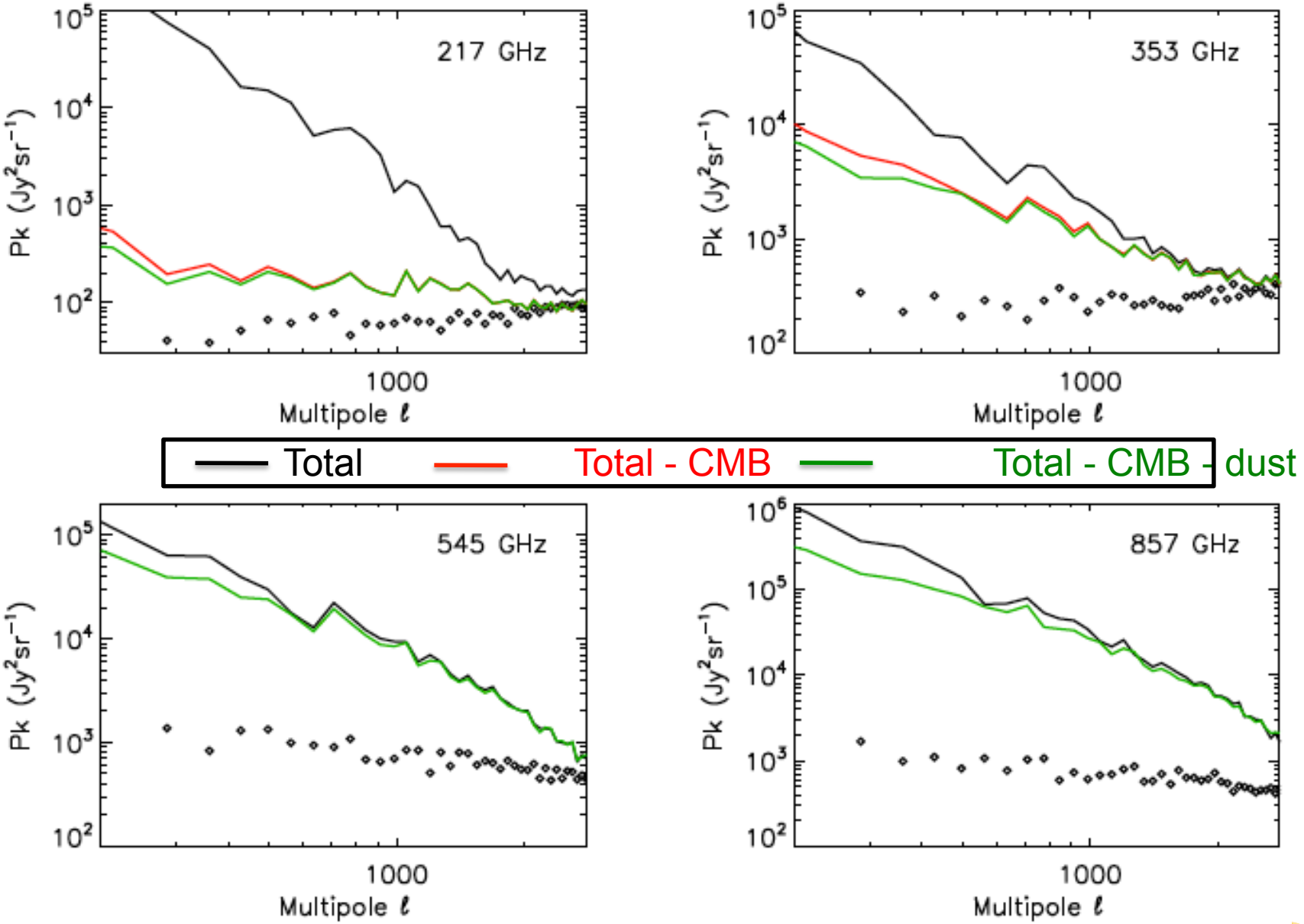

Planck Early Results:
Power spectrum of CIB anisotropies with Planck/HFI

Cosmic Infrared Background records much of the radiant energy released by processes of structure formation that have occurred since the decoupling of matter and radiation following the Big Bang.

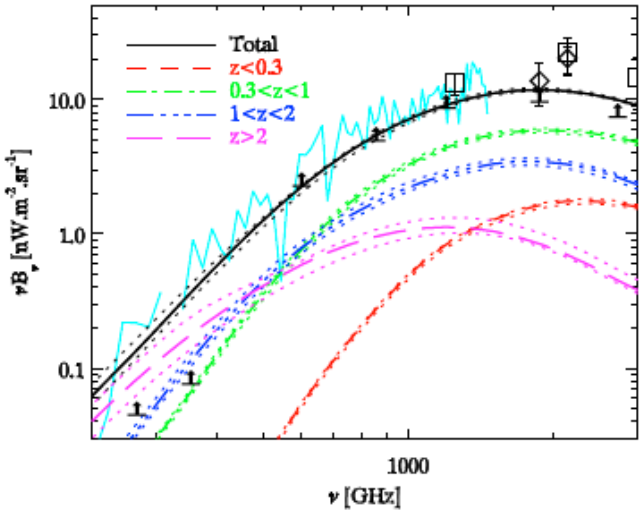

Contribution to the CIB per redshift slice, extracted from Bethermin et al. (2010b). Black solid line: CIB spectrum predicted by the model.

Due to its frequency coverage from 100 to 857 GHz, the HFI instrument onboard Planck is sensitive to the complete history of star-formation and is thus ideally suited to probe the dark matter/star-formation connection.

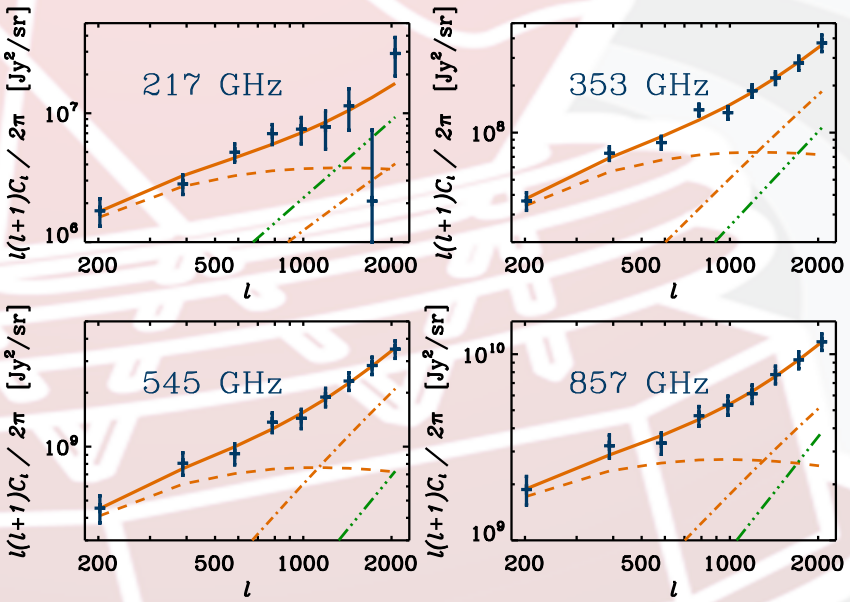

Power spectra are measured independently for the 6 fields and are then combined.

- First measurements at those wavelengths and spatial scales;

- We measure strong frequency-correlated structures consistent with the expected CIB signal. The correlation decreases with increasing frequency;

- No significant difference between the frequency spectrum of the CIB anisotropies and the CIB mean is observed;

Lesson from CIB

- **Planck data alone could exclude a model where galaxies trace the (linear theory) matter power spectrum with a scale-independent bias: that model requires an unrealistic high level of shot noise to match the small-scale power they observed.**
- **Consequently, an alternative model that couples the dusty galaxy, parametric evolution model of Bethermin et al. 2011 (A&A 529, A4:1-18) with a halo model approach has been developed.**
- **Characterized by only two parameters, this model provides an excellent fit to our measured anisotropy angular power spectrum for each frequency treated independently.**
- **In the next future, modelling and interpretation of the CIB anisotropy will be aided by the use cross-power spectra between bands, and by the combination of the Planck and Herschel data at 857 and 545/600 GHz and Planck and SPT/ACT data at 220 GHz.**

Current Extragalactic *Planck* Intermediate Papers

- Comparison of VLA/ERCSC fluxes
- Characterization of the first *Planck* high-z candidates
- Statistical Properties of Infrared and Radio Sources from the *Planck ERCS Catalog*
- Confirmation and first scientific characterization of new *Planck clusters from XMM validation follow-up*
- The gas content of dark matter halos: the Sunyaev-Zel'dovich stellar mass relation for central galaxies
- Physics of the hot gas in the Coma cluster
- Comparison of Sunyaev-Zel'dovich measurements from *Planck* and from the Arcminute Microkelvin Imager for 11 galaxy clusters
- The relation between galaxy cluster mass and Sunyaev-Zel'dovich effect

Galactic science (WG7)

Galactic studies with Planck

- The Planck multifrequency view of our Galaxy allowed for the first time a detailed investigation of many interesting topics
- Early studies/papers achieved crucial results on the following aspects:
  - Dark gas in the Galaxy
  - Microwave anomalous emission
  - Interstellar medium
  - Cold cores
  - Thermal dust on nearby molecular clouds

New Light on Anomalous Microwave Emission from Spinning Dust Grains

Planck, combined with ancillary radio and FIR data, has provided a unique opportunity to establish a comprehensive spectrum of AME: **present observations strongly favour the spinning dust (electro-dipole radiation) mechanism** which provides a good fit to the microwave (10 − 100 GHz) part of their spectra which peaks at ≈ 30 GHz

The two best-studied AME sources that have extensive ancillary data are in

Perseus and ρ Ophiuchus molecular clouds

Using parameters constrained at smaller angular scales, the 20 − 40 GHz AME peak in Perseus is well explained with spinning dust emission arising from dense, molecular gas (nH > 200 cm^{-3}) subjected to a few times the interstellar radiation field. The contribution from low density gas appear to only play a minor role

In the case of ρ Ophiuchus, irradiated, high density molecular gas from the PDR appears to contribute in the range 50 − 100 GHz. The picture seems to be that smaller PAHs are found in PDRs (G0 > 100) as suggested by recent Spitzer observations

- Determination of the PAH size degenerate with that of nH and G0 and quantitative conclusions will be obtained from consistent modeling of the gas state, radiative transfer and spinning dust
- At this level of modelling it is not possible to constrain the electric dipole moment of PAHs
- Planck data provide a rich source of observations that can be used as a basis for developing a realistic understanding of the AME mechanism in a range of Galactic environments

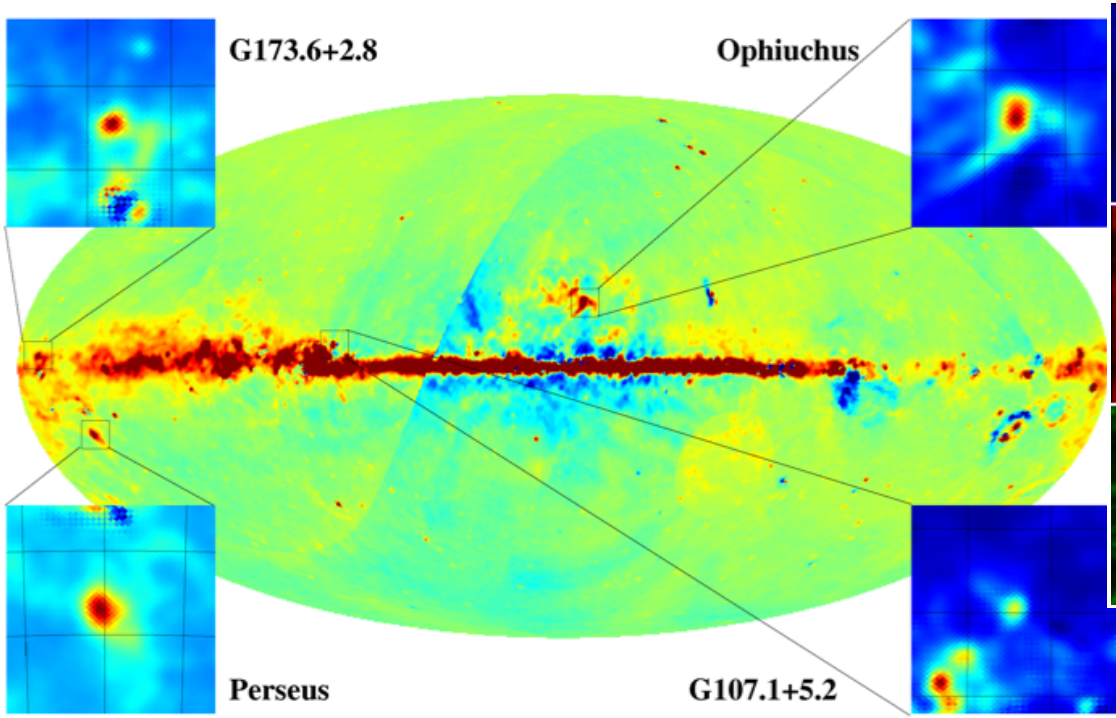

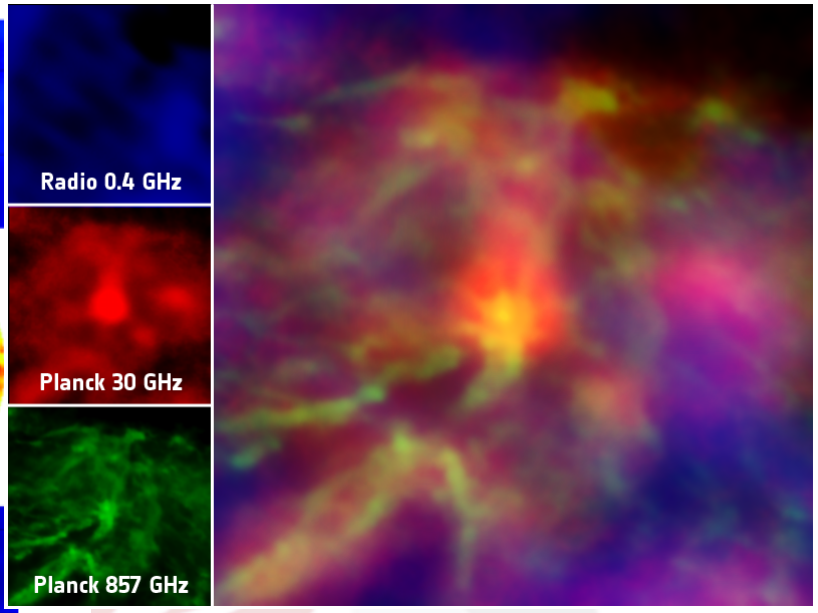

Fig. 10. Residuals in the full sky *Planck* LFI 28.5 GHz 1° smoothed map after subtraction of synchrotron, free-free and thermal dust emission (see text). 12.°5 × 12.°5 cut out maps are shown for the Perseus and ρ Ophiuchus molecular clouds, and the two new regions of AME, G107.1+5.2 and G173.6+2.8.

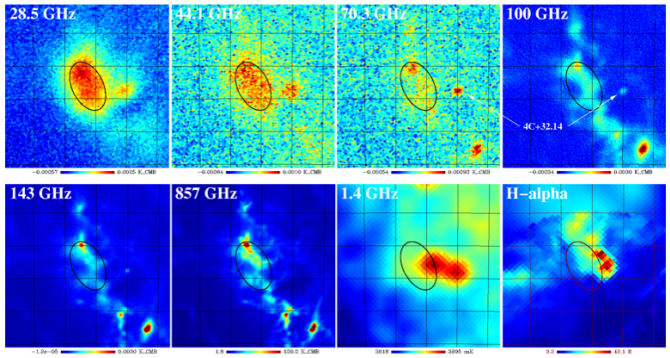

Fig. 1. Maps of the Perseus molecular cloud region at their original angular resolution. From left to right, top row: *Planck* 28.5, 44.1, 70.3 and 100 GHz, bottom row: *Planck* 143 and 857 GHz, 1.4 GHz and Hα. The maps cover 5° × 5° centred on $(l, b) = (162.°26, -18.°62)$ and have linear colour scales. The graticule has 1° spacing. The FWHM of the elliptical Gaussian model used to fit the flux density in the filtered maps (see text) is shown. The strong AME is evident at 30 – 70 GHz.

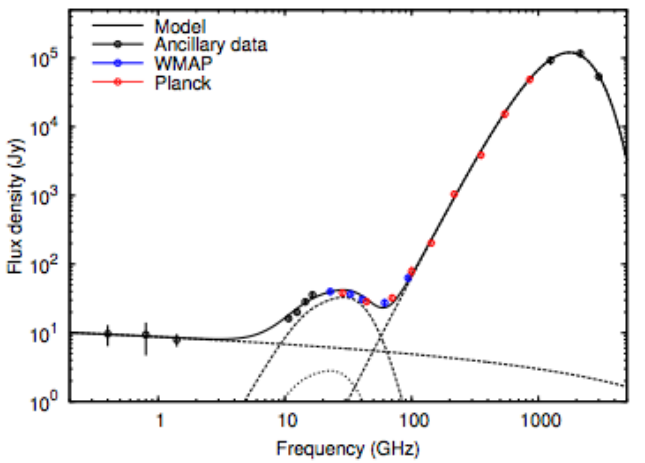

Fig. 4. Spectrum of G160.26-18.62 in the Perseus molecular cloud. The best-fitting model consisting of free-free, spinning dust (2 components), and thermal dust is shown.

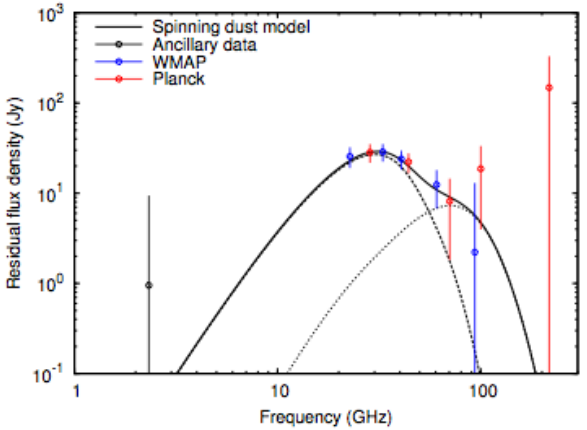

Fig. 9. Spectrum of G353.05+16.90 in the ρ Ophiuchus molecular cloud after subtracting the best fit free-free, CMB and thermal dust components. A theoretical spinning dust model consisting of two components (dark cloud and PDR; see text), is shown.

The Galactic Cold Core Population revealed by the first all-sky survey - I

- Statistical properties of **the first version of the Cold Core Catalogue of Planck Objects (C3PO)**, in terms of their **spatial distribution, temperature, distance, mass, and morphology**
- Statistics of the Early Cold Core Catalog (ECC): it is a subset of the complete catalogue that contains only the most reliable detections
- ECC is delivered as a part of the ERCSC
- CoCoCoDeT algorithm to extract **about 10 thousands cold sources**
- The method uses the **IRAS 100μm data as a warm template** that is extrapolated to the Planck bands and subtracted from the signal, leading to a detection of the cold residual emission
- **Cross-correlation with ancillary data** to increase the reliability of our sample, and to derive other key properties like distance and mass
- **Temperature and spectral index values** derived using the fluxes in the **IRAS 100 μm band** and the **three highest frequency Planck bands**

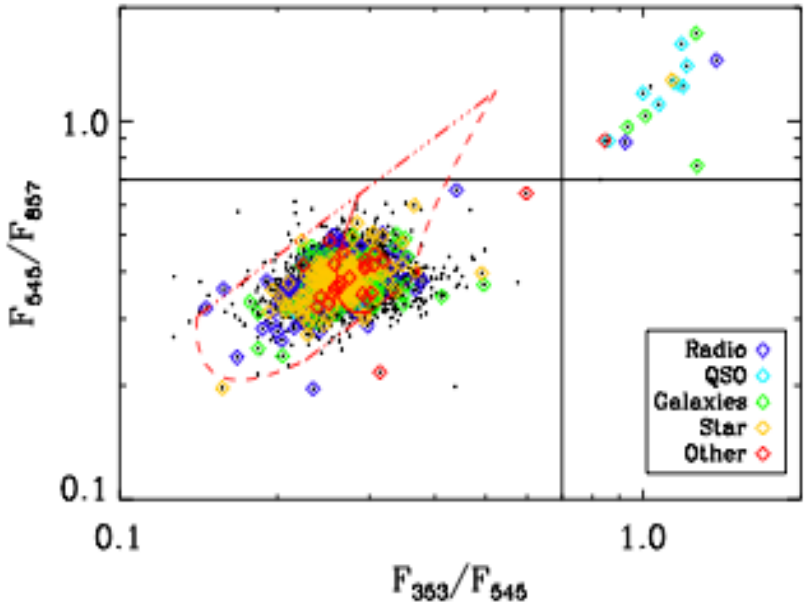

Fig. 1. Color-Color diagram of the catalogue. The over-plotted symbols stand for the positive cross-macthes with non ISM objects. The red contours give the domain of the diagram filled by Archeops cold cores assumed to follow a grey-body law, with a temperature ranging from 6 K < T < 25 K, and a spectral index β given by Désert et al. (2008).

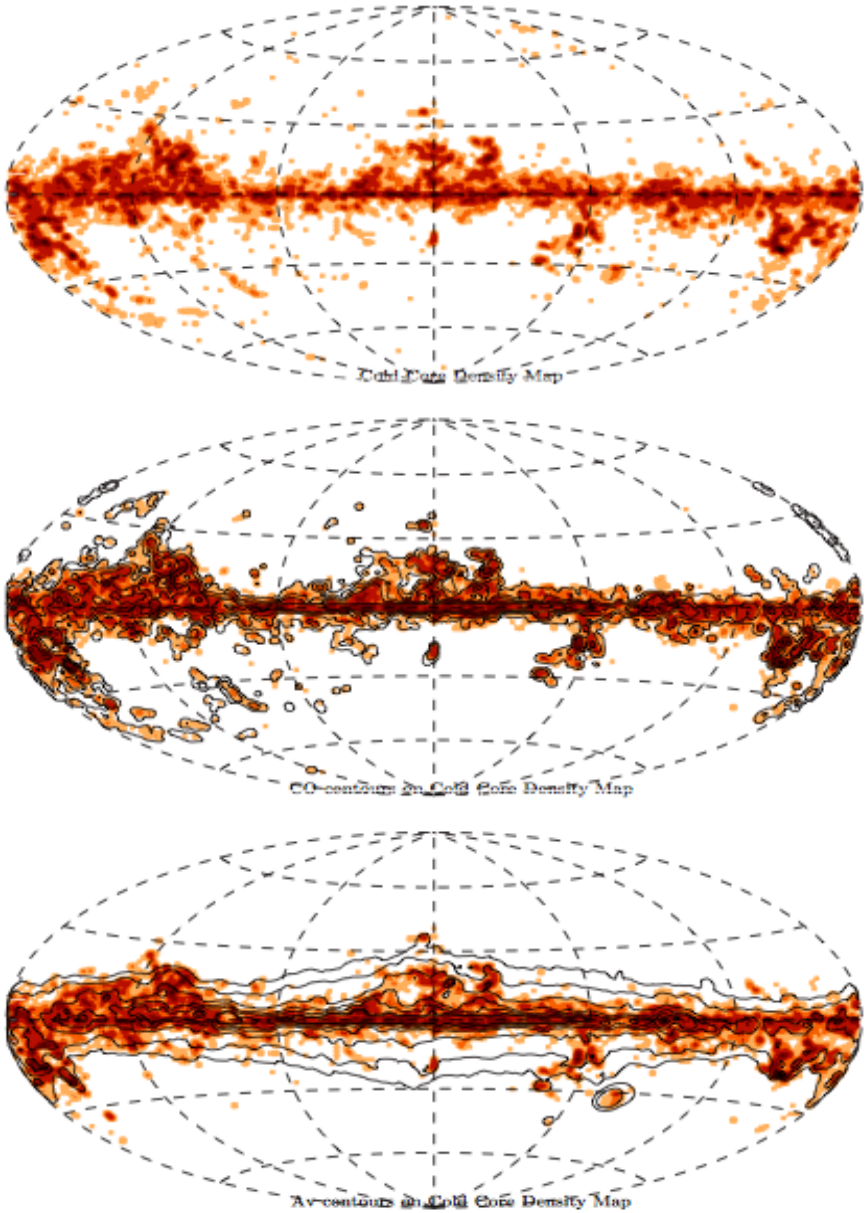

Fig. 3. Upper panel: All-sky density map of the C3PO *Planck* Cold Clumps, smoothed at 3°. Middle panel: CO contours are over-plotted on the C3PO density map which is set to 0 where CO map is not defined. Lower panel: Av contours are over-plotted on the C3PO density map which is set to 0 where Av map is lower than 0.1 Av.

v1.0

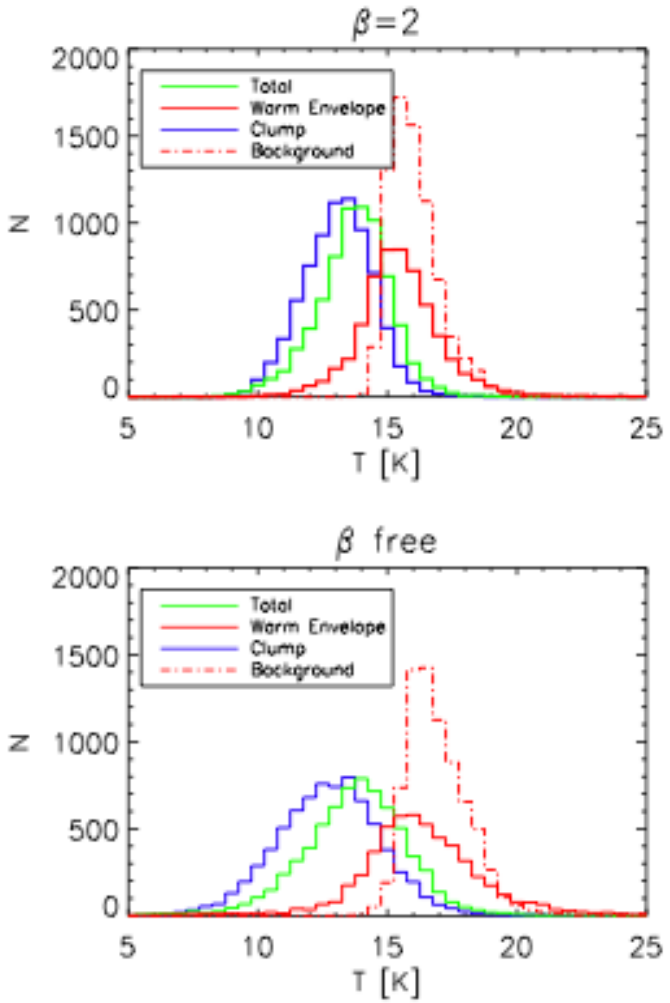

Fig. 6. Distribution of the temperature of the cold clumps (blue), of the warm envelope (red) and of the total (green) estimated inside the elliptical gaussian of the clump itself. The averaged temperature of the local background is plotted in red dot-dash line.

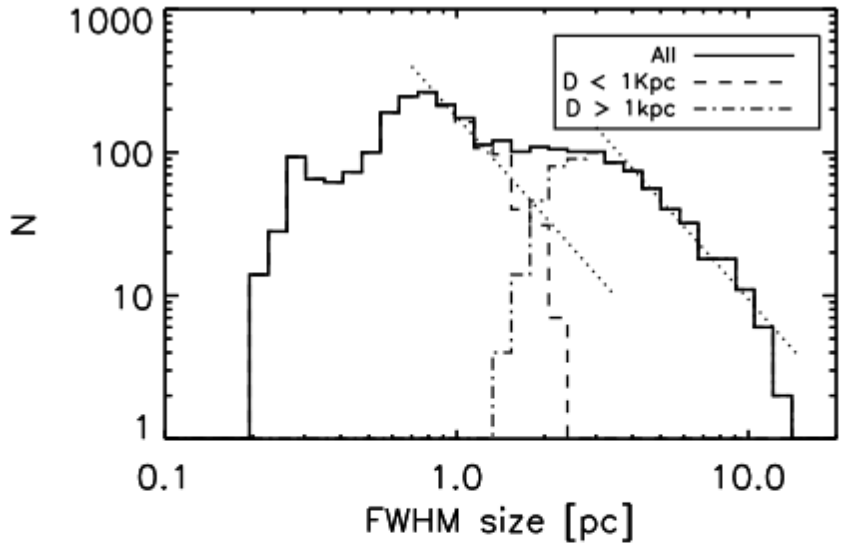

Fig. 9. Distribution of the physical size of the cold clumps in pc. The distinction is done between the local sample ($D < 1$kpc, dashed line) and the distant sample ($D > 1$kpc, dot-dash line). A power law with $\alpha = -2.3$ is overlaid in dotted line over the 2 subsets.

Current Galactic *Planck* Intermediate Papers

- Anomalous microwave emission in Galactic HII regions and Galactic clouds
- Component separation in the Gould Belt System
- A map of CO extracted from *Planck*
- The Galactic Haze as seen by *Planck*
- Galactic PNe with *Planck*
- Herschel observations of selected *Planck* cold clumps

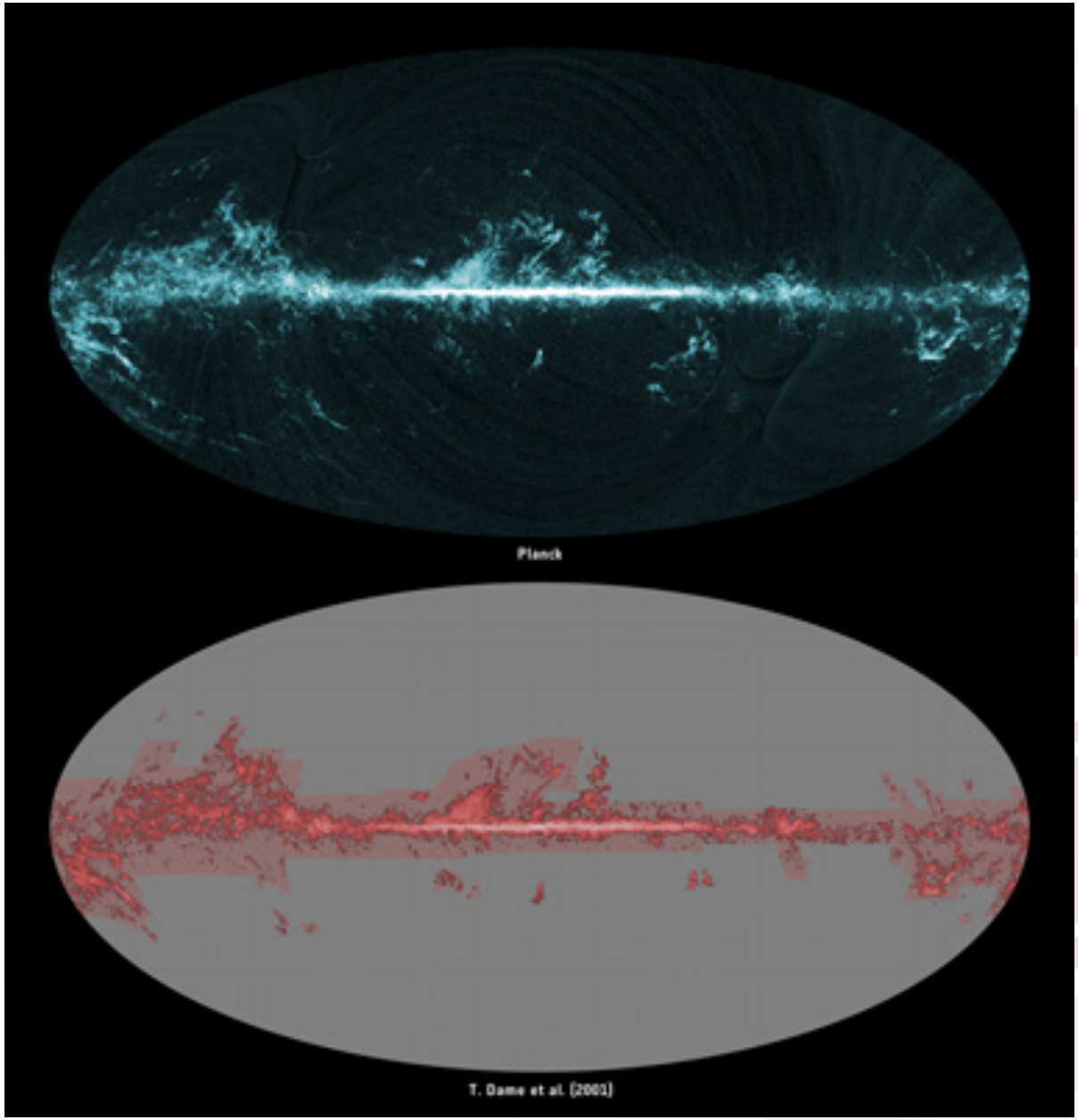

CO map

This all-sky image shows the distribution of carbon monoxide (CO), a molecule used by astronomers to trace molecular clouds across the sky, as seen by Planck (blue).

Carbon monoxide (CO) emits a number of rotational emission lines in the frequency range probed by Planck's High Frequency Instrument (HFI).

A compilation of previous surveys (Dame et al. (2001)), which left large areas of the sky unobserved, is shown for comparison (red).

CO map & specific sky areas

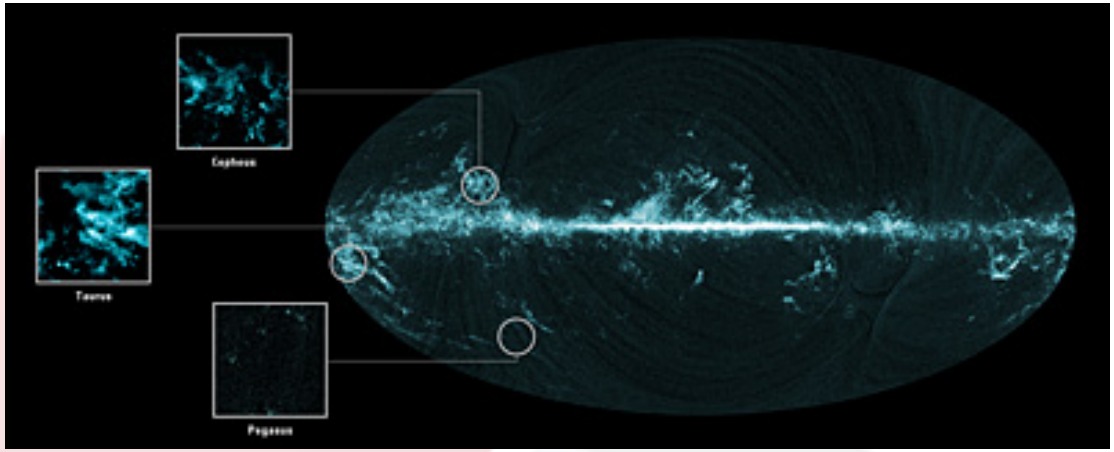

The inserts provide a zoomed-in view onto three individual regions on the sky where Planck has detected concentrations of CO: Cepheus, Taurus and Pegasus, respectively.

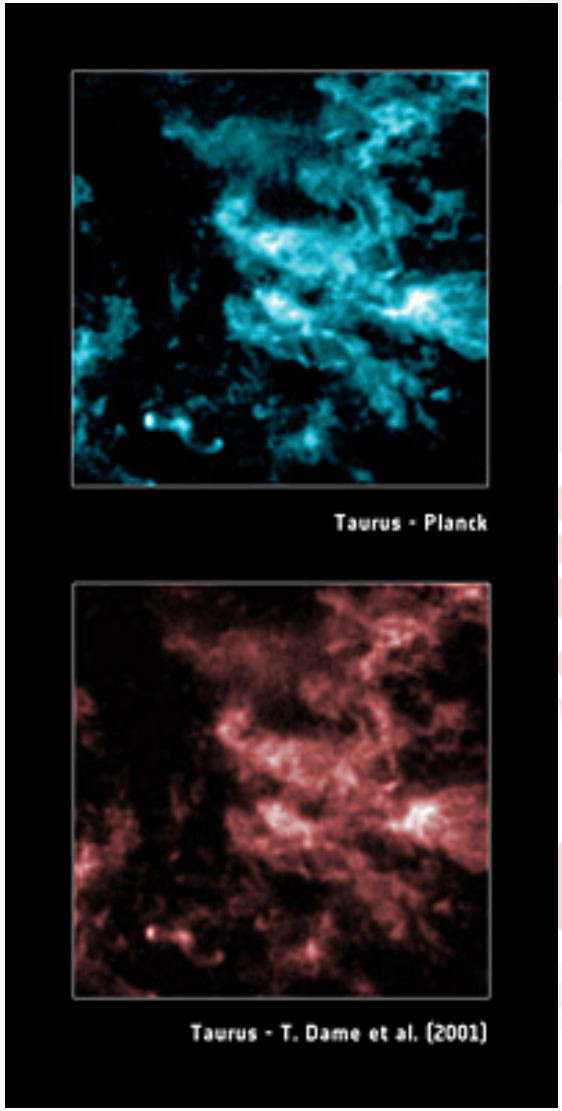

Taurus molecular cloud complex as seen through the glow of carbon monoxide (CO) with Planck (blue). The same region is shown as imaged by previous CO surveys (Dame et al., 2001) for comparison (red).

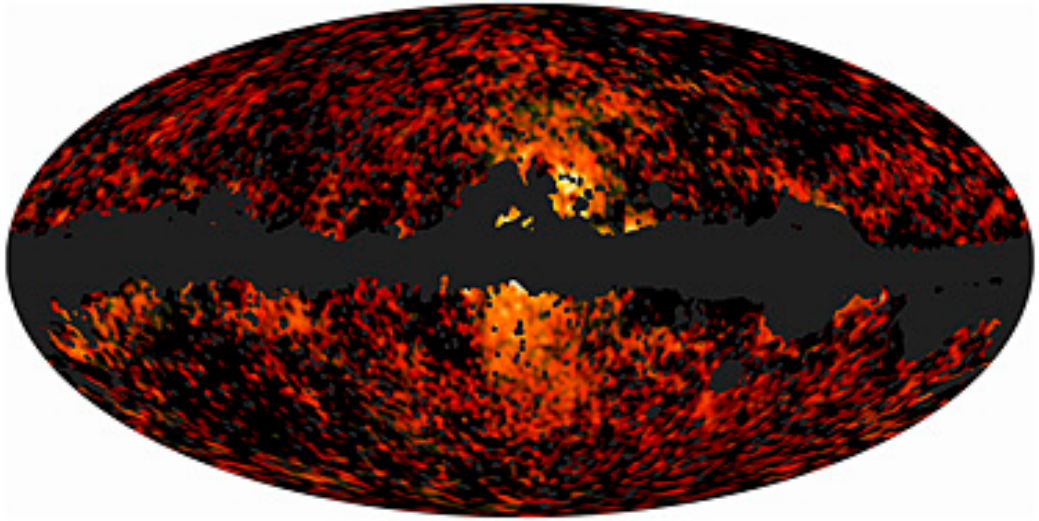

Haze with *Planck*

❖**Galactic Haze at 30 and 44 GHz, extracted from the Planck observations.** In addition to this component, other foreground components such as synchrotron and free-free radiation, thermal dust, spinning dust, and extragalactic point sources contribute to the total emission detected by Planck at these frequencies. The prominent empty band across the plane of the Galaxy corresponds to the mask that has been used in the analysis of the data to exclude regions with strong foreground contamination due to the Galaxy's diffuse emission. The mask also includes strong point-like sources located over the whole sky.

❖The **Galactic Haze** is seen to be distributed **around the Galactic Centre** and its **spectrum is similar to that of synchrotron emission.** However, compared to the synchrotron emission seen elsewhere in the Milky Way, the Galactic **Haze has a 'harder' spectrum**, meaning that its emission **does not decline as rapidly with increasing frequency.** Diffuse synchrotron emission in the Galaxy is interpreted as **radiation from highly energetic electrons** that have been accelerated in shocks created by supernova explosions.

Haze with *Planck & Fermi*

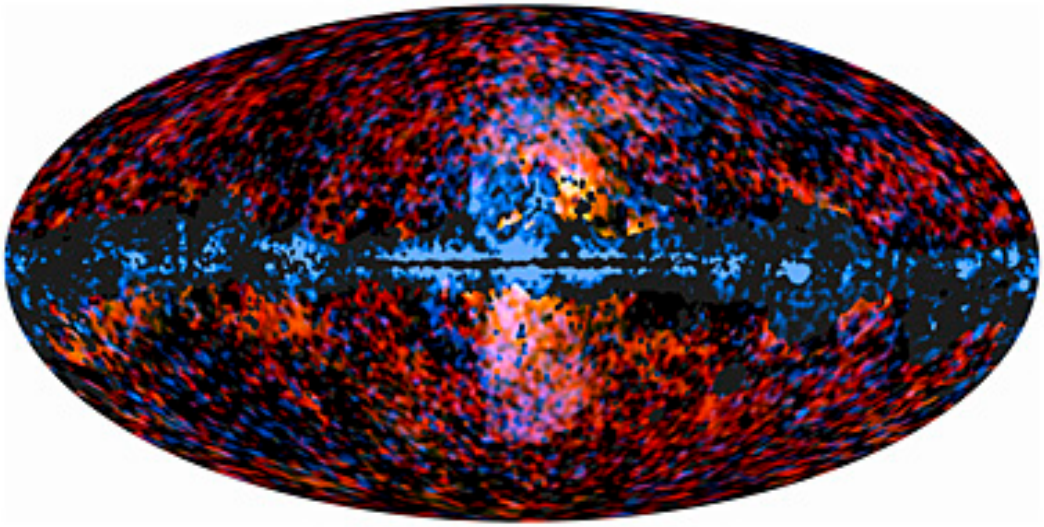

❖The **Fermi** data (shown here in blue) correspond to observations performed at energies **between 10 and 100 GeV** and reveal **two bubble-shaped, gamma-ray emitting structures** extending from the Galactic Centre.

❖The two emission regions seen by **Planck and Fermi** at two opposite ends of the electromagnetic spectrum **correlate spatially quite well** and might indeed be a **manifestation of the same population of electrons** via different radiation processes.

← Distribution of the Galactic Haze seen by ESA's Planck (shown here in red and yellow at LFI frequencies of 30 and 44 GHz) mission at microwave frequencies superimposed over the high-energy sky as seen by NASA's Fermi Gamma-ray Space Telescope.

❖**Several explanations** have been proposed for this unusual behaviour, including ***enhanced supernova rates, galactic winds and even annihilation of dark-matter particles.*** Thus far, none of them have been confirmed and the issue remains open.

On-going / Future studies

Topics: Galactic science

- (a) Construction of a model of the large scale ordered magnetic field in the Galaxy, based on the polarised Planck maps.
- (b) Study of the diffuse warm ionized gas in the Galaxy, based on the Planck map of free-free emission.
- (c) Reconstruction of the Galacto-centric distribution of emission of the different phases of the interstellar medium in the Galaxy (H2, HI, H), by correlation of the Planck maps to tracers of each phase.
- (d) Study of the diffuse synchrotron emission from the Galaxy, in particular its spectrum and its spatial structure.
- (e) Study of the physical characteristics of the circumstellar environment of various types of stellar objects in the final phases of their evolution.
- (f) Construction and analysis of a catalogue of compact and ultra-compact HII regions and massive young stellar objects.
- (g) Construction and analysis of a catalogue of cold pre-stellar cores in the Galaxy.

Topics: Galactic science

- (h) Study of the spectral energy distributions of Supernova Remnants across the Planck bands.
- (i) Study of the spatial and spectral distribution of thermal dust polarisation to elucidate the nature of dust in the various phases of the interstellar medium.
- (j) Establishment of the spatial and spectral properties of the anomalous emission so far attributed to spinning dust particles.
- (k) Combination of Planck maps with lower frequency large-scale ground based surveys to study the relationships between the various phases of the Galactic interstellar medium (atomic, molecular, ionized, relativistic, magnetic, etc.).
- (l) Study of the properties of dust in regions at high Galactic latitudes and in intermediate and high velocity clouds, using the Planck data in combination with other tracers such as HI, IRAS/IRIS etc.
- (m) Study of the Planck maps to determine the structure and distribution of mass in molecular clouds.
- (n) Study of the structure and intensity of the magnetic fields (ordered and tangled components) within nearby inter-stellar clouds, in relation with their density and velocity structure.

Detailed characterization of Galactic diffuse components

- 1. Synchrotron: pattern, spectral behaviour
- 2. Free-free: its relevance in particular close to the Galactic plane
- 3. Thermal dust: cold, warm components
- 4. Anomalous emission (spinning dust?)
- 5. Haze (astrophysics vs DM annihilation ?)
- → Galactic magnetic fields
  (ordered vs turbolent components)

see interesting recent papers
by Fauvet et al. 2011, 2012

- Dust grain properties
- ISM history

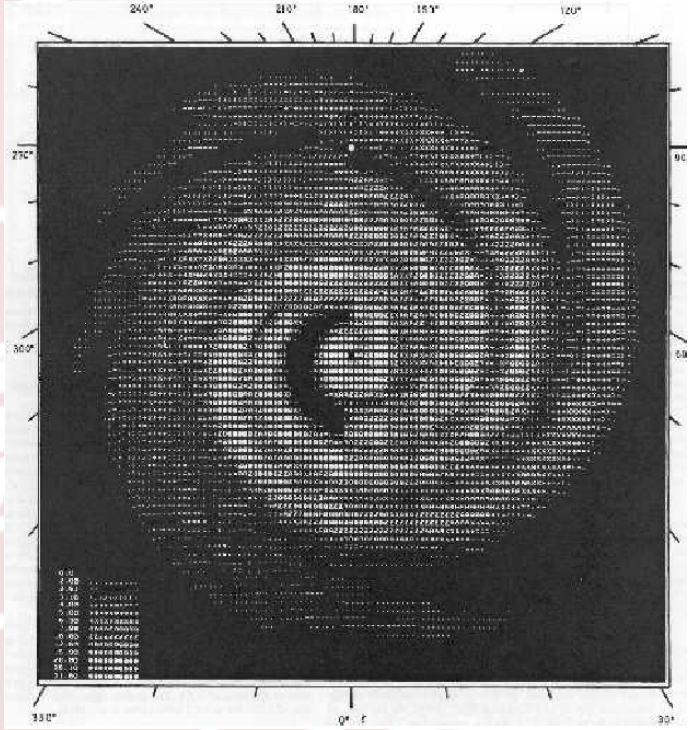

FIG 5.7.— Top view of the 3-D model of synchrotron emissivity derived from the Haslam map by Beuermann et al. (1985). The model contains assumptions on the Galactic magnetic field orientation and degree of alignment along the spiral arm, and therefore can be used to synthesize a map of synchrotron polarisation around the Sun (filled circle).

• Synchrotron Polarization

- Info from WMAP
- Info from radio surveys
- Relevance of Planck

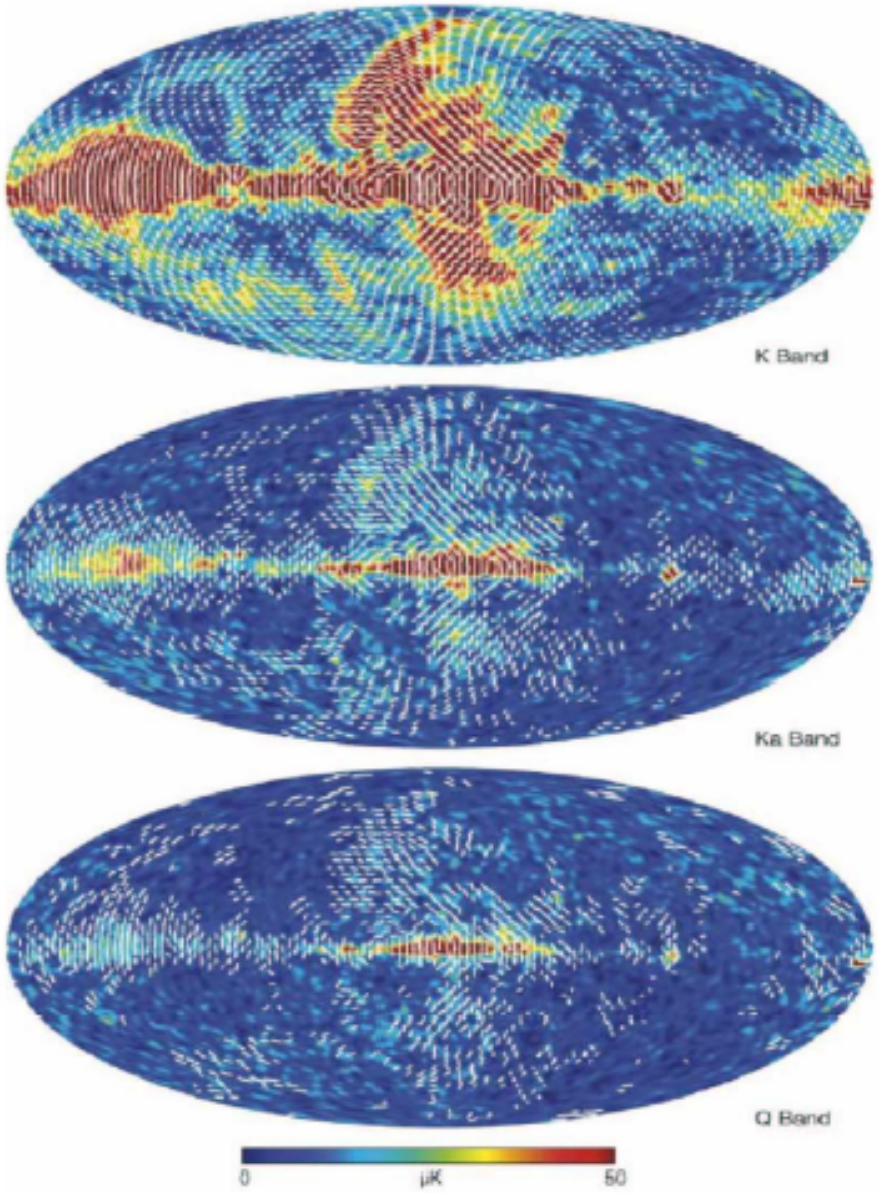

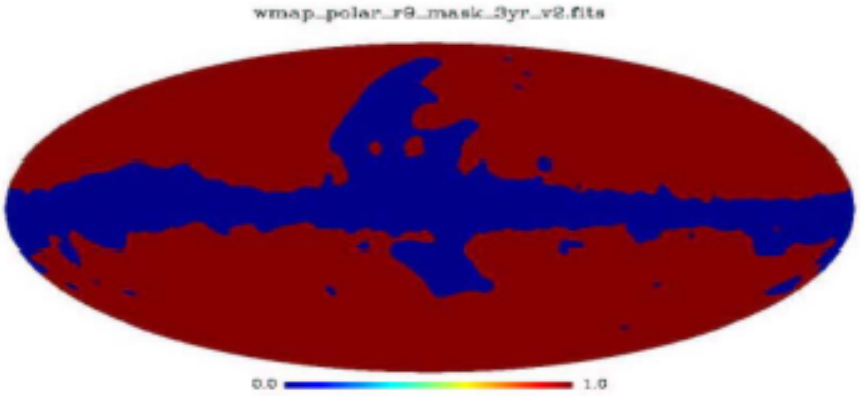

WMAP 3 yr Pol. maps and mask.

Polarization: Comparison of radio 1.4 GHz surveys with WMAP

Polarized Intensity

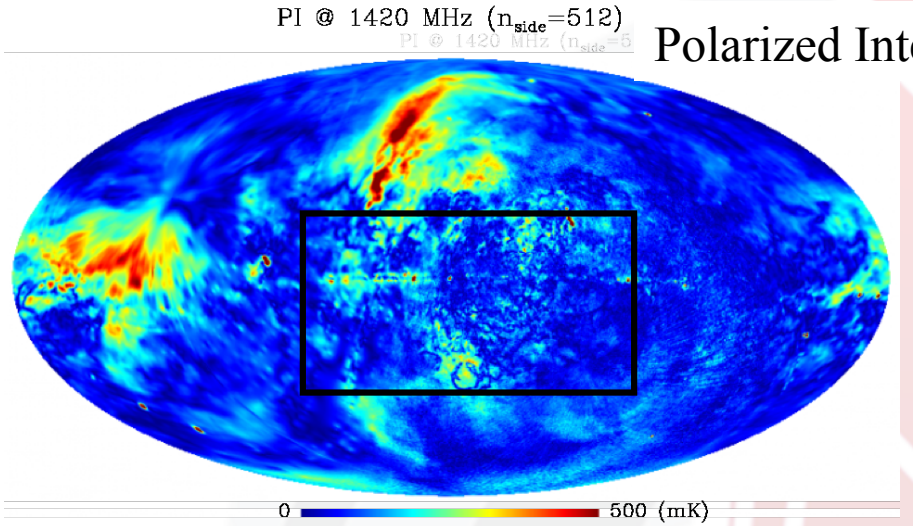

Polarized Intensity

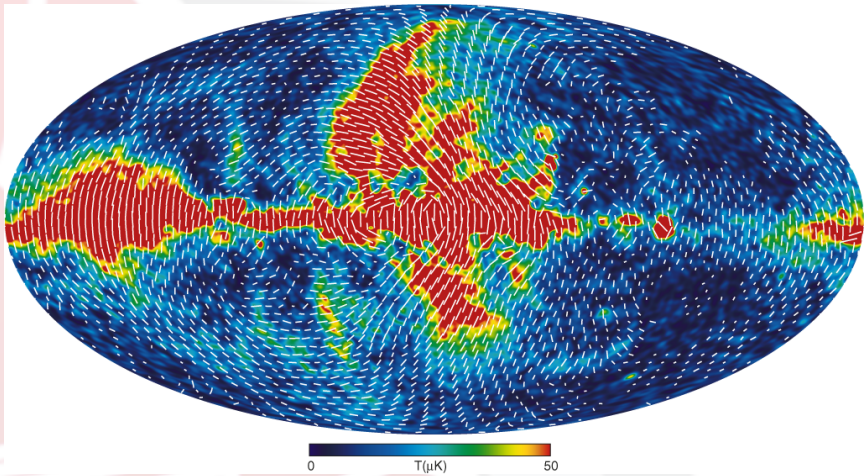

Polarization Angle

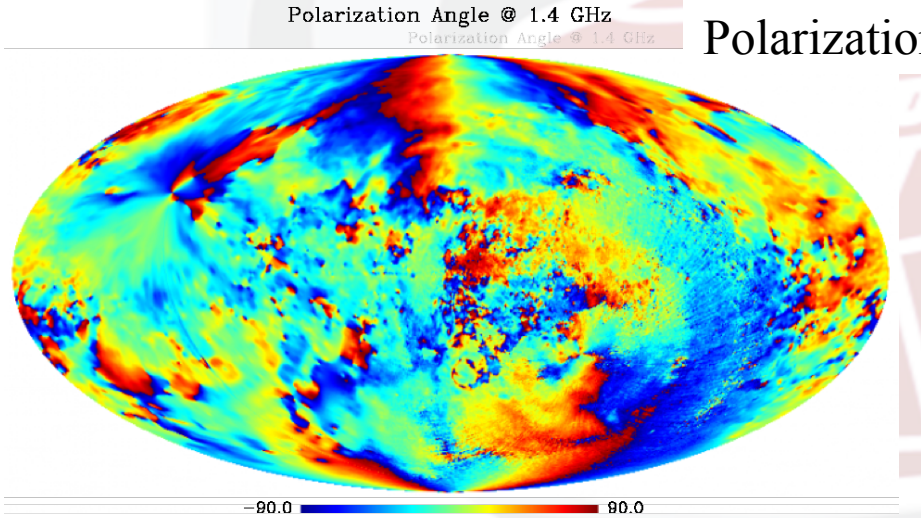

Polarization Angle + 90°

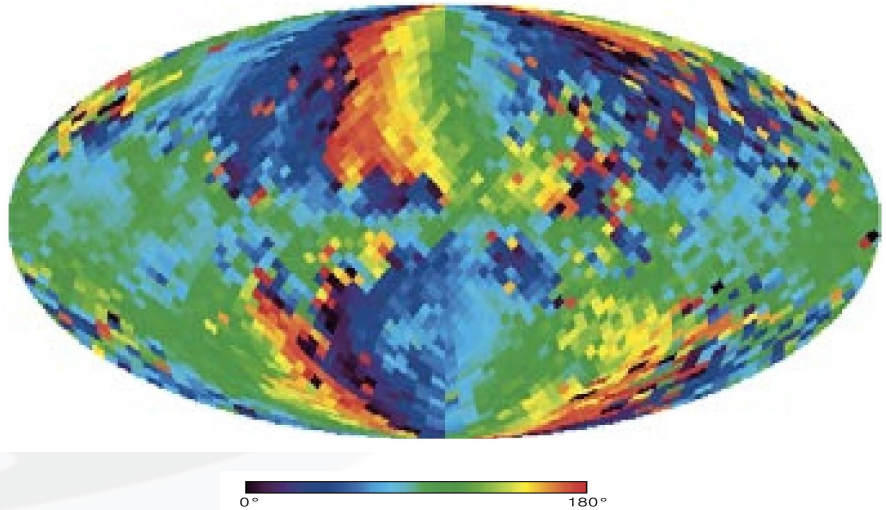

1.4 GHz *[Reich et al., in preparation]*

WMAP 23 GHz *[Page et al. 2006]*

Polarization: radio vs WMAP

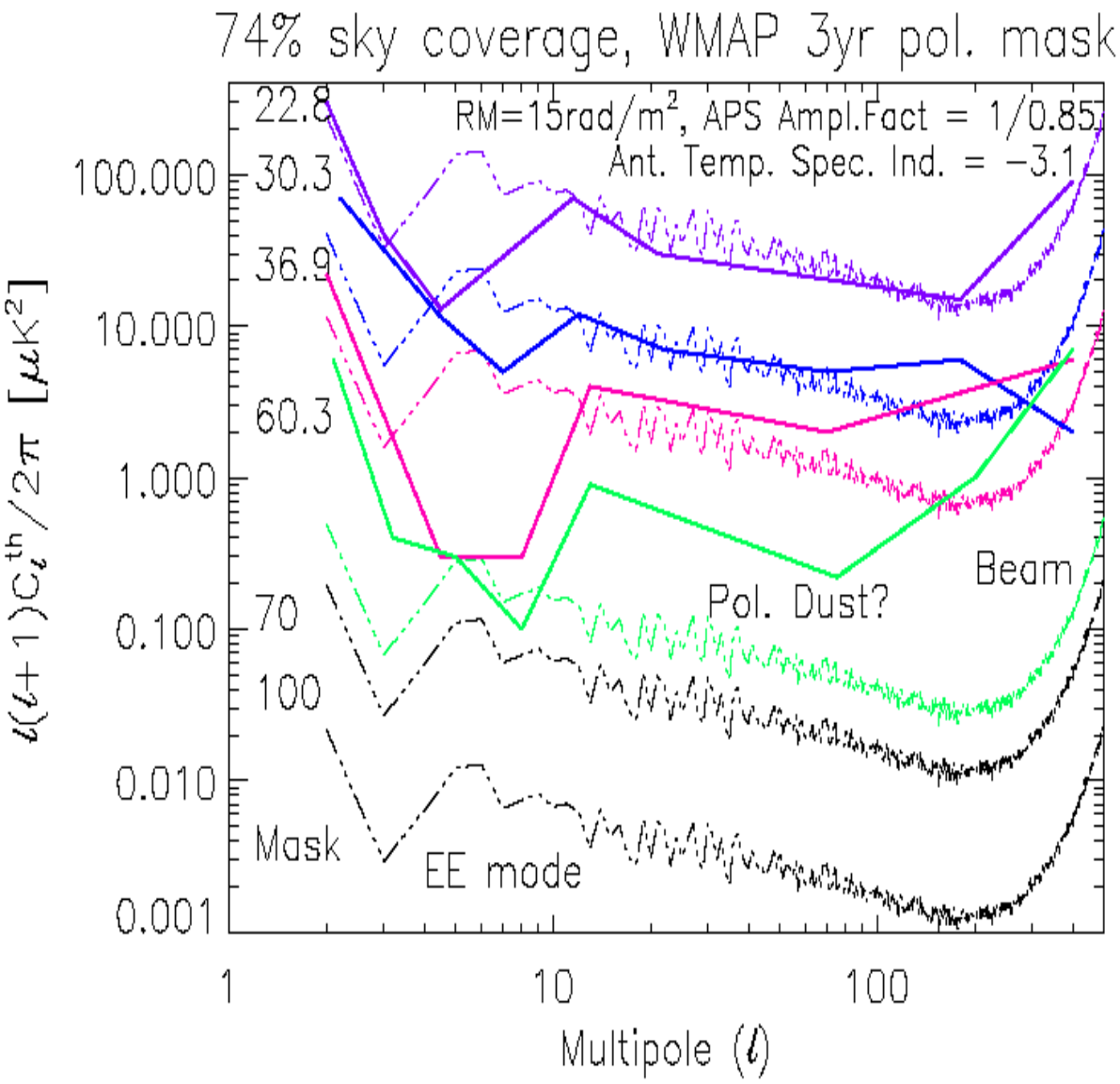

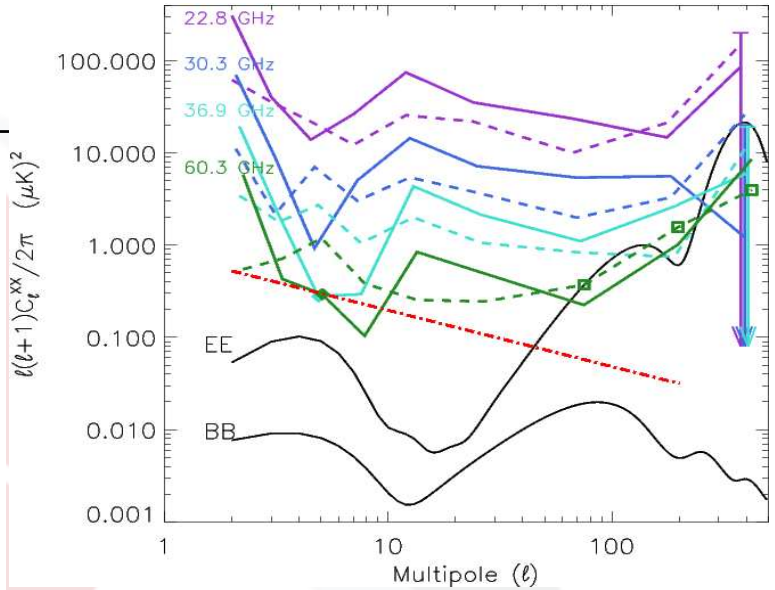

In agreement with WMAP results at intermediate ℓ (~ 10-100) within a factor ~ 2 or better, @ ν ≤ of about 40 GHz. Dust important @ higher ν

1.4 GHz new polarization maps good template of the large scale synchrotron emission

Burigana et al. 2006, PoS(CMB2006)016

KBOE - Large Scale Traces of Solar System Cold Dust on CMB Anisotropies

M. Maris, C. Burigana, A. Gruppuso,
F. Finelli. J.M. Diego - MNRAS 2011, 415, 2546

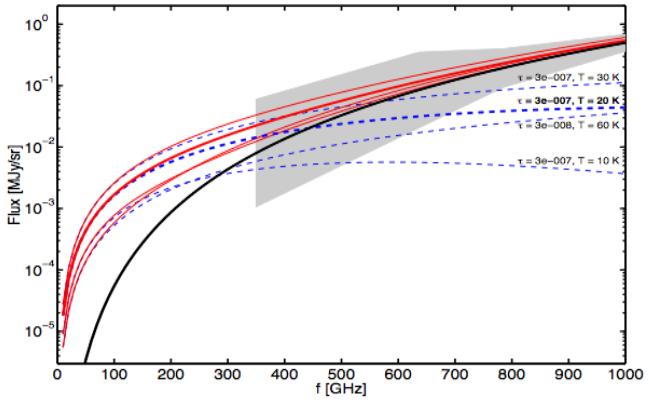

Figure 1. Comparison of ZLE fluxes compatible with COBE/FIRAS data (Fixsen & Dwek 2002) and a set of possible models of KBOE (Stern 1996). The black solid line shows the ZLE derived from the best fit model to COBE/FIRAS data and extrapolated to lower frequencies. The gray band represents a sketch of the allowed region obtained from the error bars in Fixsen & Dwek (2002). The blue dashed lines display four different models of KBOE corresponding to different values of τ and T. The resulting fluxes, sum of KBOE and ZLE, are represented by the red solid lines. Note that the classical ZLE (estimated on the basis of COBE data) is negligible in practice at WMAP frequencies, whereas KBOE might not be ignored.

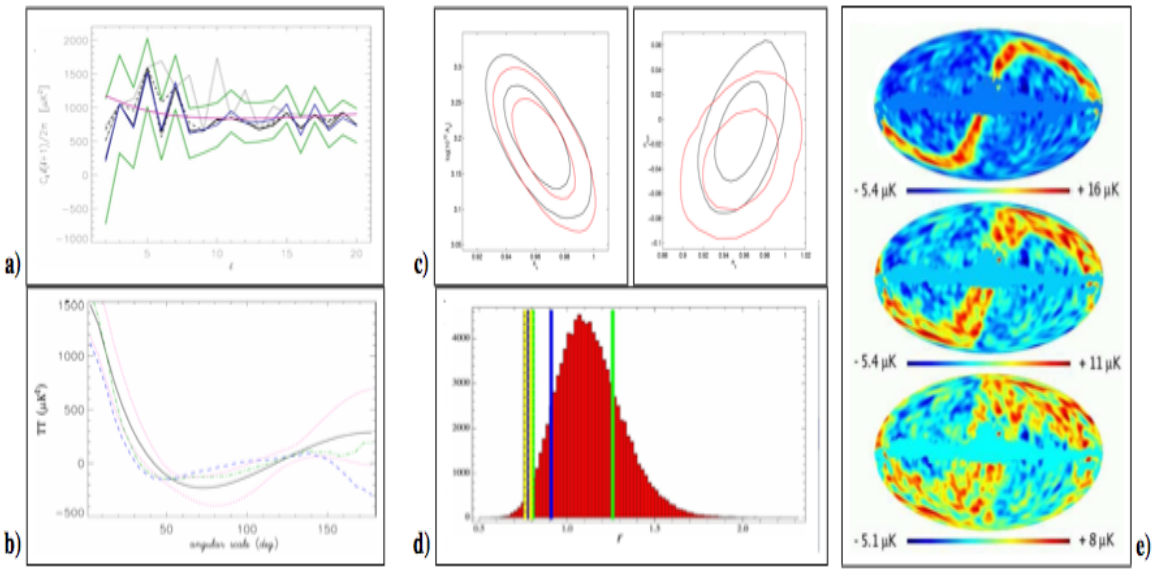

Figure 2. Panel a): APS at low multipoles as derived by the WMAP team analyzing the ILC 7 yr map (blue solid line) with its 1σ errors (green solid lines); APS of the ILC 7 yr map derived using `Anafast` (black solid line); APS of the ILC 7 yr map after the subtraction of our KBOE template with $H_{\rm KBOE} = 70°$, 35° and 17.5° (black dotted–dashed line, dashed line, and dotted line, respectively). The dust model with $\tau = 3 \times 10^{-7}$ and $T = 30$ K (CM) and the V band is here considered. The red solid line shows APS of the best fit ΛCDM model for the WMAP 7 yr map. Panel b): two-points correlation function computed for maps at HEALPix resolution $N_{\rm side} = 16$. The solid line displays the average of 10^5 MC realizations of CMB anisotropy maps extracted from the WMAP 7 yr best fit ΛCDM model APS shown in panel a). The red dotted lines show the corresponding 1σ level fluctuations of the MC simulation. The blue dashed line refers to the ILC 7 yr map. The green dotted-dashed line refers to the map derived subtracting from the ILC 7 yr map one of our KBOE model, namely that obtained for the CM with $H_{\rm KBOE} = 17.5°$. Panel c): Two dimensional marginalised probability distributions for cosmological parameters by removing (black lines) or not removing (red lines) the KBOE template for the CM with $H_{\rm KBOE} = 35°$ (curves are the 68% and 95% confidence level). To the left (right) the plot for A_s ($n_{\rm run}$) vs n_s for a standard ΛCDM model (including running of the scalar spectral index). Panel d): parity anomaly of the estimator $r = P_+/P_-$ as defined in the text with $\ell_{max} = 22$. The histogram (in red) displays the distribution of r obtained from 10^5 MC realizations. Vertical lines correspond to the maps considered in this work: the black solid line (on the left) refers to the ILC 7 yr map; colored solid lines refer to the CM; colored dashed lines refer to the WM. Green, blue, and yellow lines are for $H_{\rm KBOE} = 17.5°$, 35°, and 70°, respectively. Panel e): predicted signal in the combination $V + W - 2Q$ from the CM with $H_{KBOE} = 70°$ (bottom), $H_{KBOE} = 35°$ (middle), and $H_{KBOE} = 17°$ (top). The map units are μK and it has been smoothed with a 7° Gaussian. Compare this plot with Fig. 1 of Diego et al. (2010) based on WMAP data: the model with $H_{KBOE} = 70°$ seems to agree better with the observations.

Can residuals of the Solar system foreground explain low multipole anomalies of the CMB?

M. Hansen, J. Kim, A.M. Frejsel, S. Ramazanov, P. Naselsky, W. Zhao, C. Burigana, arXiv:1206.6981

Topics: extragalactic sources

- (a) Analysis of the statistical properties and evolution of radio and sub-mm sources, and their classification into dominant populations.
- (b) Survey of extreme radio sources, i.e. those with unusual, sharply peaked, or inverted spectra.
- (c) Construction and analysis of a catalogue of quasars and BL Lac objects, combining Planck data with data from a wide variety of other wavelengths. Specific effort is being made to detect flaring sources and follow them up quickly with ground facilities.
- (d) Construction and analysis of a catalogue of nearby galaxies, and the detailed study of a small number of resolved galaxies (LMC, SMC, M 31, M 33).
- (e) All-sky survey and analysis of bright high-redshift dusty galaxies, and possibly proto-clusters.
- (f) Extraction of the cosmic far-infrared background believed to consist of unresolved galaxies, and analysis of the angular power spectra of this component.

Extragalactic (radio)sources
Ancillary data / Almost coeval data / Synergy with different observatories

Acquisition & analysis of ancillary data in many frequency bands

(Tool by Massardi & Burigana 2010, POFF) **Some examples:**

- Coeval observations of blazar with Planck, Swift & Fermi
- New survey at high frequency of northern sky (K-band Northern Wide-area Survey – KNOWS, PI: E. Carretti)
- Observations with the Medicina radiotelescope coeval with Planck of samples of radiosources (SiMPlE - PI: M. Massardi)
- Data analysis of AT20G survey (Australian Telescope 20 GHz, PI: R.D.Ekers):
- ATCA observations, many of them coeval with Planck, of samples of radiosources (project PACO)
- Identification of sub-mm sources detected by Planck in the survey Herschel-ATLAS
- Selection of sub-mm sources with strong gravitational amplification of fluxes

Topics: clusters & secondary anisotropies

- (a) Production and analysis of a catalogue of Sunyaev-Zeldovich (SZ) sources detected by Planck.
- (b) Analysis of the combination of Planck SZ-selected galaxy clusters with a wide range of other observations (X-ray, optical, near-IR, sub-mm), either from existing surveys or by dedicated follow-up, to study their physicsand evolution.
- (c) Reconstruction of the ionisation history of the Universe.
- (d) Estimation of the Integrated Sachs-Wolfe effect and its constraints on cosmological parameters e.g. the dark energy equation of state.
- (e) Extraction and analysis of diffuse and kinetic Sunyaev-Zeldovich components.

Extension to all modes (B-modes) beyond simple tau-approximation

- Future of CMB polarizatione anisotropies:
  - towards B-modes & full exploitation of all modes
- New original implementation of reionization models in CAMB code considering all modes & in particular B-modes
- → T. Trombetti & C. Burigana, 2012, arXiv: 1205.0463
- Inclusion of
  - Phenomenological models (high/low z)
  - Astrophysical models
  - Mix of models
- Typical cases →

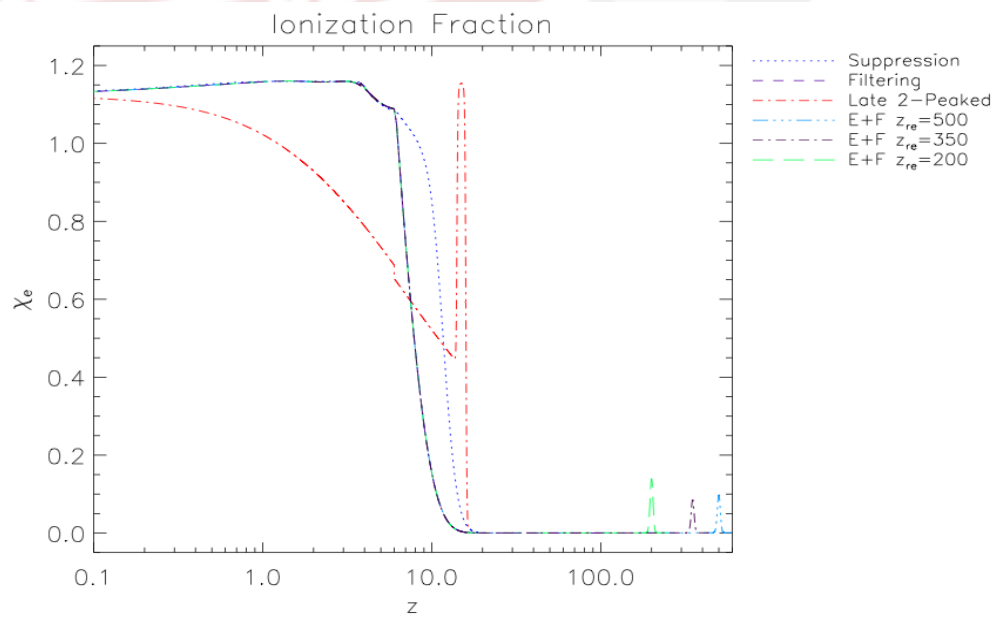

BB predictions

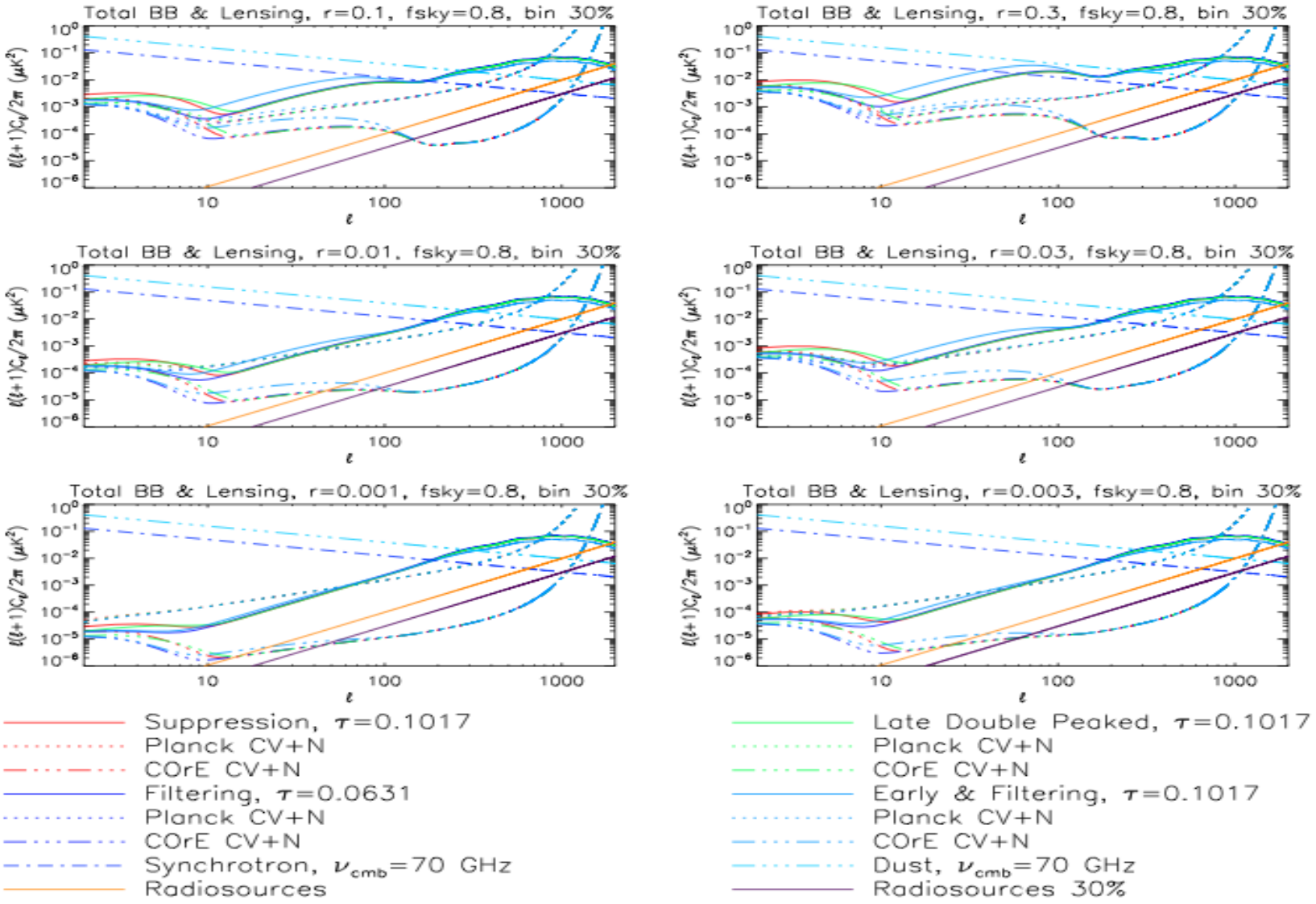

From T. Trombetti & C. Burigana, 2012, arXiv: 1205.0463

BB: comparing models & experiments

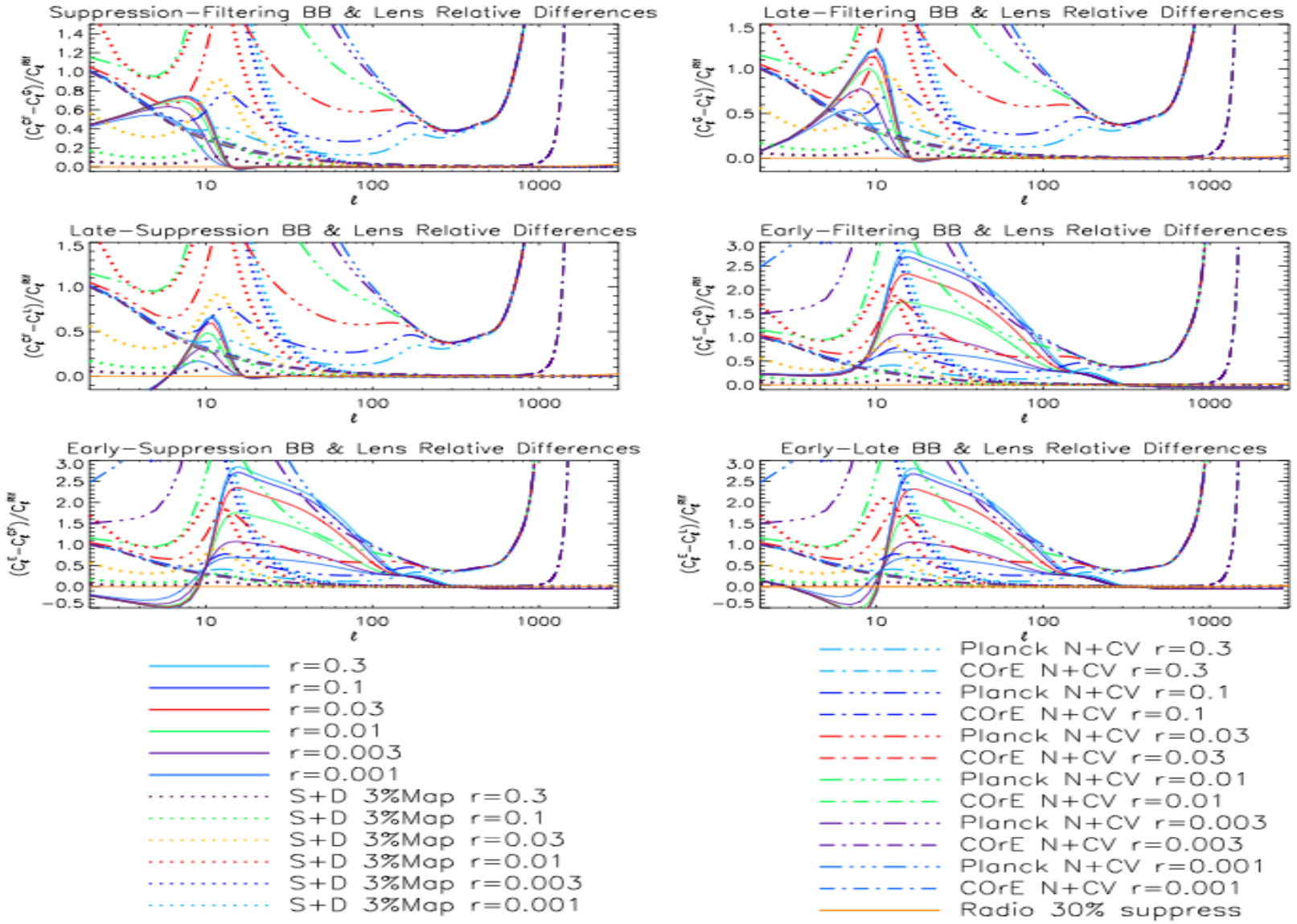

From T. Trombetti & C. Burigana, 2012, arXiv: 1205.0463

Conclusions

- *Planck* is working as expected
- DPCs, instruments, CTs, WGs are working well & intensively to produce accurate TOD, frequency maps, component maps, source catalogs & to scientifically analyze data
- *Planck is probed to be a powerful "astrophysical surveyor" & we are working to deliver products & cosmological results since 2013*
- So … the future will be bright for
  - CMB & cosmological "main" science
  - Galactic & extragalactic "secondary" science

Thanks for your attention!